Don A. Doutre

THE DEVELOPMENT AND APPLICATION OF A RAPID METHOD OF EVALUATING MOLTEN METAL CLEANLINESS

Department of Mining and Metallurgical Engineering

Ph.D. May 1984 Copy 1

THE DEVELOPMENT AND APPLICATION OF A RAPID METHOD OF EVALUATING MOLTEN METAL CLEANLINESS

by

Don A. Doutre

A Thesis Submitted to the Faculty of Graduate Studies and Research
in Partial Fulfilment of the Requirements for the Degree of
Doctor of Philosophy

Department of Mining and Metallurgical Engineering
McGill University
Montreal, Canada

A RAPID METHOD OF MEASURING MOLTEN METAL CLEANLINESS

ABSTRACT

The presence of inclusions in metals is often detrimental to product quality. Despite a widespread need for a rapid means of assessing metal cleanliness, most techniques currently available are either far too slow to be useful for process control or lack the sensitivity required to detect the relatively small inclusions which occur at very low concentrations in most molten metals.

The first part of the present work describes the development of a rapid, quantitative and extremely sensitive means of evaluating metal cleanliness. The method provides both the concentration and the particle size distribution of suspended inclusions while sampling directly from the molten metal.

In the second part of the study the method was used to investigate metal cleanliness at a number of production centers. The beneficial effects of settling and filtration on the concentration of suspended inclusions in a variety of aluminium alloys were examined and the results compared to those obtained using an independent (metallographic) means of assessing metal cleanliness.

RESUME

La présence d'inclusions non-metalliques est souvent préjudiciable à la qualité des produits manufacturés. Malgré la demande généralisée pour une méthode capable d'évaluer rapidement le niveau de propreté du métal, les techniques présentement disponibles sont ou trop lentes pour être utiles en controle de procédé, ou trop peu sensible pour détecter les inclusions de dimensions relativement faibles présentes en très petites concentrations dans la plupart des métaux en fùsion.

La première partie du présent travail décrit le développement d'une technique rapide, quantitative et hautement sensible pour évaluer la propreté du metal. Cette méthode détermine a la fois la concentration, la dimension et la répartition des inclusions, et ce pendant un échantillonage direct du métal en fusion.

En deuxième partie, cette technique a été appliquée à l'étude de la propreté du métal dans divers centres de production. Les effets bénifiques de la sédimentation et de la filtration sur les niveaux d'inclusions en suspension ont été mesurés pour une gamme d'alliages et les résultats obtenus sont comparés a ceux dérivés d'une méthode indépendante (métallographique) d'évaluation de la propreté du métal.

ACKNOWLEDGEMENTS

I would like to thank Prof. R.I.L. Guthrie not only for his advice and encouragement but also for the faith he showed in emptying a good part of his research budget to buy the necessary test equipment to try out an untested idea. I am also deeply indebted to Mr. G. Dubé of the Arvida Laboratories of Alcan International for making available the facilities of the experimental foundry where much of the development work took place and for making the arrangements necessary to carry out the in-plant testing.

Special thanks go to Mr. D. Roy, Mr. S. Néron and Mr. H.M. Bouchard for their assistance in carrying out the hot metal testing and to the staff of the Metallography Department of the Alcan Arvida Laboratories for providing the PoDFA analyses and the electron micrographs of the sampling tubes. Discussions with Mr. C. Tremblay and Mr. G. Deschêne, both of the Arvida Instrumentation Laboratory, concerning the finer points of minimizing electronic noise were most useful and are greatfully acknowledged.

The Natural Sciences and Engineering Research Council, the Québec Ministry of Education and Alcan International are all gratefully acknowledged for the scholarships they provided to the author.

Above all I owe a debt of gratitude to my wife, Lise, both for her unwavering support and for enduring, without complaint, the prolonged periods of absence during which she assumed the entire burden involved in raising two young children.

TABLE OF CONTENTS

INTRODUCTION

Metal quality is a major concern in the aluminium industry. One aspect of metal quality that is becoming increasingly important is metal cleanliness, where cleanliness depends on the number and size of non-metallic inclusions suspended in the metal. One area in which metal cleanliness is of paramount importance is in the production of can body stock. American shipments of this product represented 1.3×10^9 kilograms in 1981, over 20% of all domestic American aluminium shipments. Over 50% of this metal was recycled scrap. This, owing to its large surface to volume ratio and its tendency to oxidize, represents a very "dirty" starting material for the secondary producers. With such large and increasing proportions of recycled metal and the trend towards the production of lighter gauge sections, it is becoming necessary to produce metal from increasingly dirty starting material that is free from increasingly smaller inclusions.

There is a wide variety of melt cleaning techniques that are currently being used by aluminium producers. These include fluxing the metal with active gases (principally containing chlorine), inert gases or mixtures of the two, fluxing with halide salts, decantation, filtration through packed beds or ceramic foam filters and specialized process units which combine gas fluxing and mechanical agitation. Examples of the latter systems include Consolidated Aluminium's MINT reactor, Union Carbide's SNIF and Alcoa's 622 System. Fluxing aluminium with chlorine containing gas mixtures serves the dual purpose in that, in general, it lowers both the hydrogen concentration and the level of suspended inclusions. Regarding hydrogen, there exists today fast and reliable instrumentation for the measurement of dissolved hydrogen in aluminium and well established production procedures that ensure

satisfactorily low hydrogen levels in the metal prior to casting. The situation with respect to inclusions has not reached a comparable state of development due largely to the absence of a quantitative analytical technique for measuring the size and concentration of suspended inclusions.

The initial goal of the present work was to study the effectiveness of the inclusion removal techniques currently used in the aluminium industry. It was soon appreciated that the existing methods of metal cleanliness evaluation were not capable of providing particle size distribution data and that furthermore most methods were semi-quantitative and extremely time consuming. It was therefore decided that a fresh attempt should first be made to develop a rapid, quantitative technique for the determination of the concentration and size distribution of inclusions in molten metals. This development is described in Part I of this report. Part II then describes some applications of the method developed including in-plant monitoring of molten metal cleanliness.

PART I

THE DEVELOPMENT OF A RAPID QUANTITATIVE METHOD FOR THE MEASUREMENT OF THE CONCENTRATION AND SIZE DISTRIBUTION OF INCLUSIONS SUSPENDED IN MOLTEN METALS

ABSTRACT

A new method and apparatus for the measurement of the concentration and the size distribution of suspended inclusions in molten metals is described. The method is based upon measuring the change in resistance of a small fluid element as the particles pass through it displacing the conductive fluid. The amplitude of the resistance change is a measure of the particle size and by counting the frequency of such changes, the concentration of the particles can be deduced. The method is extremely rapid, providing results in approximately one minute.

1. INTRODUCTION

The presence of non-metallic inclusions in liquid metals often gives rise to undesirable consequences in the final products. In the case of aluminium these can include pin-holes in foil, razor-streaks in bright trim, perforations and tears in deep drawn forms such as beverage cans, surface defects in sheet products and increased breakage rates in wire drawing operations. Inclusions can also serve as nucleation sites for hydrogen gas thus causing blistering in annealed ingots. In extreme cases inclusions can increase the rates of tool and extrusion die wear and cause damage to rolling surfaces. The origins, composition and effects of inclusions have been the subject of a recent review by Langerweger [1].

There is an extensive body of literature concerning the nature and effects of inclusions in steel where inclusions are known to affect the strength, corrosion resistance, fatigue properties and formability of steel products. Steel cleanliness has been the subject of a recent conference [2].

The size at which an inclusion is considered undesirable depends of course upon the application. In wrought aluminium alloys it is safe to say that any inclusion larger than 15 μm is potentially harmful. In plain carbon steels alumina inclusions as small as 10 μm have been reported to affect the polishability of lens moulds used for forming plastics [3]. The most common inclusions present in aluminium and its alloys are listed in Table 1.

TABLE 1

COMPOSITION AND PROBABLE SOURCE(S) OF NON-METALLIC INCLUSIONS COMMONLY OCCURRING IN ALUMINIUM.

Composition	Source(s)
Al_2O_3	Exposure to O_2, H_2O
MgO	Exposure to O_2, H_2O
$AlMgO_4$	Exposure to O_2, H_2O
Al_4C_3	Carried over from reduction cells
	Reaction with graphite tools
TiB_2	Grain refiner additions
	Recycled, grain-refined scrap
(Ti-V)B	Addition of boron to increase electrical conductivity
Salts	Salts fluxes
	Chlorine fluxing.
Entrained refractories	

It can be seen that most sources of inclusions are, generally unavoidable. For instance, the metal is normally transferred down open launders and thus exposed to atmospheric oxygen and water vapour, boron additions are routinely made to electrical conductor grade aluminium to precipitate vanadium in the form of complex titanium-vanadium borides, titanium diboride is widely used as a grain refining agent, aluminium carbide is sometimes formed by the reaction of aluminium with graphite cathodes during the reduction process, etc. Indeed, most of the commonly occurring inclusions are too small to be detrimental in all but the most exacting applications. Even

large inclusions can be tolerated if they are fragile enough to be broken down during forming operations.

However a very low concentration of large hard inclusions can render the metal unfit for some applications. A good example of such an application is in can body stock (Alloy AA-3004) where the production and filling of the cans is highly automated and a defect rate of 1 can per 10,000 is usually considered to be unacceptably high.

Despite the acknowledged need within the aluminium industry for a rapid method of monitoring metal cleanliness, limited progress towards that end has been achieved to date. The present paper describes the operating principle and the development of such a device.

2. REVIEW OF PREVIOUS WORK

In view of the importance of the level of inclusions on metal quality is not surprising that a variety of approaches for evaluating metal cleanliness have been developed. These can be divided into four main categories:

1. Chemical Methods
2. Optical Methods
3. Operational Methods
4. Physical Methods.

This review emphasises techniques that have been used for the evaluation of cleanliness in aluminium. A brief review of methods available for measuring the cleanliness of steel is included separately at the end of this section.

2.1 Chemical Methods

Gross chemical analysis is of little use in measuring the inclusion content of aluminium. This is due to the fact that measuring the bulk concentration of an element or compound tells nothing about how it is distributed within the metal. For instance, it has been established that there is no correlation between the oxygen concentration and the inclusion level in aluminium. Typical oxygen levels in commercial aluminium range from five to fifty parts per million (ppm) with most of this oxygen present in the form of very thin (<2 μm) oxide films. If there were one 50 μm Al_2O_3 particle per ml the oxygen level due to this inclusion would be about .050 ppm and would thus be indistinguishable above the background oxygen concentration.

Similarly total carbide levels can be measured by reacting them with H_2O to form methane which can be detected at very low levels by gas chromatography. However once again this approach provides no indication of particle size [4].

The gravimetric determination of the residue remaining after dissolving the metal matrix would also be of little use for reasons similar to those given above and in addition would be technically difficult. If, 100 g of metal containing one 50 μm Al_2O_3 particle per ml were dissolved the residue would weigh approximately 11 μg (assuming separation of the oxide films). Although analyses of this type are possible the chances of gross contamination arising from the reagents, glassware or imperfect separation from films would be very high and extreme care would have to be taken during all steps. Of course the residue need not necessarily be determined gravimetrically. In the case of metal containing TiB_2 or TiVB particles such a residue could be redissolved and measured by, for example, atomic absorption spectroscopy. However, such a procedure would be a) prone to error, b) time consuming and c) provide limited information about the size of the inclusions.

Siemensen [5] has reported on the use of a resistive-pulse type particle size analyser for measuring the particle size distribution of extraction residues. Apart from uncertanties concerning the loss of inclusions or the production of artifacts during extraction this procedure is slow and unsuitable as a candidate for a rapid method of quality control.

2.2 Optical Methods

Perhaps the most obvious method of assessing the inclusion content in aluminium is the direct examination of polished sections. However, at the concentrations typically encountered in reasonably clean aluminium (approximately 5 to 20 particles per ml 20 μm or larger), preconcentration of the inclusions is necessary in order to observe a significant number of particles within a reasonable area. One early method of preconcentration was the IMFA (In Mould Filtration Apparatus) test [6]. This test involved

passing a fifty pound sample of metal through a glass filter cloth, allowing the metal to solidify while some metal still remained on the upstream side of the filter, cutting out the filter and metal and finally sectioning and polishing the filter cake. Since the filter cloth was relatively coarse, this method depended upon the formation of a cake of Al_2O_3 films which then acted as the filter medium in retaining other forms of inclusions. Thus the cleanliness rating depended both upon the level of inclusions of interest and upon the level of oxide film. This tended to give erratic results particularly when relatively unoxidized metal was sampled. In addition, the large quantity of metal sampled, while good from the point of view of obtaining a large and thus presumably representative sample, made the test cumbersome and time consuming.

Attempts to refine the IMFA test led to the development of the PoDFA [6] (Porous Disk Filtration Apparatus) technique initially calling for a thirty pound sample and later, a five pound sample. The PoDFA technique essentially consists of forcing a measured mass of molten aluminium through a porous filter disc under pressure. The pressure is relieved while some metal still remains upon the filter, the overlying metal is allowed to solidify and the filter cake is recovered and examined metallographically. (The IMFA and PoDFA techniques were developed by ALCAN during the 1950's and 1960's and have evolved since).

Other manufacturers have developed similar methods of pre-concentration. These include the Union Carbide particulate tester in which the sample is aspirated directly from a transfer launder using a porous graphite disc [7] and the Olin frit test in which a twenty pound sample is forced through a porous silica disc [8]. Bates and Hutter of the Anaconda Aluminium Company have also described a vacuum-type metal sampler in which an eight

pound sample was filtered through a porous ceramic disc [9]. Undoubtedly the other major aluminium producers have developed their own versions of this type of test.

These techniques require care during sampling to avoid fouling the filter surface with oxide films during initial contact with the metal and, at least for the PoDFA test, are very sensitive to the permeability of the filter and the metal flow rate. Erratic results may also occur, particularly with fairly "dirty" metal due to the formation of a filter cake with inclusion capture characteristics different from those of the porous disc.

Due to nature of these techniques there is necessarily a substantial (>1 hour) time delay between sampling and obtaining results and the tests are subjective in the sense that some interpretation on the part of the metallographer is required. Despite some twenty years of development the PoDFA technique remains "semi-quantitative". On the positive side, however, these techniques provide some indication of particle size and can be used to deduce the composition of the inclusions, a fact that has been useful in tracing the source of inclusions in unsatisfactory metal.

Another method of concentrating inclusions is the use of a hot metal centrifuge. Most inclusions being more dense than molten aluminium tend to settle, and centrifuging the melt accelerates the rate of sedimentation. Mollard et al [10] and later Siemensen [5] reported on the use of liquid metal centrifuges in studies of metal cleanliness.

Bauxman [11] has described a different approach based on the observation that defects (inclusions) larger than twenty microns act as light scattering centers if the metal is heavily anodized. The reported procedure involved diamond milling a 10 by 10 cm section, followed by anodizing and counting the number of light scattering centers visually.

Apart from a minimum dimension (20 μm) this technique provides no size distribution data and obviously none concerning composition. In addition the volume of metal examined is relatively small (10 cm x 10 cm times the depth of the anodized layer) and again there is a substantial time delay in obtaining results.

The examination of the surface of fractured metal specimens was used by Hedjazi et al [12] during an evaluation of filter media but the report gives no indication of sample to sample variation (values were reported as the mean of thirty measurements). Levy et al [13] applied a penetrant dye to the fractured surfaces of 144 test bars and were able to detect only one inclusion, this despite the fact that the metal had been intentionally "dirtied".

2.3 Operational Methods

In view of the lack of an entirely adequate method to evaluate metal quality, reliance has been placed upon the measured performance of production or product materials as a guide for the development of plant practices and melt treatment devices. This includes, for example, the rate of tool wear in machining, extrusion die longevity, quantity of wire drawn per break, pin holes per unit area of foil, surface defects per unit area of sheet, failure rates in beverage cans, etc. Although these types of "tests" are undeniably relevant in that they measure actual production or product performance, this approach inevitably leads to costly rejects and does not measure true cleanliness. While this approach does serve to develop empirical production procedures that are satisfactory for specific individual applications, it does not permit any possibility of on-line process control.

2.4 Physical Methods

In contrast to the techniques discussed in the previous three sections physical methods have the advantage that, at least in principle, they can be carried out relatively rapidly and therefore allow some hope of implementation as process control techniques.

Filtration Rate Tests:

The rate of liquid metal filtration at constant differential pressure has been investigated by Alcan [6]. However this approach was abandoned when it became evident that the rate was influenced by all particles suspended in the metal, including any very small oxide films and grain refiner nuclei. This together with the relatively low concentrations of larger, detrimental inclusions resulted in the latter exerting little, or no, detectable effect on the filtration rate. The Union Carbide particulate tester (mentioned earlier in the optical methods section, 2.2) has also been used for filtration rate testing [7]. In this case the sampler was equipped with a load cell and the measured weight-time curves fitted to an equation of the form:

$$W = AT^B$$

where W is as weight of metal filtered, T the elapsed time, and A and B curve fitting constants which were claimed to depend upon the cleanliness of the metal.

By interfacing a microprocessor to the load cell and mounting the sampler in a transfer trough this technique has been used "on-line". However it gives no indication of particle size and the results are probably seriously affected by very small particles and oxide films.

Levy et al [13] investigated the rate of the rise of the differential pressure developed across the porous frit of the Alcoa telegas probe and reported that the results were "encouraging". However it is virtually certain that this method would be subject to the same limitations noted for filtration rate testing at constant differential pressure. The fact that inclusions can act as nucleation sites for hydrogen gas bubble formation in the Straupe-Pfeiffer (vacuum-gas) solidification test led to the development of the test as a qualitative tool for estimating metal cleanliness [14]. Despite obvious limitations in providing independent data concerning either the hydrogen level or inclusion content this approach has proved useful as a quick "pass/fail" test of overall metal quality.

Ultrasonics

Ultrasonic technology for the nondestructive testing of solid materials is well established. Indeed, the method is used routinely to inspect welds, extrusion ingots, etc. for macroscopic defects. In general, the size of the defects detected by routine ultrasonic inspection are relatively large, typically several millimeters, through resolutions of the order of 0.1 mm are reportedly possible [15].

An attempt to correlate the ultrasonic attenuation of solid samples with their inclusion concentration was reported by Levy et al [13] who concluded that the former was more a measure of the porosity of the sample than of its inclusion content.

In 1968 Pitcher and Young [16] demonstrated that ultrasonic techniques could be applied in molten metals and at the present time there is considerable interest in the application of ultrasonic techniques to measure the cleanliness of molten aluminium. Alcoa [6] and Reynolds [17] both have development programs underway and Alcan has been considering a major

expansion in its ultrasonics program. The promise of ultrasonics is that, with modern, high speed signal analysis capabilities, the reflected signals may provide information on particle size and shape as well as on particle concentration.

T.M. Mansfield of the Reynolds Aluminium Company presented a paper at the 1982 AIME conference describing Reynold's developments in this field [17]. He described a system capable of making four types of measurements directly in molten aluminium: attenuation, discontinuity detection, velocity and spectrum analysis. Attenuation measurements were reportedly capable of indicating the overall level of suspended particles within the melt, with particles as small as one tenth the wavelength of the imposed ultrasonic oscillation contributing to the attenuation. Since the oscillator described was operated at 10 megahertz and the velocity of sound in molten aluminium is approximately 4700 m/sec [18] the detection limit for attenuation measurements would be $4700/10^7 \cdot 10 = 47$ μm. Discontinuity measurements can in theory detect individual particles no smaller than one half of the ultrasonic wavelength; 235 μm in the system described by Mansfield. The velocity measurements refer to the determination of the velocity of sound in the melt and not to any measure of metal cleanliness. Finally the spectrum analysis measurements refer to a potential use of the technique to measure attenuation as a function of frequency which would apparently be subject to the same size of detection limitation as are discontinuity measurements (i.e. $\lambda/2$ or 235 μm in the case at hand).

In view of the relatively large particle size detection limit it is difficult to understand the current level of interest in ultrasonic devices for application in molten aluminium except to underscore

the fact that a rapid technique for determining melt cleanliness has been badly needed for some time. Since the particle detection limit of ultrasonic techniques is inversely proportional to the excitation frequency, it is evident that the detection limit could in principle be made as small as desired by using a higher frequency source. This approach is apparently not feasible due to the necessity of using wave-guides (generally titanium) to conduct the vibrations from the source (generally an oscillating crystal) to the metal. The ultrasonic attenuation of the the wave guides rises rapidly with increasing frequency and thus there is a practical upper limit to the inspection frequency [19].

Despite the relatively coarse limit of detection Mansfield was able to qualitatively demonstrate the detrimental effect on metal cleanliness of disturbing a filter and the beneficial effect of allowing a settling period prior to casting metal from a furnace. In contrast to most alternatives, ultrasonic measurements of liquid samples have the distinct advantage of providing a rapid indication of melt cleanliness. Nevertheless, it would seem that considerably more development work remains to be done before the technique can provide quantitative measurements of metal cleanliness.

2.5 The Measurement of Steel Cleanliness

The American Society for Testing Materials has published a standard practice for the determination of the inclusion content of steel [20] in which four testing procedures are specified. These are:

1. The Macroetch Test: in which the steel surface is etched with hot hydrochloric acid and examined visually or at low magnification for the presence of inclusions.

2. The Fracture Test: in which, as the name implies, a metal sample is fractured and the surface examined for inclusions at up to 10X magnification.
3. The Step Down Method: in which the specimen's surface is machined and subsequently examined for inclusions.
4. The Magnetic Particle Method: in which a machined surface is powdered with small magnetic particles to reveal the presence of non-metallic inclusions.

The resolutions of methods 1, 3 and 4 are reportedly 0.4 mm whereas the stepdown method (3) is used to determine the presence of inclusions larger than 3.2 mm (1/8 inch) in diameter. The limitations of these tests both in terms of resolving power and the time required are obvious.

Lagneborg [21] has reported the application of an electron microscope coupled with an image analyser to the investigation of steel cleanliness, and there are automatic image analysis systems interfaced with optical microscopes commercially available.

Flinchbaugh [22] has reported the use of a modified Coulter counter to size and count inclusions after chemical dissolution of the steel matrix.

The firm Electro-Metals [23] reportedly makes use of an electron beam to melt button samples in which insoluble inclusions float to the surface where, in the presence of the beam they luminesce and can be distinguished from the metal.

From this brief review it is evident that the measurement of inclusions in steel is no more advanced than it is in aluminium and that it is unlikely that there is any technique developed for use in steel that would provide a rapid means to measure the cleanliness of aluminium.

3. THEORY

Despite a large amount of effort and expenditure on the part of many investigators, the previous section indicates that there has, to date, been no report of any technique capable of providing a rapid quantitative estimate of the cleanliness of molten metals. This section describes the operating principle and the theoretical basis of such a technique, which has been dubbed LiMCA for Liquid Metal Cleanliness Analyzer (Analysis).

3.1 Principle of Operation

The LiMCA is based upon the resistive pulse principle of particle size analysis. This technique was developed by Coulter [24] in the 1950's and has since been widely applied to aqueous and organic suspensions at or near room temperature. Examples of its application include heamatology measurements (heamotocrit, lymphocyte and platelet counts), particle size distribution measurements of powders, including alumina in Bayer process plants and biological applications ranging from measuring the growth rates of nematodes to investigations of the prey size preferences of fish, insect larvae and a variety of aquatic and marine invertebrates.

The principle of the resistive pulse technique is shown in Figure 1.

The particles to be analysed are suspended in an electrically conducting fluid and the latter is drawn through an orifice in an electrically insulating vessel. At the same time a constant current is maintained through the orifice which completes the circuit between two terminals of a power supply. When a particle enters the orifice it displaces its volume of the conducting fluid causing a temporary rise in the electrical resistance of the orifice. This resistance change, in the presence of the applied current, causes a voltage pulse, of a duration approximately equal to the

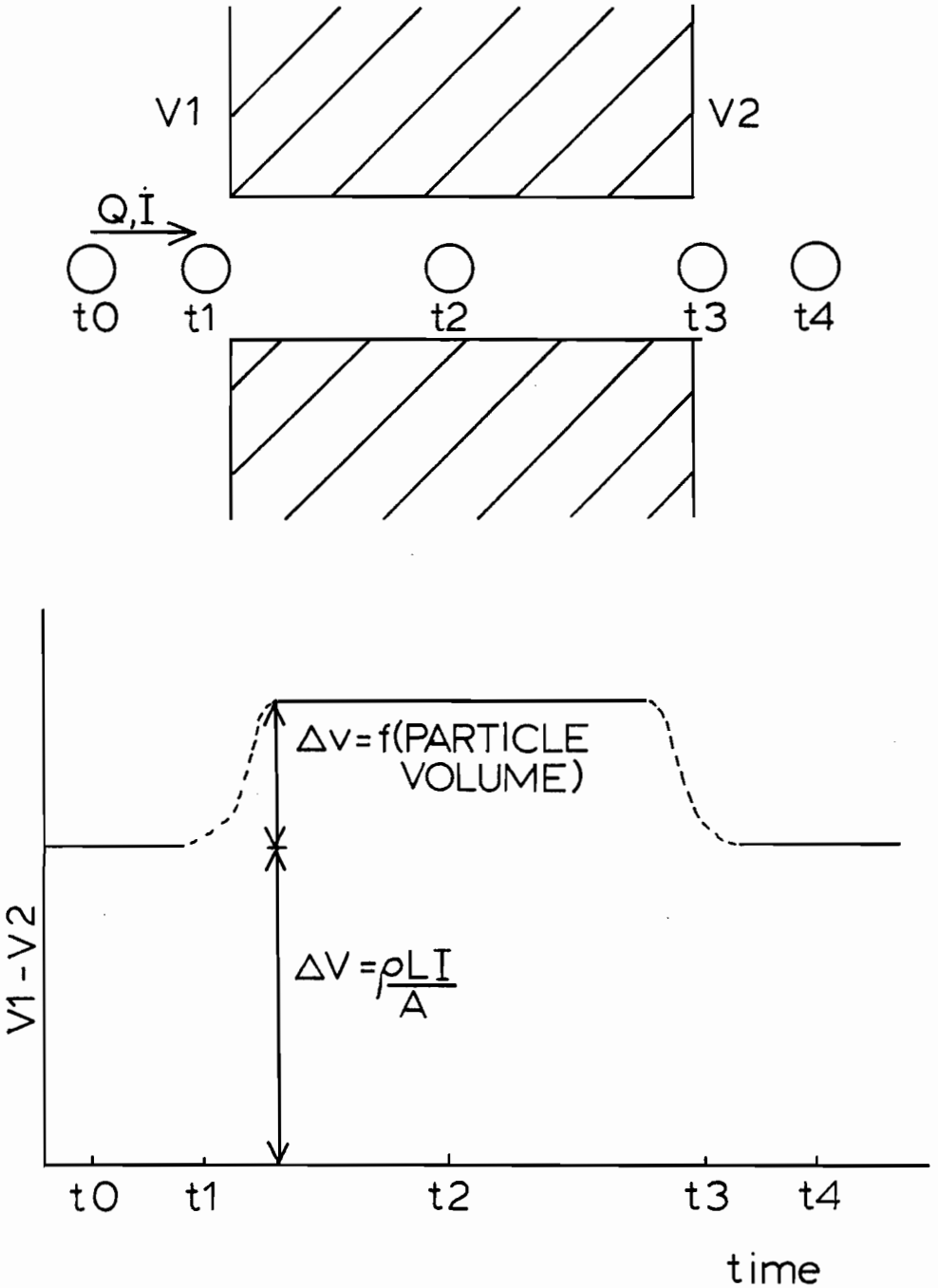

FIGURE 1: The Resistive Pulse Principle of Particle Size Measurement. During its passage, the particle changes the resistance of the orifice. In the presence of an applied current, a voltage change is produced which can be related to the volume of the particle.

transit time of the particle, to appear across the orifice. Alternatively, a constant voltage source can be used in which case current pulses are observed.

The amplitude of the voltage (or current) change is, as a first approximation, proportional to the volume of the particle. Thus by measuring and counting each pulse, the particle size distribution and concentration of the suspended particles can be deduced.

3.2 Prediction of the Magnitude of the Resistive Pulse

The central theoretical problem of the resistive pulse technique is the prediction of the magnitude of the change in electrical resistance (ΔR) caused by the introduction of a non-conducting particle of equivalent diameter (d) into a sensing volume (normally a right circular cylinder) of diameter (D) and length (L). There is no simple analytical solution to this problem valid for all values of (d/D) ranging from 0 to 1.

Deblois and Bean [25] have shown that for (d/D) < ~0.4 a relation first proposed by J.C. Maxwell can be used to derive an explicit expression for ΔR. Maxwell showed that, for a dilute suspension of insulating spheres the effective resistivity could be expressed as:

$$\rho_{eff} = \rho \left(1 + \frac{3}{2} f + \ldots \right) \qquad (1)$$

where (f) is the volume fraction occupied by the spheres. For a cylindrical sensing volume of length (L) and diameter (D) filled with a fluid of conductivity (ρ) the resistance is:

$$R_1 = \frac{\rho L}{A} = \frac{4 \rho L}{\pi D^2} \qquad (2)$$

When a sphere of diameter (d) is introduced, the value of (f) becomes

$$f = \frac{V \text{ sphere}}{V \text{ cylinder}} = \frac{2\ d^3}{3\ D^2 L} \tag{3}$$

Substituting (3) into (1) into (2) gives the resistance of a cylinder with a small non-conducting sphere contained within it:

$$R_2 = \frac{4\ \rho L}{\pi\ D^2} \left(1 + \frac{d^3}{D^2 L} + \ldots \right) \tag{4}$$

Substracting (2) from (4) then gives the desired expression for ΔR:

$$\Delta R = \frac{4\rho\ d^3}{\pi\ D^4} \tag{5}$$

This expression correctly predicts that the resistive pulse is independent of the length of the sensing volume and can be recast in terms of the particle volume (V_p):

$$\Delta R = K\ V_p \tag{6}$$

where the constant K is determined by the resistivity of the fluid and the diameter of the sensing volume:

$$K = \frac{24\ \rho}{\pi^2\ D^4} \tag{7}$$

This is the basis for the contention that resistive pulse type particle size analyzers respond to particle volume. In theory, the factor K should be calculable from a knowledge of ρ and D. However in practical analyzers the existence of entrance and exit effects, implicitly neglected in the use of equation (1) and the fourth order dependency upon D preclude this approach and calibration with standard spheres is universally recommended.

Smythe [26,27] analyzed the problem of predicting ΔR using a numerical technique and has published correction factors (with a stated accuracy of 1 part in 10^7) for equation (5) of the form:

$$\Delta R = \frac{4\rho\, d^3}{\pi\, D^4} f\,(d/D) \qquad (8)$$

Smythe's values of f(d/D) are shown in Table 2.

TABLE 2

CORRECTION FACTORS (f(d/D)) FOR PARTICLE TO ORIFICE DIAMETER RATIOS (d/D) FOR USE WITH EQUATION (8) AFTER DEBLOIS ET AL [28]

d/D	F (d/D)	d/D	f(d/D)
0.1	1.000798	0.6	1.208438
0.2	1.006416	0.7	1.379503
0.3	1.021988	0.8	1.710860
0.4	1.053744	0.9	2.556723
0.5	1.110694	0.95	3.861028

It can be seen that for (d/D) ≃ 0.4 the error in the use of equation (5) is in the order of 5% and decreases to insignificance when (d/D) is less than 0.2. Deblois et al [28] showed that the correction factor f(d/D) could be expressed as:

$$f(d/D) = \left[1 - 0.8\ (d/D)^3\right]^{-1} \qquad (9)$$

with an error of 3×10^{-6} at (d/D) = 0.1 and less than 1% at (d/D) = 0.8. Thus equation (8) can be written explicitly as:

$$\Delta R = \frac{4\rho\ d^3}{\pi\ D^4\ [1-0.8(d/D)]} \qquad (10)$$

valid for (d/D) ranging from 0 to 0.8 with an accuracy of 99%.

The case where (d/D) approaches one is of considerably less technological interest due to the practical problem of physical blockage of the orifice by such particles. However in this case a relatively simple analytical solution exists. Consider a sphere within a right circular cylindrical conductor:

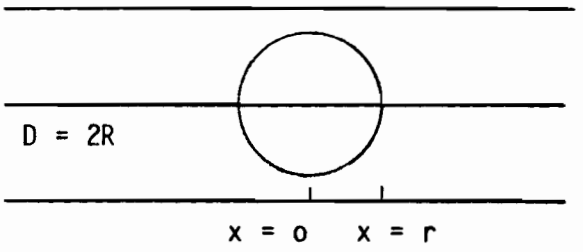

Ohm's law in differential form is:

$$R = \rho \int \frac{dx}{A(x)} \qquad (11)$$

In this case A(x) represents the area of each annular conductor element:

$$A(x) = \pi R^2 - \pi(r^2 - x^2) \tag{12a}$$

$$A(x) = \pi (R^2 - r^2 + x^2) \tag{12b}$$

Substituting (12b) into (11) gives:

$$R = \frac{\rho}{\pi} \int_{x=-R}^{x=+R} \frac{dx}{\sqrt{(R^2 - r^2)^2 + X^2}} \tag{13}$$

Integrating gives:

$$R = \frac{\rho}{\pi} \frac{\tan^{-1}\left(x \Big/ (R^2 - r^2)\right)^{1/2}}{(R^2 - r^2)^{1/2}} \Bigg|_{x=-r}^{x=r} \tag{14a}$$

$$= \frac{\rho}{\pi} \frac{\sin^{-1}(x/R)}{\sqrt{R^2 - r^2}} \Bigg|_{x=-r}^{x=r} \tag{14b}$$

and since $\sin^{-1}(X) = -\sin^{-1}(-X)$

$$R = \frac{2\rho}{\pi} \frac{\sin^{-1}(r/R)}{\sqrt{R^2 - r^2}} \tag{15}$$

The resistance of the cylinder without the particle is:

$$R = \frac{\rho L}{A} = \frac{\rho\ 2\ r}{\pi\ R^2} \tag{16}$$

Substracting (16) from (15) and factoring gives:

$$\Delta R = \frac{2\rho}{\pi R} \left[\frac{\sin^{-1}(r/R)}{\sqrt{1 - (r/R)^2}} - \frac{r}{R} \right] \tag{17}$$

Or, in terms of diameters:

$$\Delta R = \frac{4\rho}{\pi D}\left[\frac{\sin^{-1}(d/D)}{\sqrt{1-(d/D)^2}} - \frac{d}{D}\right] \qquad (18)$$

Equation (18) has been shown to predict ΔR accurately for $(d/D) > 0.8$ [29]. Greig and Steidly [30] showed that equation (18) could be expressed as a power series as:

$$\Delta R = \frac{8\rho\, d^3}{3\pi\, D^4}\left[1 + \frac{4}{5}\left(\frac{d}{D}\right)^2 + \frac{24}{35}\left(\frac{d}{D}\right)^4 + \ldots\right] \qquad (19)$$

which as (d/D) tends to zero converges to:

$$\Delta R = \frac{8\rho\, d^3}{3\pi\, D^4} \qquad (20)$$

which differs from equation (5) by a factor of 3/2. The reason for the discrepency arises from the behaviour of the electric field in the region of the discontinuity. Maxwell [31] verified that the voltage drops resulting from gradual changes in the cross-sectional area of a conductor (i.e. gradual changes in annular area in the case of a large sphere) could be treated by equation (11)(Ohms law). However in the case of a small sphere direction changes in the electric field are locally more marked and Ohms law in the form of equation (11) can no longer be applied.

In practice voltage rather than resistance changes are measured, the magnitude of which are predicted by multiplying equation (8) by the applied current (I):

$$\Delta V \doteq I\Delta R = \frac{4\ I\rho}{\Pi}\ \frac{d^3}{D^4}\ f\left[\frac{d}{D}\right] \qquad (21)$$

Figure 2 is a plot of ΔV as a function of particle diameter under the following conditions:

$\rho = 25 \times 10^{-8}\ \Omega\cdot m$ (Molten Aluminium)

$I = 60$ amperes.

It can be seen that the amplitude of the signals caused by particles of a size likely to be encountered in molten aluminium (20 to 100 μm) are quite small (tens of microvolts to millivolts) thus requiring good shielding from external noise and sensitive measurement equipment. (The choice of operating parameters for the LiMCA are discussed more fully later).

3.3 Effect of Particle Shape and Trajectory

So far only the case of spherical particles has been considered; with non-spherical particles the situation becomes much more complicated. Smythe [27] addressed the question of the effect of particle shape on the magnitude of the resistive pulse and his results show that for oblate and prolate ellipsoids of eccentricity 2 and (d/D) less than 0.4 the error arising from determining d using equation (9) is approximately 10%. Smythe's work was actually concerned with fluid flow around spheres and spheroids in circular tubes. However as he pointed out, the governing equations are the same for the case of the current distribution through a cylinder in the presence of non-conducting particles.

The effect of off-axis particle trajectories has also been investigated by Smythe [32] who calculated that significant changes in the value of ΔR occur as the gap between the off-axis particle and the cylinder

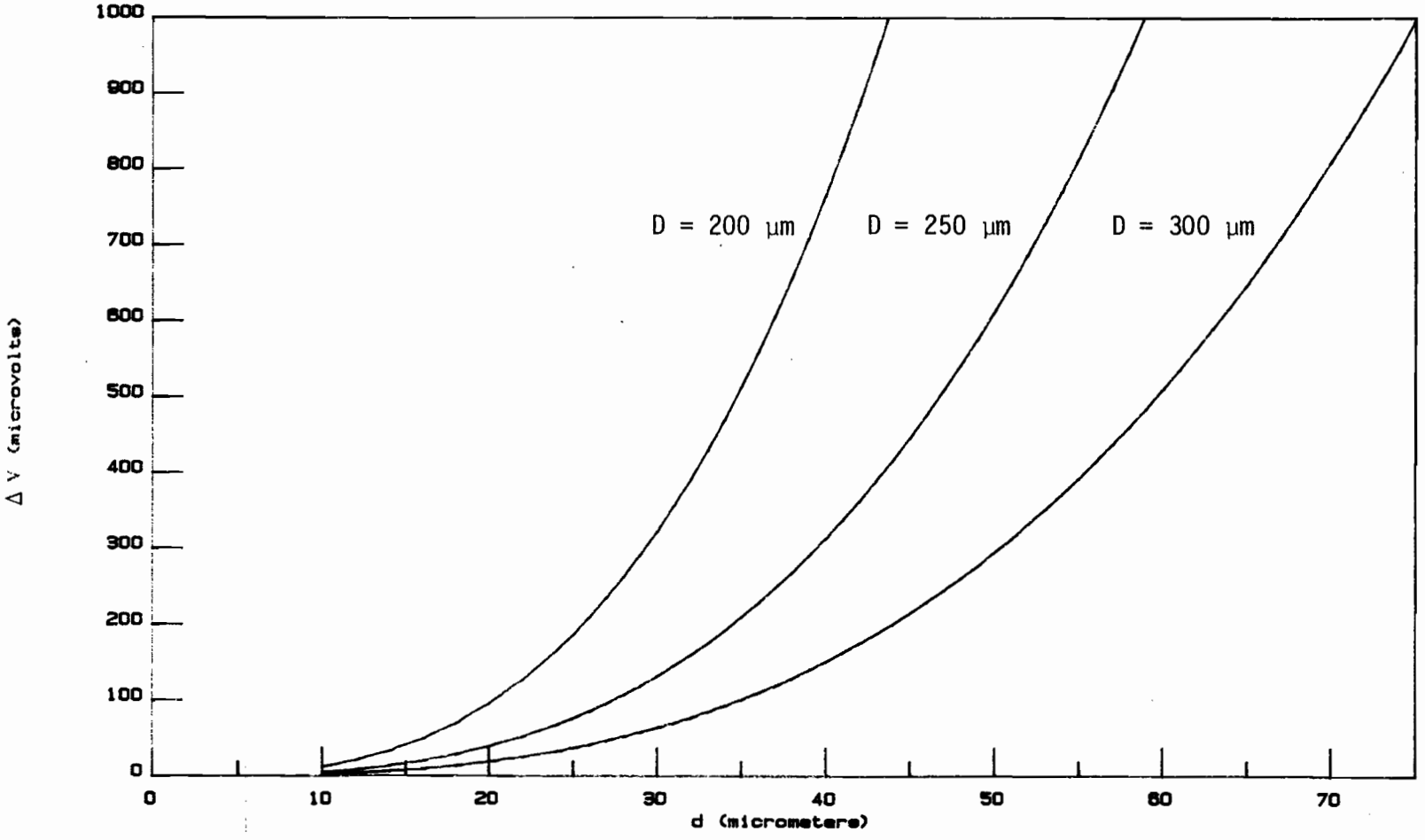

Figure 2: The magnitude of the voltage pulse in aluminium as a function of the particle diameter (d) and the orifice diameter (D)

wall approaches zero. This question has also been addressed by Davies et al [33] who predicted and observed a variety of distorted peaks as function of the angle of entry and the axis of passage of spherical particles through cylindrical sensing volumes. Kahrun et al [34] showed that these effects could be minimized by the use of a smoothly tapered entrance to the sensing volume. These observations have resulted in the introduction of hydrodynamic focusing in conventional resistive pulse analyzers in which the particles to be analysed are introduced into the system through a narrow capillary in-line with the central axis of the sensing volume [35].

4. APPARATUS

The apparatus is shown schematically in Figure 3. It consisted of an insulating sampling cell containing a small orifice through which the metal to be sampled was drawn under reduced pressure. The flow of current through the orifice was established with a constant current power supply and two electrodes, one inside the sampling tube and the other immersed in the metal outside. The voltage across the two electrodes was observed using an oscilloscope and the peaks caused by the passage of particles through the orifice were amplified and recorded using a multichannel analyser which measured and recorded the amplitude of each peak and after each test provided a histogram display of the number of peaks observed as a function of their magnitude.

Since the object of this project was to seek a technique capable of rapidly measuring molten metal cleanliness the apparatus per se was under a continuous state of development and many modifications were made during the course of the investigation.

For descriptive purposes it is useful to divide the apparatus into three major subsystems:

1. A pneumatic metal sampling system (including the sampling cell).
2. A high amperage constant current DC power supply.
3. A voltage pulse measurement system.

4.1 Metal Sampling System

The sampling system is shown in detail in Figure 4. The sampling tube was held in a gas tight brass fixture with an "O" ring (Viton) seal. An inlet through the top of the fixture was connected via the valve assembly to the atmosphere, a low pressure argon gas supply, or to a

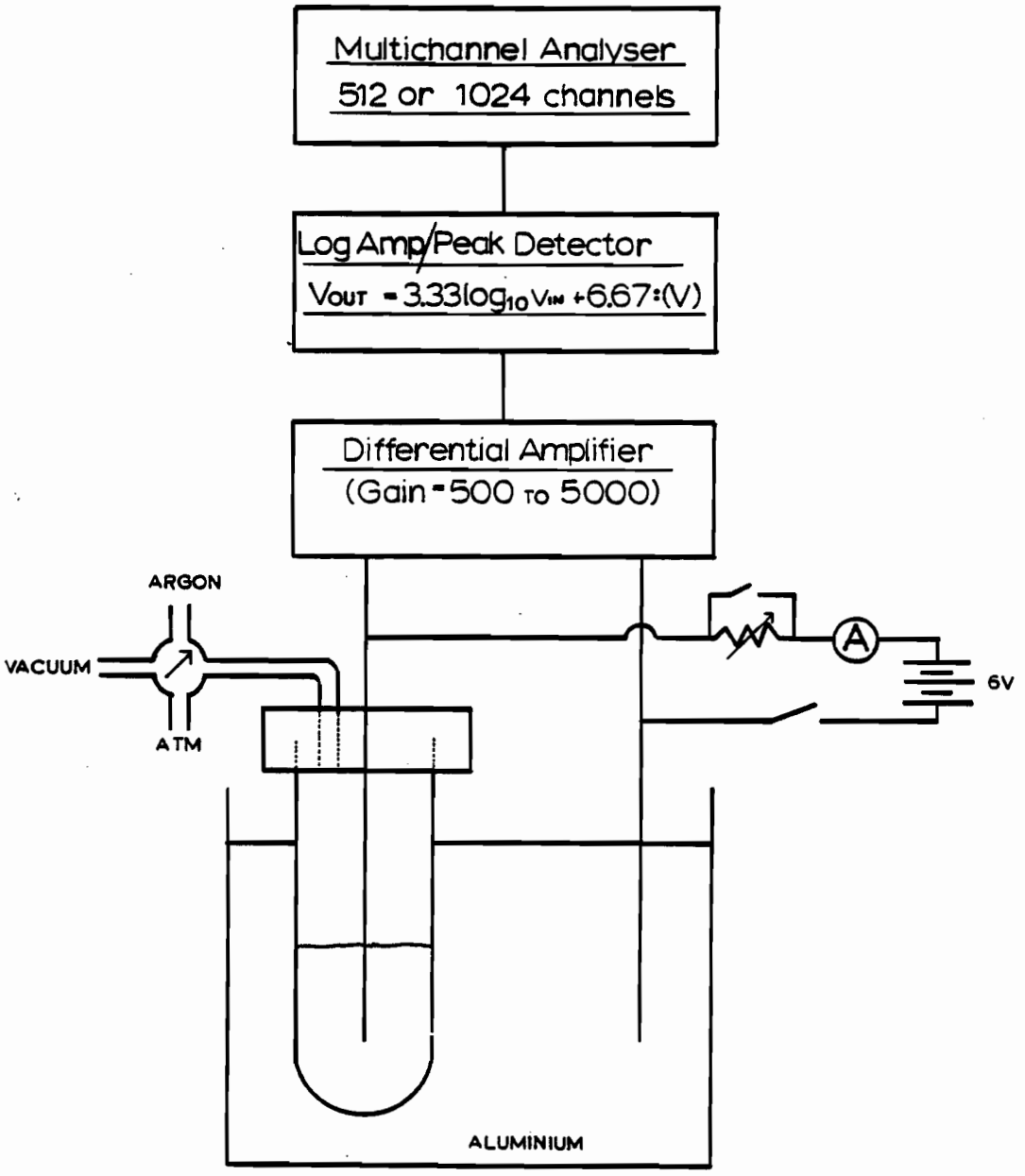

Figure 3: A schematic diagram of the LiMCA apparatus.

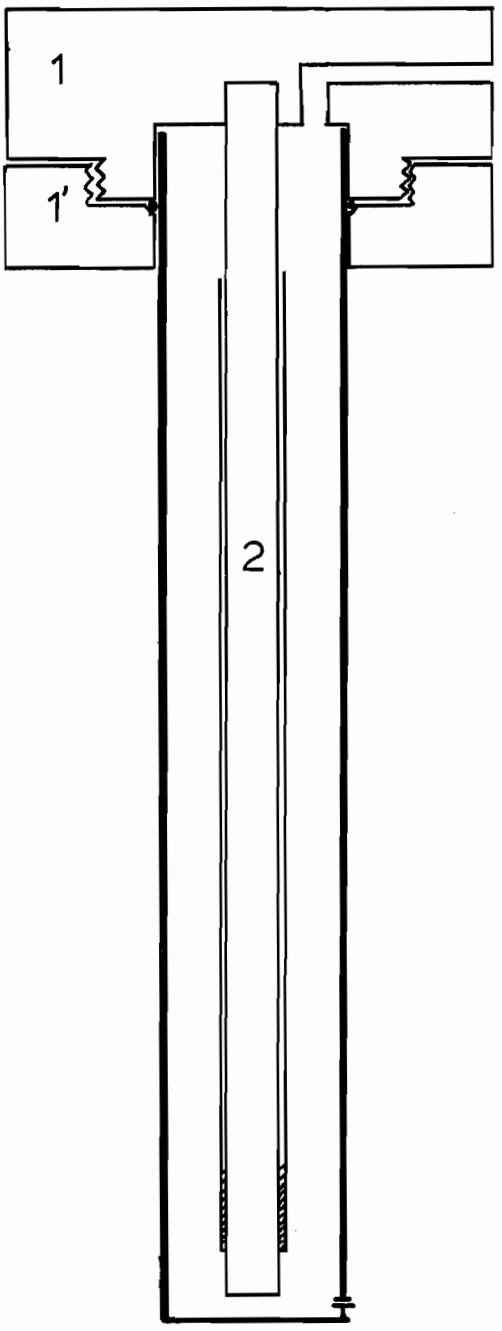

Figure 4: A cross sectional view of the sampling cell holder (1,1') and of the sheathed current carrying electrode (2).

vacuum source. In order to avoid pulsatile flow, the vacuum source was a 10 l reservoir which was pumped down when necessary with a standard laboratory vacuum pump. The purpose of the argon was two-fold: 1) it allowed the tube to be emptied under moderate positive pressure (15 kPa) and reused without having to remove the sampling assembly from the bath and 2) positive argon pressure was applied during the introduction of the tube into the melt to avoid entrainment of the surface oxide film across the orifice. The outlet to the atmosphere was included to permit neutral pressure to exist in the tube for safety during its removal.

Initially 25 mm diameter by 200 mm Kimax brand borosilicate culture tubes were used with orifice diameters ranging from 0.18 to 0.4 mm. These combined the advantages of being commercially available at low cost in closed tube form, reasonable chemical and thermal resistance to molten aluminium at temperatures up to 725°C and the ease with which the orifice could be produced in the wall of the tube. Vycor and Quartz tubes were tested but were difficult to fabricate, reacted more readily with the melt and were much more expensive than Kimax tubes. Pyrex brand borosilicate tubes were also tested but were found to be less heat resistant than Kimax brand tubes, collapsing after approximately 5 minutes exposure at 720°C.

4.2 Constant Current Power Supply

The power supply consisted of a 6 volt lead-acid battery (heavy-duty automative) with an appropriate ballast resistance. All connections were made with #4 gauge copper wiring (battery cables). The ballast consisted of one to ten 0.5 ohm 100 watt resistors mounted in parallel. This allowed the current to be adjusted in approximately 12 ampere increments over the range 12 to 90 amperes (at high currents the resistances of the other circuit elements, principally the cables and the electrodes, limited

the current). Two switches were installed, one to open the circuit after a test to avoid draining the battery while emptying the sampling tube between measurements, while the other was mounted in parallel with the ballast resistors allowing the battery to be short-circuited through the sampling cell. The latter was used to provide an intense current, 200 to 300 amperes, through the orifice to ensure that the walls were wetted by the aluminium and to burn out any material partially blocking the orifice. This was generally necessary at the beginning of each run.

The current could be controlled by changing the ballast resistance and was monitored with a 0-100 A DC ammeter. This allowed the value of I for equation (21) to be measured and gave an indication as to when the batteries needed recharging. The batteries were recharged when necessary with a 6 V heavy duty battery charger. All electrical cables were kept as short as possible and, when feasible, were twisted around one another to minimize noise pickup.

4.3 Voltage Pulse Measurement System

Referring to Figure 3, each time a particle passed through the measurement volume a voltage pulse was generated. The voltage difference between the two feeder electrodes was carried to the oscilloscope input along RG-59 U co-axial cables. The shield of each cable was grounded at the oscilloscope input, the two cables were twisted around one another and further shielded within a flexible braided wire sheath also grounded at the oscilloscope. The oscilloscope used was a Tektronix model 5223, 10 MHz digitizing storage scope equipped with a model 5A22N differential amplifier with switch selectable high and low pass RC filters and a model 5B10 digital time base. The oscilloscope was used both to observe the stability of the baseline and the voltage pulses and as a pre-amplifier. When used as a

pre-amplifier the oscilloscope provided a fixed output of 50 mV per screen division. Normally the instrument was used at a setting of 50 μV per division, in which case the pre-amplifier gain was 1000 (gains of up to 5000 could have been used by increasing the input sensitivity).

By using an AC coupled differential amplifier the voltage drops due to the resistances of the electrodes and the stable component of the orifice voltage were ignored and only the changes in voltage occurring within the frequency "window" between the high and low pass filters were amplified. The high and low pass filters were normally set at 0.1 and 10 kHz respectively to eliminate both high and low frequency noise.

The pre-amplified signals were then fed to a Tracor-Northern model TN 1214 logarithmic amplifier whose output response was:

$$V_{out} = 3.33 \log_{10} (V_{in}) + 6.67 \quad \text{(volts)}$$

Using a logarithmic amplifier had the effect of increasing the resolution in the lower ranges of particle sizes. In addition to serving as a logarithmic amplifier this instrument also served as a peak detector which used a "sample and hold" circuit to generate short (2 μs) voltage pulses from the relatively long (ca 500 μs) peaks produced by the passage of the particles. These short duration pulses were required in order for a conventional multi-channel analyzer (MCA) to be able to process the signals. (Most MCAs are designed for use in applications such as X-ray fluorescence where the pulse duration is extremely short).

The multichannel analyzer used was a Tracor-Northern model 1206. This device had a 10 bit analogue to digital converter which divided a 0-8 volt input range into 1024 equal channels and counted up to 10^6 - 1 events per channel at overall count rates of >1 MHz. Alternatively the memory

could be partitioned into two 512 channel portions allowing two distributions to be obtained before having to record them. The MCA thus provided a 512 channel histogram of particle number versus channel number. Each channel of the MCA corresponded to a unique particle size range depending upon the experimental conditions chosen. The correspondence between the particle diameters, d, and the channel numbers was calculated as follows:

The original signal appearing across the orifice was

$$\Delta V = \frac{4\rho\ I d^3}{\pi\ D^4}\ f(d/D) \tag{21}$$

This was amplified by the oscilloscope with a gain of G:

$$\Delta V^1 = G\ \Delta V \tag{22}$$

Then fed to the logarithmic amplifier whose output, ΔV^{11}, was

$$\Delta V^{11} = 3.33\ \log_{10}(\Delta V^1) + 6.67 \tag{23}$$

And finally appeared as a count in channel number, #:

$$\# = \Delta V^{11} \times \frac{512}{8} \tag{24}$$

Therefore, once the operating conditions for any particular experiment were determined (current, pre-amplifier gain, orifice diameter) the channel numbers corresponding to the particle diameters were fixed.

Since 512 channels provided more precision than was justified or desired, normally the sums of counts between channels corresponding to fixed intervals were taken. For instance under conditions of I = 60 amperes, G = 1000 and D = 300 μm the following correspondence between channel number and particle diameter exists (Table 3).

TABLE 3

CORRESPONDENCE BETWEEN THE CHANNEL NUMBERS OF THE MULTICHANNEL ANALYZER AND THE PARTICLE DIAMETER

(Equation (24) I = 60 A, G = 1000, D = 300 μm, fluid = aluminium)

Channel Numbers	Particle Diameters (μm)
0 - 60	16 to 20
61 - 122	20 to 25
123 - 172	25 to 30
173 - 215	30 to 35
216 - 252	35 to 40
253 - 285	40 to 45
286 - 314	45 to 50
>315	>50

All counts appearing within desired limits were added using the "Region of Interest" option of the MCA. Alternatively the entire memory contents could be stored on magnetic tape for later recall.

5. EXPERIMENTAL

5.1 Preliminary Experiments in Gallium

Once the theoretical feasibility of detecting particles in molten metals had been established, the first step carried out was to search for voltage peaks in a low temperature liquid metal system. Gallium was chosen for these initial experiments for a number of reasons including:

1. Its low melting point (29.8°C).
2. Its ability to wet glass.
3. The relatively large quantity on hand (1 kg).
4. Its relatively low density (5900 kg/m^3).
5. The fact that its electrical resistivity in the liquid state is virtually the same as that of molten aluminium (24.8×10^{-8} Ωm and 25.0×10^{-8} Ωm respectively).

The advantages of points 1, 3 and 5 are obvious, point 2 (wets glass) suggested that it would be possible to disperse silica flour in the melt, while point 4 (low density) meant that there would be less tendency for the dispersed particles to float out than there would be in the case of, for example, mercury (ρ = 13500 kg/m^3).

The initial apparatus is shown in Figure 5. It consisted of a 10 cc hypodermic syringe with the needle removed and the protective sheath sealed into place. A piece of glass capillary tubing 1.3 mm long with an internal diameter of 160 μm was cemented with cyanoacrylate glue into a small hole passing through the base of the protective sheath. A current of four amperes was established using a six volt battery and two 3 Ohm resistors mounted in parallel. Contact leads were made with 12 gauge copper wiring, one lead being submerged in the melt while the other passed through a hole at the base of the syringe barrel. The voltage across the orifice was measured with the Tektronix 5223 oscilloscope described earlier.

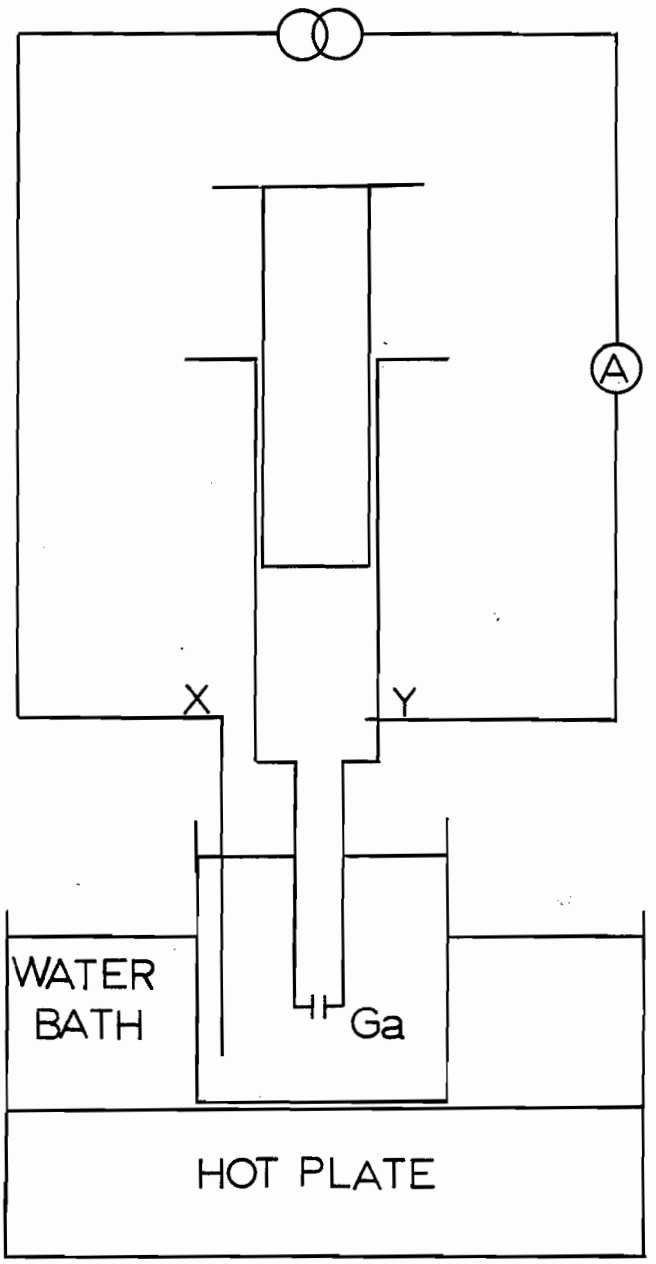

Figure 5: A schematic diagram of the apparatus used for preliminary experiments to demonstrate the feasibility of the technique in gallium. Voltage measurements were made between the points 'x' and 'y'.

Silica particles were dispersed in the melt (Silico-Sil 200, -200 mesh) and the suspension forced through the orifice by alternately with-drawing and inserting the syringe plunger. The peaks observed were stored in the oscilloscope's memory and photographed. Two of these peaks, typical of particles passing through an orifice, are shown in Figure 6.

Having established the practicality of the idea, the next two years were dedicated to overcoming problems involved in applying the principle to making measurements in molten aluminium.

5.2 Choice of Experimental Conditions for Aluminium

Equation (21):

$$\Delta V = I\Delta R = \frac{4\rho I}{\pi} \frac{d^3}{D^4} f\left(\frac{d}{D}\right)$$

predicts that the amplitude of the voltage pulses produced by the passage of non-conductive particles is:

- proportional to the applied current,
- inversely proportional to the fourth power of the orifice diameter,
- proportional to the particle volume.

The decision was made to aim for a particle detection limit of 20 μm (equivalent spherical diameter) while maximizing in so far as possible the orifice diameter (to maximize the sampling rate and to reduce the chance of plugging). The conditions ultimately chosen thus represent a compromise between the detection limit, the sampling rate and the size of the current supply system. Since the measurement of unusually small amplitude signals was involved, much effort went into eliminating electrical noise pickup in the circuit. The final conditions chosen were:

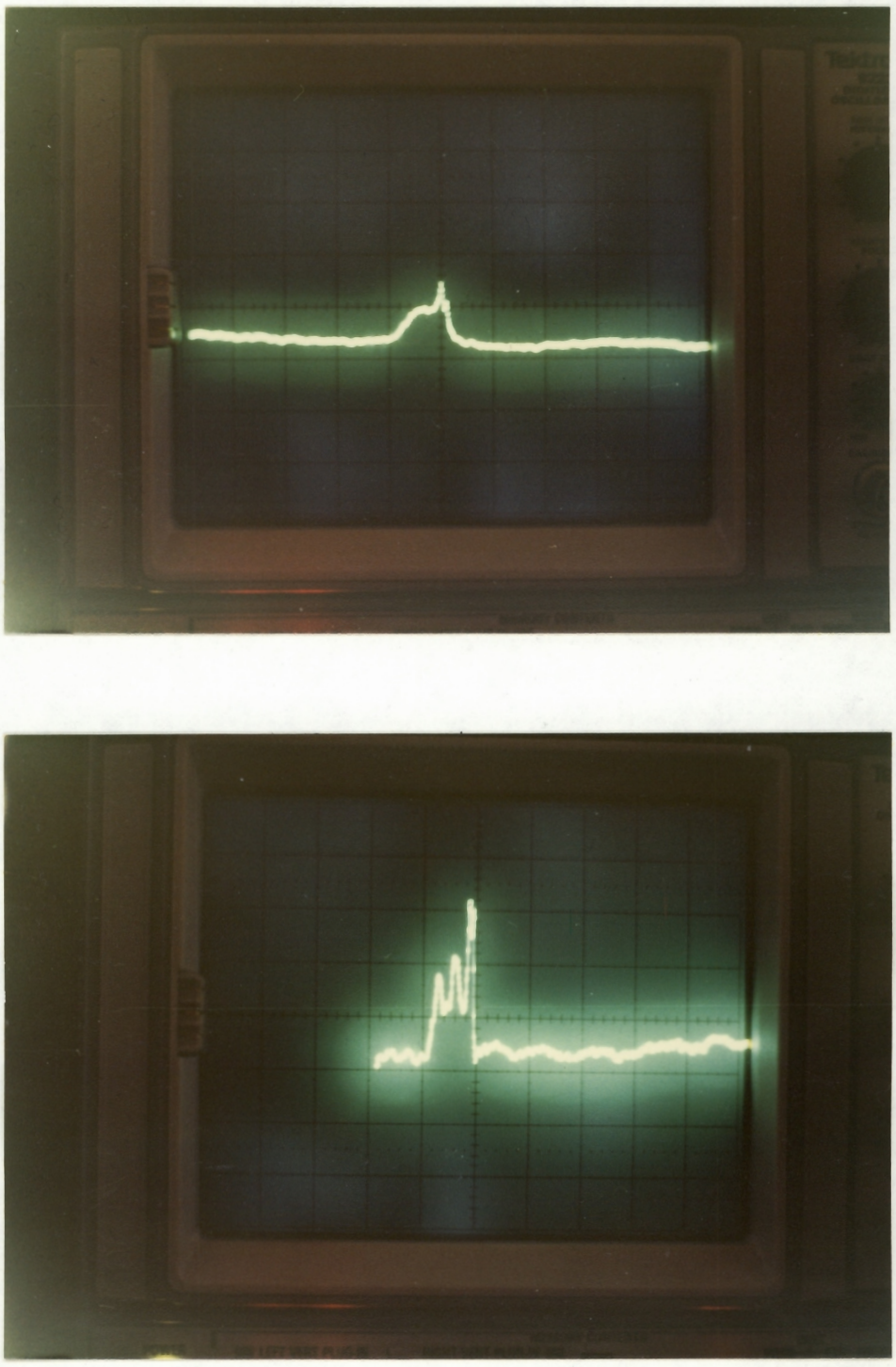

Figure 6 Transient voltage increases caused by silica particles dispersed in gallium passing through a 160 μm orifice in the presence of a current of 4 amperes. The vertical scale is 50 μvolts per major division; the horizontal scale is 1 ms per major division.

orifice diameter	300 μm
current	60 amperes
pre-amplifier gain	1000

under these conditions a particle 20 μm in diameter produced a voltage pulse of 19 μV compared to a typical background noise level of 5 μV (peak to peak).

5.3 Development of the Sampling Cell

As mentioned in the APPARATUS sections, KIMAX brand borosilicate culture tubes offered satisfactory thermal and chemical resistance to molten aluminium combined with ease of fabrication of the orifice. A number of methods for producing small holes in glass tubes were attemped, including*

1. drilling relatively large holes (0.6 mm) with a carbide dental bur and heat shrinking the holes to the desired diameter;
2. drilling the holes using diamond coated micro-drill bits;
3. cutting the hole with a micro-torch.

Drilling the holes with a micro-drill was by far, the quickest method (ca. 30 seconds/tube), however the reproducibility of the orifice diameters was poor. Method 1 (heat shrinking), while more time consuming (ca 5 min/ tube), produced uniform orifices with smooth surfaces and tapered (trumpet shaped) entrances and exits. This shape of orifice has been shown to be useful in avoiding distorted peaks in conventional resistive pulse particle size analysers [34]. Method 3 involved heating a small zone at the base of the tubes while applying pressure to the inside of the tube with a blow pipe.

---

* A review of methods to produce small holes in glass and ceramic materials appeared in Rev. Sci. Inst. V. 48, p. 64.

This method produced orifices similar in form to those produced using method 1 but required more skill.

The sampling tubes were routinely produced by the author using method 1 and later, by M. Bédard of the Société d'Électrolyse et de Chimie Alcan using method 3.

5.4 Development of the Electrodes

In order to obtain the sensitivity required, large currents had to be carried into the aluminium bath. The final electrode design is shown in Figure 4. The glass sheath was used to ensure a constant area of contact in order to avoid the noise that was sometimes caused by changes in the metal level when the electrodes were not sheathed. (The resistance of the electrodes, though small, was not negligible, without the sheath the circuit resistance changed as the metal rose in the sampling cell.)

In order to ensure good electrical contact between the electrodes and the metal, oxidation of the electrode surfaces had to be avoided. With new electrodes this was done by applying a flux and coating the exposed surface areas with solder. This layer melted off during first use and in subsequent runs the layer of aluminium adhering to the electrodes protected the interface from oxidation.

Towards the end of the project it was discovered that well wetted steel electrodes could be prepared by an initial immersion in aluminium at 900°C. This procedure was carried out in a small table top furnace with the molten metal covered with approximately 20 mm of a molten salt flux (50/50 (weight) NaCl/KCl). The electrodes were brushed to remove loose rust and held in the furnace for five to ten minutes at 900°C. Using these "well-wetted" electrodes it was found that the glass sheathing was not always necessary. At the time of writing this question is still unresolved, although for most work the sheathing has been retained.

Other electrode materials tried included:

- copper, which dissolved too rapidly to allow more than two or three samples to be taken before the electrodes had to be replaced;
- titanium, which performed satisfactorily but not better than steel electrodes;
- copper rods tipped with steel or titanium and sheathed so that only the tip was exposed to the metal, however, upon repeated use the tips tended to loosen which resulted in a poor contact and consequently the generation of excessive electrical noise;
- stainless steel (304 and 316), which performed satisfactorily but, owing to their high resistivity, limited the current.

Thus no material was found which had any clear advantage over steel as the electrode material.

Although the steel electrodes were slowly attacked by molten aluminium it was found that they could be used for periods of up to ten hours before replacement was necessary.

6. RESULTS AND DISCUSSION

6.1 Observations in Molten Aluminium

Typical voltage peaks observed while aspirating molten aluminium under the following conditions are shown in Figure 7:

Orifice diameter	0.30 mm
Current	60 amperes
Metal temperature	705°C
Pre-amplifier gain	1000
Low and high pass filters	0.1 and 10 kHz

It can be seen that the signals are well defined with respect to the background noise level. These signals were obtained in remelted, commercially pure (99.7%) aluminium. Supporting evidence for the contention that these signals are the result of particles suspended in the melt includes:

1. All signals were of the predicted polarity.
2. All signals were of the predicted duration.
3. If the current was switched off no signals were observed.
4. Stirring the melt or adding dirty metal (e.g. scalper chips) increased the number of observed signals.
5. Increasing the amplifier gain and/or the applied current increased both the size and numbers of the observed signals.
6. Signals of opposite polarity were observed when the metal was cooled to the melting point and stirred (solid aluminium is approximately 2 1/2 times more conductive at the melting point than liquid aluminium).

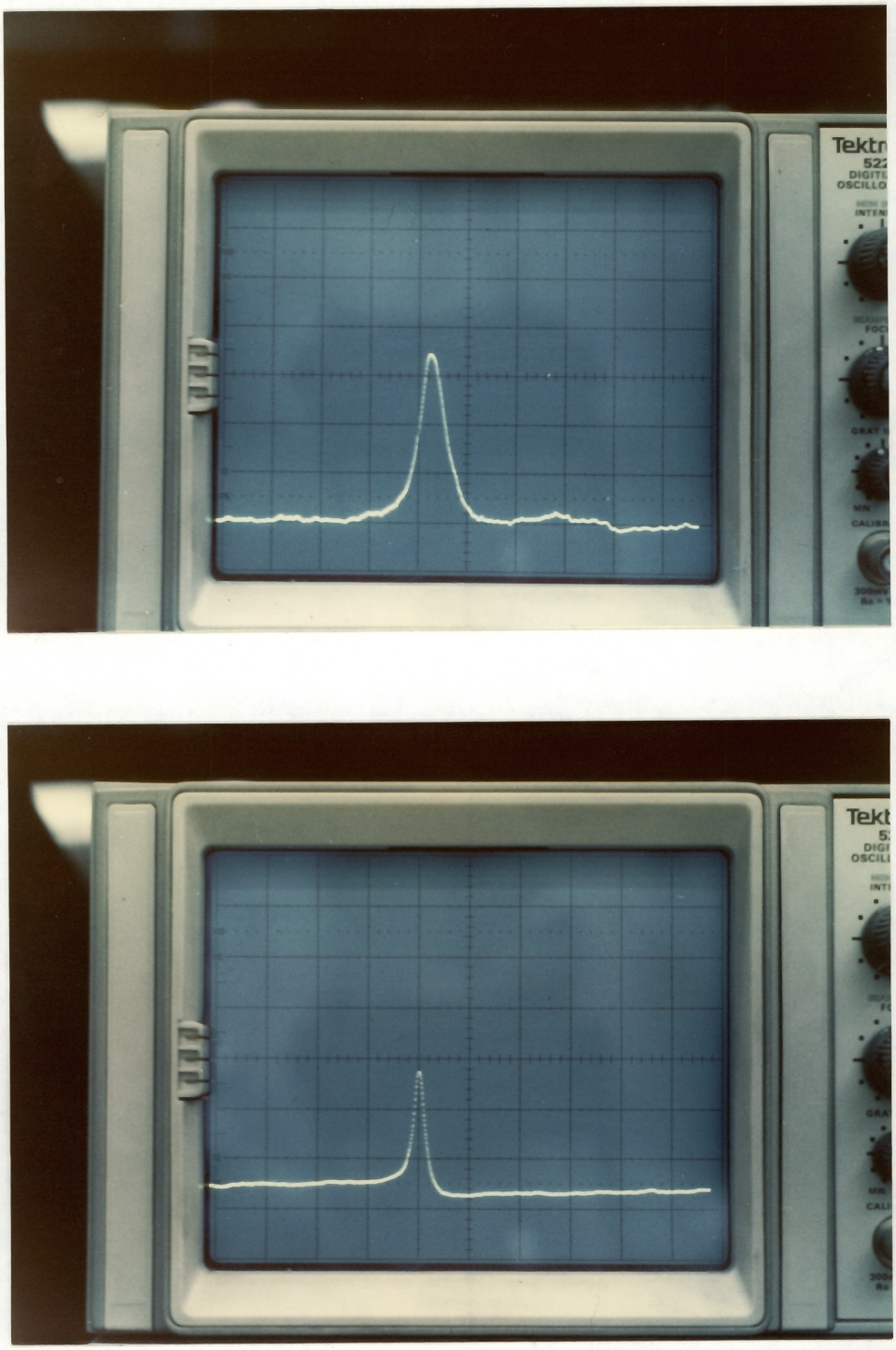

Figure 7 Typical signals observed while aspirating aluminium through a 300 μm orifice in the presence of an applied current of 60 amperes. The vertical scale is 50 μvolts per major division; the horizontal scale is 0.5 ms per major division.

7. Extensive testing, described in Part II, both in the laboratory and in the plant showed that there was excellent agreement between LiMCA results and those obtained by a metallographic method of metal cleanliness assessment.
8. Changing the metal flow rate changed the duration of the signals.

6.2 Orifice Stability

Due to the fourth-order dependency of the signal amplitude on the diameter of the orifice it was crucial that the sampling cell possess a dimensionally stable orifice. The dimensional stability of the orifices was verified by measurements before and after use. Tubes that had been used for periods of up to one hour in aluminium at 710°C were emptied, removed from the apparatus, wrapped in insulation and allowed to cool slowly to room temperature. Any adhering aluminum was dissolved with 30% W/V NaOH or 6 N HCl before measurement. The results are shown in Table 4.

Figure 8a shows a scanning electron micrograph of the area around the orifice in an unused KIMAX sampling tube. Figure 8b shows the same zone in a tube that had been used for 90 minutes in aluminium at 710°C. These figures and the results of Table 4 indicate that although some surface erosion had occured there were no major changes in either the shape or the dimensions of the orifices in the KIMAX sampling tubes. On the other hand Vycor brand (96% SiO_2) and quartz (>99% SiO_2) tubes eroded rapidly presumably due to their high free silica content which led to their being chemically reduced by the aluminium.

a)

b)

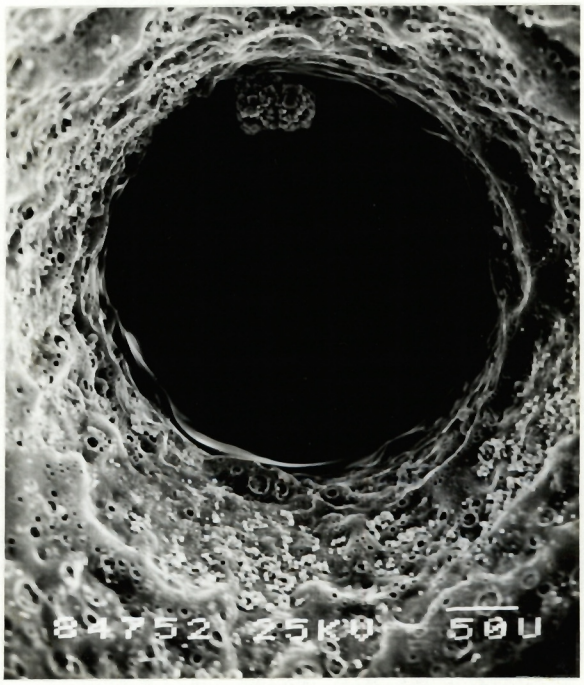

Figure 8 Scanning electron micrographs of the orifice in borosilicate (KIMAX) tubes a) before use and b) after one hour of use in aluminium at 710 °C.

TABLE 4

EVALUATION OF THE DIMENSIONAL STABILITY OF ORIFICES IN SAMPLING TUBES MADE OF KIMAX (BOROSILICATE) GLASS, VYCOR AND QUARTZ

Material	Immersion Time in Al, minutes	Cleaning Agent	D before µm	D after µm
KIMAX	0 (Control)	NaOH	240	250
"	0 (Control)	HCl	300	300
"	30	NaOH	280	270
"	45	NaOH	290	270
"	30	NaOH	300	300
"	60	NaOH	290	295
"	60	HCl	300	300
"	60	HCl	290	300
"	60	HCl	305	305
"	60	HCl	300	300
Vycor	0 (Control)	NaOH	300	300
"	10	NaOH	300	400
"	10	NaOH	300	340
Quartz	0 (Control)	NaOH	320	320
"	30	NaOH	315	380
"	30	NaOH	300	360

6.3 Sample Volume

In order to obtain quantitative inclusion concentration measurements, some means was required of assuring that the same volume of metal analyzed during each sampling cycle. To this end a two electrode on/off level detector was built and installed. Its principle of

operation was as follows. During sampling the metal rose within the sampling tube and when the level reached the lower limit electrode the potential between it and the current carrying electrode fell to zero. This change in potential activated the mutichannel analyzer which then began to acquire data. After a pre-determined volume of metal had been sampled, the level reached the upper limit electrode, again causing a change in potential between it and the current carrying electrode which stopped the data acquisition.

Unfortunately this system did not work reliably in molten aluminium because the surface skim tended to stick to and hang from the limit electrodes thus changing their effective lengths, and thus the sample volume. Because of this difficulty, this approach was abandoned and instead measurements were taken over a fixed period of time while maintaining a constant low pressure in the sampling cell by means of a vacuum reservoir.

The contention that, at constant differential pressure, the amount of metal sampled over a fixed period of time was constant, is supported by the results presented in Table 5. For these tests, water was aspirated into a series of tubes of orifice diameter 300 ± 10 μm for a period of one minute. These results indicate that the error associated with the assumption of a constant sample volume was valid to better than +/- 10% error, i.e. $\frac{2xS_3}{V} \times 100$

TABLE 5

REPEATABILITY OF THE VOLUME OF WATER

ASPIRATED IN ONE MINUTE BY 6 SAMPLING TUBES

Dia. (mm)	Volume (ml)	Ave. ± S.D. (S_2)
0.30	23, 24, 24, 24, 23	23.6 ± 0.55
0.30	24.5, 25, 24.5, 25, 24.5	24.7 ± 0.27
0.31	26.5, 25.5, 23, 26, 26	25.4 ± 1.38
0.31	25.5, 25.5, 24.5, 25, 25	25.1 ± 0.42
0.29	23.5, 24, 24, 25, 24	24.1 ± 0.54
0.29	23, 22.5, 23, 23, 23.5	24.3 ± 1.0 (S_3)

For quasi-steady flow through a submerged orifice Bernoulli's equation for the discharge velocity (u, m/s) can be written in the form:

$$u = \left[\frac{2\ (\Delta P + \rho g\ \Delta h)}{\rho}\right]^{\frac{1}{2}} \qquad (25)$$

where ΔP is the differential pressure applied by the vacuum reservoir (Pa), ρ is the fluid density (kg/m^3), g is the acceleration due to gravity (m/s) and Δh the difference in the fluid levels outside and inside the tube. The latter term varies (decreases) as the fluid rises within the tube. Numerically however, the ΔP term dominates and as an approximation, Δh has been taken as half the depth of submergence of the orifice and a constant filling rate assumed.

Multiplying (25) by the area of the orifice and substituting the appropriate numerical values gives the theoretical volumetric flow rate:

$$Q_{th} = Au=(150 \times 10^{-6})^2 \pi \left[\frac{2 \times [16920 + 0.05 \times 9.81 \times 1000]}{1000}\right]^{\frac{1}{2}} \quad (26)$$

$$\times 60 \times 10^{-6} = 25.0 \text{ mL/min}$$

The coefficient of discharge (C_D) for these orifices was thus

$$C_D = \frac{Q \text{ actual}}{Q \text{ theoretical}} = \frac{24.3}{25} = 0.97 \quad (27)$$

This allows an estimate of the volume of aluminium sampled per minute under similar conditions to be made:

$$Q_{Al} = C_D A \left[\frac{2(\Delta P + \rho_{Al} \Delta h)}{\rho_{Al}}\right]^{\frac{1}{2}} \times 60 \times 10^{-6} = 16 \text{ mL/min} \quad (28)$$

6.4 The Resistor By-pass (conditioning) Effect

The most unexpected discovery made during the course of the development of the LiMCA was the beneficial effect of briefly short-circuiting the battery through the orifice. Under these conditions the current was limited only by the resistances of the battery, cables and steel electrodes and was of the order of 200 to 300 amperes. When this was done the baseline voltage could be stabilized and any obstructions to metal flow through the orifice removed. It is hypothesized that these beneficial effects were due to intense localized heating of the metal in the orifice which ensured complete wetting of the orifice wall by:

a) removing any adsorbed gases,

b) accelerating the reaction between the aluminium and the silica in the glass making the surface more easily wettable, and

c) lowering the viscosity of the metal and lowering the contact angle, both of which promote the wetting and removal of any inclusions sticking to the orifice wall.

This procedure was carried out routinely each time a new sampling cell was first used and performed when necessary (as evidenced by decreased flow rates or baseline instability) thereafter. Figure 9 shows waveforms recorded before and after "conditioning" a new orifice. It is hypothesized that the damped oscillation observed in Figure 9a was the result of incomplete wetting of the wall of the orifice leading to the formation of a free jet of metal within the orifice; the passage of the particle through the orifice then disturbed the metal jet profile leading to the observed oscillation. The signal shown in 9b was recorded using the same sampling tube a short while later after having "conditioned" the orifice by the application of a brief, intense current.

6.5 Other Metals

The resistive pulse technique should, in principle, be applicable in all metals. Having successfully observed the predicted signals in gallium and aluminium, trial runs were performed in the laboratory using molten zinc and molten lead. Since the melting points (420°C and 327°C respectively) and the chemical "aggressivity" of both these metals are significantly lower than those of liquid aluminium no problems were encountered in using the sampling tubes previously described.

In the case of zinc, tests were performed in a 2 l crucible at 460°C using an orifice diameter of 0.40 mm and a current of 60 A. Tests with lead were conducted at 400°C using an orifice diameter of 0.30 mm and a current of 60 A. Signals similar to those seen in aluminium were observed

a)

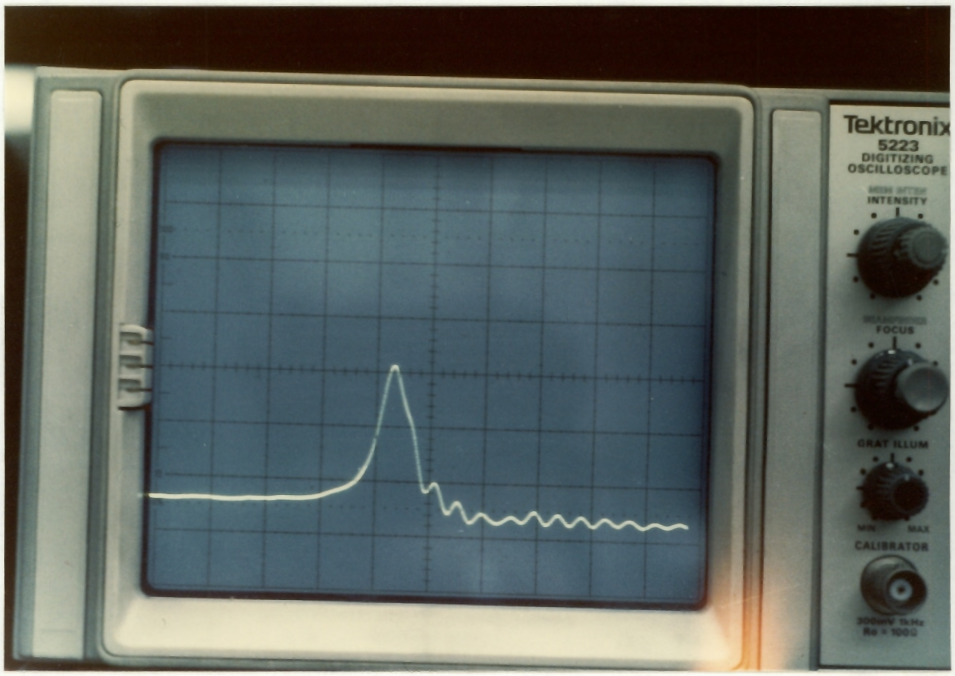

b)

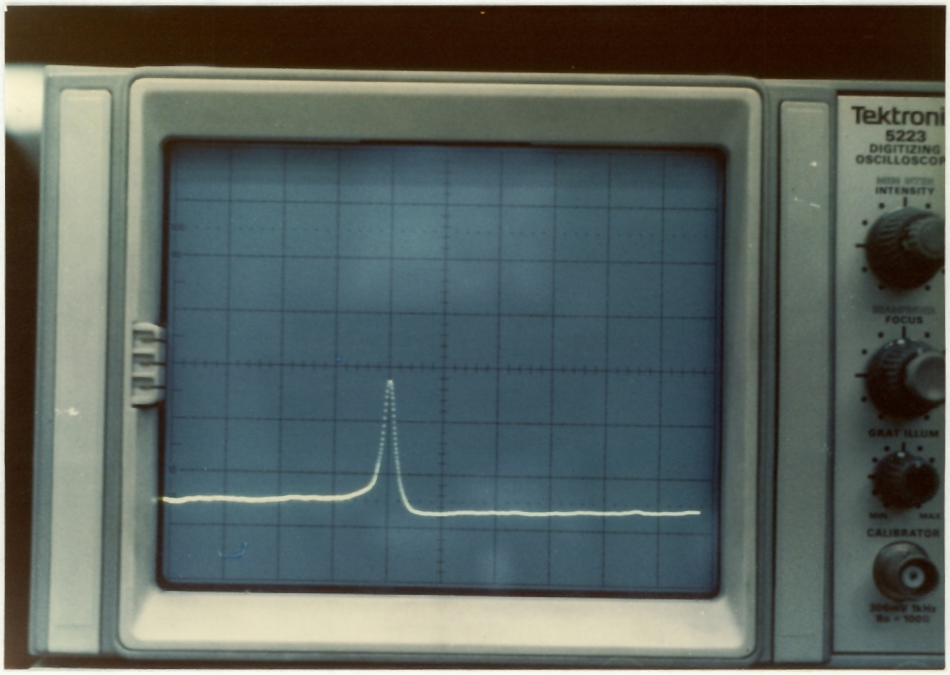

Figure 9 The "Conditioning" Effect. The waveform "a" was recorded using a new sampling cell. After passing 200-300 amperes through the orifice briefly the same sampling cell produced signals of the form "b". The vertical scale is 50 μvolts per major division; the horizontal scale is 1 ms per major division

and in both cases no degradation of the sampling cell occurred. The count rates observed , the corresponding equivalent spherical diameters (Eq. 21 and 24) and the estimated volumetric sampling rates for each metal are shown in Table 6.

TABLE 6

APPLICATION OF THE LiMCA APPARATUS IN MOLTEN LEAD AND ZINC

Particle equivalent spherical diameters (d) were calculated using equations 24, 23, 22 and 21. Metal flow rates were estimated using equation 28.

Channel Number	LEAD		ZINC	
	d (μm)	CPM	d (μm)	CPM
61-122	13-15	131	27-34	97
123-172	16-18	54	35-40	43
173-215	19-21	17	41-46	11
216-252	22-24	8	47-53	5
253-285	25-27	3	54-59	3
286-314	28-30	1	60-65	1
>315	> 30	3	> 65	2
	I = 60 Amps D = 300 μm Q ≈ 9.2 ml/min		I = 60 amps D = 400 μm Q ≈ 13 ml/min	

Based upon these observations it appears that there are no major problems to be overcome in applying the technique to other, low melting point metals and alloys.

7. DISCUSSION

The resistive pulse method of particle size analysis was initially developed by Coulter in the early 1950's. Since then, it has been widely used in aqueous and organic systems. While the LiMCA is based upon the same principle, a number of special problems were encountered in its application in molten metals. The most obvious difficulties lie in the hostile thermal and chemical environment encountered in most liquid metal systems which necessitated the development of a heat resistant sampling cell. A more fundamental problem arose from the resistivities of the fluids involved. As shown by Equation 21 the signal amplitude is proportional to the resistivity of the fluid. As Table 7 indicates, liquid metals are about one million times less resistive than the saline solutions commonly employed in conventional devices so that, for a given current, the signals produced in liquid metals are a million times smaller.

This disadvantage was partially overcome through the use of larger currents, 60 amperes versus milliamperes in conventional equipment.

A basic difference between conventional instruments and the one described herein lies in the mechanism of current conduction. This is electronic in liquid metals as opposed to ionic in saline solutions. As a result, problems of concentration polarization and noise due to gas evolution at electrode surfaces did not arise. In addition the orifice was submerged in a mass of molten metal which provided a nearly ideal Faraday's cage for minimizing noise pickup. The net effect of these differences was that background electrical noise proved to be substantially lower than that of conventional analyzers, allowing high gain amplifiers to be used for signal detection. For a signal to noise ratio of 2.0 the mininum detectable

TABLE 7

RESISTIVITIES OF MOLTEN METALS AND AQUEOUS ELECTROLYTES [36,37,38,39]

Fluid	Resistivity Ω·M	Temperature (°C)
Cu	2.2×10^{-7}	1084
Ga	2.48×10^{-7}	30
In	2.9×10^{-7}	157
Fe	13.9×10^{-7}	MP ~1540
Pb	9.79×10^{-7}	340
	10.1×10^{-7}	400
Mg	2.74×10^{-7}	650
Hg	9.84×10^{-7}	50
	10.3×10^{-7}	100
Rb	2.3×10^{-7}	122
Zn	3.53×10^{-7}	413
K	1.36×10^{-7}	64
Sn	4.5×10^{-7}	232
Cd	3.4×10^{-7}	400
Bi	12.9×10^{-7}	300
Ca	3.3×10^{-7}	839
Al	2.5×10^{-7}	700
.9% NaCl (Physiological Saline)	7.1×10^{-1}	25
0.1 N KCl	8.3×10^{-1}	25

signal was 10 μV corresponding under standard conditions (D = 300 μm, I = 60 A, G = 1000) to a particle of 14 μm equivalent spherical diameter. This was 4.7% of the orifice diameter, close to the value of 4% commonly quoted for conventional resistive pulse analyzers.

For a fixed orifice diameter the sensitivity can be increased by increasing the current. Currents as high as 100 A in 300 μm orifices were used without any noticeable problems. The major drawback with using higher currents lies in the shortened life of the batteries.

At 60 amperes the current density in a 300 μm orifice was 8.5×10^8 A/M^2 and the power density was 1.8×10^{11} W/M^3. This is roughly three orders of magnitude larger than the power densities developed in the core of a liquid metal fast breeder reactor. So long as the metal is flowing its residence time within the orifice, 0.5 m/sec, was short enough that the metal was heated by less than 1°C during is passage.

Comparing this technique to a common standard method of assessing metal cleanliness, filtration and metallographic examination of the residue, it should be noted that the latter typically requires approximately one man-hour of labour and provides a semi-quantitative result only after a substantial time delay. Once installed, the labour requirements of the LiMCA technique are minimal, involving positioning the sampling assembly and occasionally changing the sampling tube and the electrodes. The samples can be taken on line and the results are available in the form of particle size distribution histogram at approximately two minute intervals. Thus the technique has the potential of allowing "real-time" process control. In contrast, when current metallographic techniques are used, by the time the results are available, the product has been cast and is awaiting shipment in inventory. A further advantage of the LiMCA technique is that there is no human element involved in the assessment, so that problems of interpretation, boredom and fatigue are less likely to influence the results.

8. CONCLUSIONS

A resistive pulse method of particle size analysis has been developed for use in liquid metals. The technique is both more rapid and less expensive than currently used methods of metal cleanliness assessment. It provides both the concentration and particle size distribution of suspended particulates larger than a pre-determined size with the results available at approximately two minutes intervals.

A number of problems had to be overcome during the development of a workable apparatus these include the development of durable high temperature sampling cells, the production of small orifices in glassy materials and the measurement of small signals. The response of the device has been studied both in the lab and in plant trials. These studies are described in Part II of the present work.

REFERENCES

1. Langerweger, J., Nonmetallic Particles as the Cause of Structural Porosity, Heterogeneous Cell Structure and Surface Cracks in DC Cast Aluminum Products", Light Metals, The Metallurgical Society of AIME, pp 685-705, 1981.

2. Swedish Symposium on Nonmetallic Inclusions in Steel, H. Nordberg and R. Sandstrom Eds, Arranged by the Uddeholm Research Foundation, Swedish Institute for Metal Research, April 27-29, 1981.

3. Bengtsson, K., "Inclusions and Polishability", in Ref. 2 (above), pp 450-462, 1981.

4. Siemensen, C.J., "Gas Chromatographic Analysis of Carbides in Aluminium and Magnesium", Fresenius. Z. Anal. Chem., Vol. 292, pp 207-212, 1978.

5. Siemensen, C.J., "Sedimentation Analysis of Inclusions in Aluminium and Magnesium", Met. Trans. B, Vol. 12B, pp 733-743, 1981.

6. Dubé, G., Alcan International Ltd, Arvida Laboratories, Personal communication.

7. Levy, S.A., "Applications of the Union Carbide Particulate Tester", Light Metals, The Metallurgical Society of AIME, pp 723-733, 1981.

8. Dore, J.E. and Yarwood, J.C., "Ceramic Foam - A Unique Method of Filtering Molten Aluminium Alloys", Light Metals, The Metallurgical Society of AIME, pp 171-189, 1977.

9. Bates, D.A. and Hutter, L.C., "An Evaluation of Aluminium Filtering Systems using a Vacuum Filtration Sampling Device", Light Metals, The Metallurgical Society of AIME, pp 707-721, 1981.

10. Mollard, F.R., Dore, J.E. and Peterson, W.S., High Temperature Centrifuge for Studies of Melt Cleanliness", Light Metals, The Metallurgical Society of AIME, pp 483-500, 1972.

11. Bauxman, K., Bornand, J.D. and Leconte, G.B., "Impact of Purification Methods on Inclusions and Melt Loss", Light Metals, The Metallurgical Society of AIME, pp 191-207, 1976.

12. Hedjazi, Dj., Bennet, G.H.J. and Kondic, V., "Removal of Nonmetallic Inclusions and their Assessment of Al-alloy Melts", British Foundryman, Vol. 68 (12), pp 305-309, 1975.

13. Levy, S.A., Miller, J.C., McNanara, P. and Feitig, D.A., "Molten Metal Quality - Particulate Tests", Light Metals, The Metallurgical Society of AIME, pp 149-169, 1977.

14. Brondyke, K.J. and Hess, P.D., "Interpretation of Vacuum Gas Test Results for Aluminum Alloys", Trans. Met. Soc. AIME, Vol. 230, pp 1542-1546, 1964.

15. Silk, M.G., "Sizing Crack-like Defects by Ultrasonic Means", in Research Techniques in Nondestructive Testing, R.L. Sharpe Ed., Vol. 3, p 97 Academic Press, New York, 1977.

16. Pitcher, D.E. and Young, R.S., "Methods of an Apparatus for Testing Molten Metal", U.S. Patent, 3,444,726, May 20, 1969.

17. Mansfield, T.L., "Ultrasonic Technology for Measuring Molten Aluminium Quality", Light Metals, The Metallurgical Society of AIME, pp 969-980, 1982.

18. Chan, J.P., "Measurements of the Velocity of Sound in Liquid Aluminium to 1800 K", Chemical Abstracts, CA 75(22) 133242A.

19. Broom, D., Alcan International, Kingston Laboratories, Personal communication.

20. Anon, "Standard Practice for Determining the Inclusion Content of Steel", American Society for Testing Materials, Designation E45-81, 1981.

21. Lagneborg, R., Ekelund, S. and Werlefors, T., "Combined Image and X-Ray Analysis in Scanning Electron Microscope for Automatic Multiparameter Characterization of Nonmetallic Inclusions", in Clean Steel, Proceedings of the Second International Conference on Clean Steel, held on 1-3 June, 1981 at Balatonfüred, Hungary, pp 39-62, The Metals Society, London, 1983.

22. Flinchbaugh, D.A., "Use of a Modified Coulter Counter to Determine the Size Distribution of Macro-inclusions Extracted from Plain Carbon Steels", Anal. Chem., Vol. 43, No. 2, pp 178-182, 1971.

23. Chandler, H.E. "An Uptdate: What Users Should Know about Clean Steel Technology", Metal Progress, pp 25-32, October 1982.

24. Coulter, W.H., "High Speed Automatic Blood Cell Counter and Cell Size Analyzer", Proc. of the National Electronic Conf., 12, p. 1034, 1956.

25. DeBlois, R.W. and Bean, C.P., "Counting and Sizing of Sub-micron Particles by the Resistive Pulse Technique", Rev. Sci. Instr., Vol. 41, No. 7, pp 909-915, 1970.

26. Smythe, W.R., "Flow Around a Sphere in a Circular Tube", The Physics of Fluids, Vol. 4, No. 6, pp 756-759, 1961.

27. Smythe, W.R. "Flow Around a Sphere in a Circular Tube", The Physics of Fluids, Vol. 17, No.5, pp 633-638, 1964.

28. DeBlois, R.W., Bean, C.P. and Wesley, R.K.A., "Electrokinetic Measurements with Sub-micron Particles and Pores by the Resistive Pulse Technique", J. of Colloid and Interface Science, Vol. 61, No. 2, pp 323-335, 1977.

29. Anderson, J.L. and Quinn, J.A., "The Relationship between Particle Size and Signal in Coulter-type Counters", Rev. Sci. Instr., Vol. 42, No. 8, pp 1257-1258, 1971.

30. Gregg, E.C., and Steidly, K.D., "Electrical Counting and Sizing of Mammalian Cells, in Suspension", Biophys. J., Vol. 5, pp 393-405, 1965.

31. Maxwell, J.C., "A Treatise on Electricity and Magnetism (Clarendon, Oxford), 3rd Ed., Vol. 1, p 429, 1904.

32. Smythe, W.R., "Off-axis Particles in Coulter-type Counters", Rev. Sci. Instr., Vol. 43, No. 5, pp 817-818, 1972.

33. Davies, R., Karuhn, R. and Graf, J., "Studies on the Coulter Counter - Part II. Investigation into the Effects of Flow Direction and Angle of Entry of a Particle on Both Particle Volume and Pulse Shape", Powder Technology, Vol. 12, pp 157-166, 1975.

34. Kahrun, R., Davies, R., Kaye, B.H. and Clinch, M.J., "Studies on the Coulter Counter - Part I. Investigation into the Effect of Orifice Geometry and Flow Direction on the Measurement of Particle Volume", Powder Technology, Vol. 11, pp 157-171, 1975.

35. Spielman, L. and Goren, S.L., "Improving Resolution in Coulter Counting by Hydrodynamic Focusing", J. Colloid, and Interface Science, Vol. 26, pp 175-182, 1968.

36. Metals Handbook, 8th Edition, American Society for Metals, Metals Park, Ohio, 1961.

37. Metals Handbook, 9th Edition, American Society for Metals, Metals Park, Ohio, 1979.

38. Encyclopedia of Chemical Tehcnology, Kirk-Othmer, 3rd Edition, Wiley-Interscience, New York, 1978.

39. CRC Handbook of Chemistry and Physics, 57th Edition, CRC Press, Boca Raton, 1977.

LIST OF FIGURES

LIST OF TABLES

PART II

APPLICATIONS OF THE LiMCA

(Liquid Metal Cleanliness Analyzer)

ABSTRACT

The object of the second part of this study was to evaluate and demonstrate the performance of the Liquid Metal Cleanliness Analyser (LiMCA) in a variety of laboratory and production situations. Laboratory tests included measuring the effect of various additions on the inclusion content of aluminium and an off-line evaluation of two commercially available melt treatment units. Plant trials included monitoring metal cleanliness during the production of an inclusion-sensitive alloy (can body alloy AA3004B), electrical conductor grade aluminium and extrusion ingot alloy. The settling of inclusions was found to have a profound influence on melt cleanliness in all situations studied. The response of the LiMCA was compared to those obtained using a metallographic technique (the Alcan PoDFA test) and, despite the fundamental difference of the basis of the two techniques, both responded similarly to changes in metal cleanliness.

1. INTRODUCTION

As stated in the introduction to this thesis, Part Two is concerned with the application of the liquid metal cleanliness analyser (LiMCA) whose development was described in Part One. Experience has shown that it is extremely difficult to manipulate aluminium on a small scale without producing large quantities of suspended oxide films which are rarely encountered in metal prepared on a production scale. Thus, once basic problems of materials and electronic noise with the instrument had been overcome in the lab, it was considered highly desirable to proceed directly to in-plant experiments in order to avoid the qualitative difference observed in laboratory metal and to study the actual inclusions present in industrial material that give rise to the problems mentioned in the introduction to Part One.

1.1 Previous Work

It has been widely recognized that progress in the field of metal cleaning has been hampered by the lack of a reliable, quantitative method of evaluating metal cleanliness.

In a critical review of the literature concerning the fluxing of aluminium with salts and gases Siemensen[1] stated (p 35) "Most of the work carried out so far in measuring the effect of fluxing gas or salt upon the inclusions content, is qualitative, incomplete and/or not systematic. The main reason is the lack of quantitative methods for analysing low concentrations of particles in huge quantities of liquid metal."

Bauxman et al[2] in a 1978 paper stated "The lack of adequate methods to count and identify inclusions in cast products makes difficult

the assessment of the efficiency of melt cleaning practices."

Finally, Levy[3] et al in a 1977 review of methods for evaluating metal cleanliness state:

> "The goal is a sensitive, accurate test, readily performed on the cast house floor, which might allow ingots to be segregated according to their ultimate quality potential and to investigate process modifications such as in filtering or fluxing. As there is no ultimate reference standard, one is forced to determine such factors as i - reproducibility of the data from replicate samples, ii - reasonableness of the data ...."

Thus, since the instrument described in Part One was specifically designed in order to provide a quantitative evaluation of the inclusion level of molten aluminium, there was virtually no prior body of knowledge directly relevant to the present work.

Apart from the "common sense" approach mentioned by Levy et al (above) the only 'yard stick' available for evaluating the LiMCA was the PoDFA technique that had been used and developed by Alcan personnel over the last 10-15 years. As mentioned previously the PoDFA technique involves filtering a known mass of metal, typically 1-1.5 kg, through a porous disc and examining the residue captured on the surface of the disc under the optical microscope. The discs are selected, based upon their permeability so as to be selective for the capture of all particles larger than approximately 20 μm. PoDFA results are expressed as a single number

(mm^2/kg) representing the area of inclusions observed in a section passing perpendicularly through the center of the face of the disc. Due to the limited quantity of the concentrate and the low concentrations of inclusions in suspension in most commercial aluminium alloys, there are not enough particles present on the polished surface to allow any estimation of the particle size distribution. PoDFA does allow the various inclusion types to be identified and thus may provide a clue as to their origin, however, at any given casting center the major types of inclusions likely to be present are generally known and what is now needed is a rapid quantitative estimate of their size and concentration.

2. LABORATORY EXPERIMENTS

2.1 Particle Addition to Aluminium

Attempts to add particulate matter of known dimensions to molten aluminium for the purpose of instrument calibration were unsuccessful. Materials tried included silica powder, calcined alumina, glass microspheres and titanium diboride. Addition methods attempted included stirring, adding the powders into the eye of a vortex, wrapping the particles in aluminium foil and holding them beneath the surface while the foil melted back and salt coating the particles (NaCl/KCl/NaF 45-45-10 W/W). Attempts were also made to decrease the surface tension of the melt prior to adding the particles by overheating the melt ($900^{o}C$) and by adding metallic copper (1-4% W/W). In all cases metallographic examinations of

chill plates revealed no suspended particles although large quantities of oxide films were often present.

The only method found that allowed "dirty" metal to be prepared in the laboratory was the addition of a boron-rich (5% B) aluminium alloy to commercial grade aluminium. The added boron reacted with dissolved titanium and vanadium, present in commercial-grade aluminium, to precipitate (Ti-V)B particles in sizes ranging up to 50 μm in diameter. Table 1 shows the effects of boron addition, settling and stirring on melt cleanliness and was obtained as follows: Commercial-grade aluminium (99.7% Al) was melted and held in a 100 kg resistance furnace for six hours (A). The melt was stirred (B), settled for two hours (C) and treated with a 20 ppm W/W addition of boron stirred into the melt (D). Following subsequent stages of settling and stirring (E through I) a second addition of boron was made (J) followed by a final period of settling and stirring (K-M). Throughout the experiment the instrumental settings of the LiMCA were as follows:

Orifice Diameter	:	0.30mm
Current	:	60 Amperes
Pre-amplifier Gain	:	1000
Differential Pressure	:	5" Hg (16.8 kPa)
Region of Interest	:	Channels 61 to 510
(Detection Limit)	:	(d >20 μm)

All pulses corresponding in magnitude to particles of at least 20 micrometers in equivalent spherical diameter (d) were recorded. Metallographic examination of chill plates taken after the boron additions subsequently confirmed the presence of (Ti-V)B particles in the predicted size range (20 to 50 μm).

TABLE 1

EFFECT OF BORON ADDITIONS, SETTLING AND STIRRING ON THE CLEANLINESS OF COMMERCIAL GRADE ALUMINIUM

	PROCESS OPERATIONS	RESISTIVE PULSE READING (total counts per minute $d > 20\ \mu m$)
A	Metal held at 700°C for 6 hours	32
B	Melt stirred	305
C	A 2 h settling period allowed	108
D	A 20 ppm addition of boron stirred into melt	2750
E	Following a 5-minute settling period	847
F	Melt stirred	2767
G	Following a 50 minute settling period	727
H	Following a 1-hour settling period	310
I	Following a further 1 hour, ten-minute period	295
J	An 85 ppm addition of boron stirred into melt	8405
K	Following a 10-minute settling period	3527
L	Following an overnight ($\sim$ 12 h) settling period	79
M	Melt stirred	2748

2.2 Book Molds

A second approach used to obtain "dirty" metal in the laboratory was to remelt samples taken during routine production runs. In order to ensure, insofar as possible, that the samples covered a wide range of cleanliness they were taken before and after two widely used melt treatment (cleaning) devices, the Alcoa 622 and the Union Carbide Spinning Nozzle Inert Flotation (SNIF) units. The samples also represented two very different alloys, in the case of the "622" samples the alloy was CA-54311, a high magnesium alloy prone to oxidation and in the case of the "SNIF" samples the alloy was AA-1350 which contains no magnesium.

The samples, rectangular blocks of aluminium (book molds) weighing approximately 2 kg were remelted in graphite bonded silicon carbide crucibles in a resistance furnace under an argon atmosphere. When the metal temperature had attained 750°C the samples were transferred one at a time, to a small cylindrical resistance furnace, stirred and four successive thirty-second LiMCA readings were taken over a period of approximately ten minutes. The experimental conditions were as follows:

Metal Temperature	:	700-720°C
Orifice Diameter	:	0.30 mm
Current	:	60 Amperes
Pre-amplifier gain	:	1000
Region of Interest (detection limit)	:	50-510 (d >19 μm)

After sampling each crucible was returned to the melting furnace and reheated to 750°C following which the metal was filtered through a porous disc and the residue examined metallographically (the Alcan PoDFA test).

Figure 1 shows the relation observed between the LiMCA readings (expressed as the sum of the four, thirty second readings for each sample) and the PoDFA results. The LiMCA values represent all counts that appeared above channel number 50 ($d > 19$ μm equivalent spherical diameter under the conditions used). It can be seen that, in general the two techniques are in reasonable agreement. The metallographic results indicated that the samples represented by the outlying point was heavily oxidized which may have affected the PoDFA test. Table 2 shows the total counts appearing above channel number 50 ($d > 19$ μm) for each thirty second sampling, as well as the alloy and the position, relative to the melt treatment device, at which the original 2 kg samples were taken.

Inspection of Table 2 shows that, as in the previous example, particle settling was occurring rapidly, since the fourth reading on each sample was typically two to four times smaller than the first. In addition oxide films and gas porosity were observed upon metallographic examination of the first six (high magnesium) samples indicating that, despite the argon flushing of the furnace some exposure of the samples to the atmosphere was occurring. For these reasons the results of Table 2 cannot be considered a definitive evaluation of the performances of the two melt treatment devices. However, the results do agree with what previous experience would have predicted: for instance, that alloys with high magnesium levels are generally "dirtier" than low magnesium alloys and that the SNIF unit which in this instance was being used as a degassing (hydrogen removal) device, would have had little or no cleansing effect on the metal.

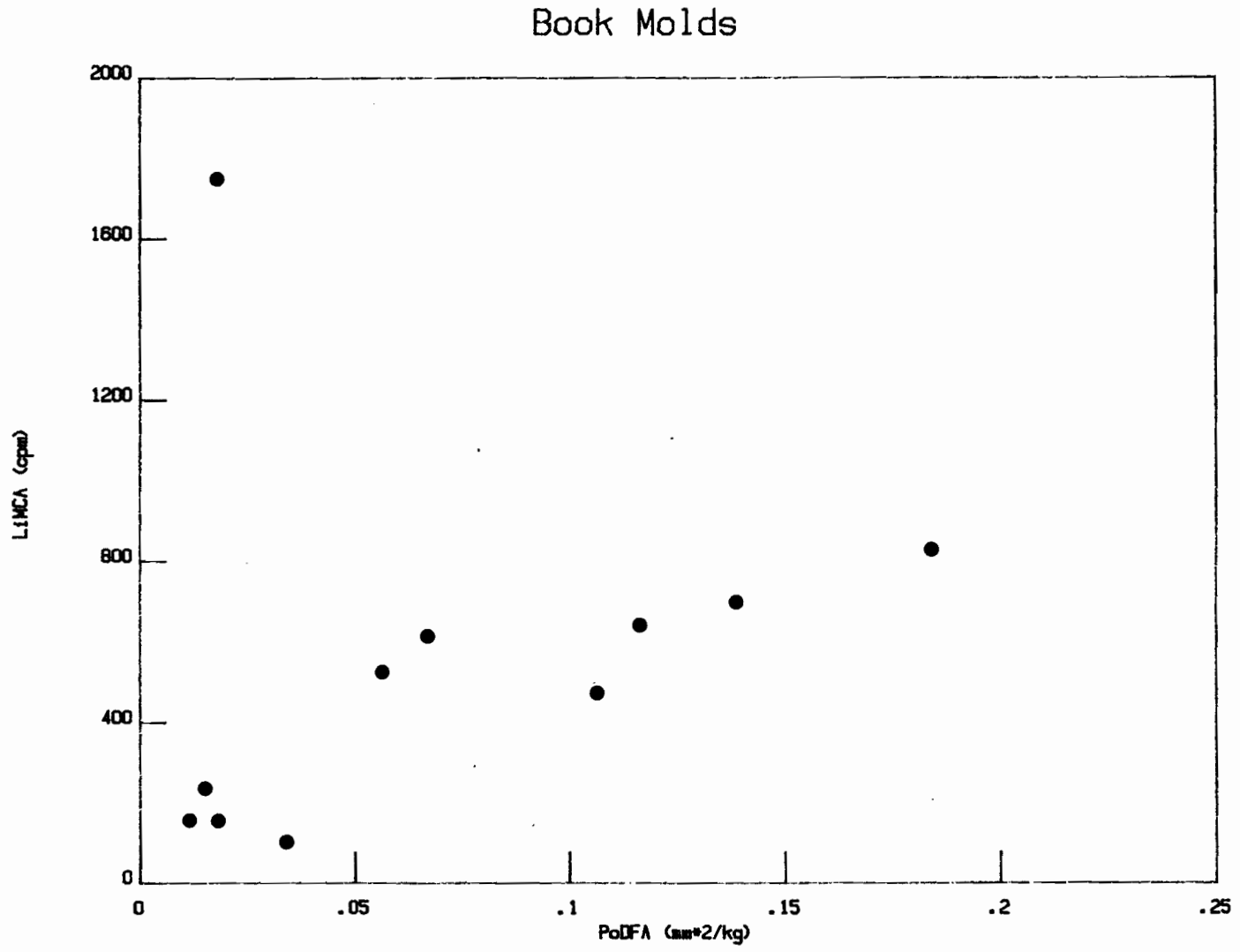

Figure 1: LiMCA (sum of four 30 second counts) as a function of PoDFA for eleven remelted samples taken before and after two melt treatment devices.

TABLE 2

LiMCA AND PoDFA RESULTS OBTAINED UPON REMELTING SAMPLES TAKEN BEFORE AND AFTER TWO MELT TREATMENT DEVICES. FOUR 30 SECOND LiMCA SAMPLES WERE TAKEN AT APPROXIMATELY 3 MINUTE INTERVALS

Alloy	Treatment Unit	Position	Sample				Total Σ 1 to 4	PoDFA mm^2/kg
			1	2	3	4		
CA-54311	Alcoa 622	Before	310	175	191	157	833	0.18
"	"	After	189	116	85	79	469	0.11
"	"	Before	378	285	85	79	658	0.12
"	"	After	250	200	119	96	665	0.066
"	"	Before	228	177	183	100	688	0.14
"	"	After	765	427	294	240	1726	0.018
AA-1350	SNIF	Before	35	9	9	15	68	-
"	"	After	63	43	24	15	145	0.011
"	"	Before	24	20	19	38	101	0.029
"	"	After	45	53	46	90	234	0.013
"	"	Before	56	32	26	26	140	0.015
"	"	After	211	138	125	110	584	0.055

2.3 Incremental Additions of Grain Refiner Rod

A third approach to the production of dirty metal in the laboratory was the introduction of grain refiner rod (5% Ti, 1% B) into the melt. Previous work by Tanaka et al[4] and Siemensen et al[5] had suggested that commercially available grain refining rod contains, in addition to small (1-3 μm) TiB_2 nuclei, substantial quantites of significantly larger TiB_2 clusters. Incremental additions of grain refiner rod (Kaweki 5% Ti 1% B) were made to a 25 kg aluminium melt held at 700°C in a resistance furnace. In order to avoid the settling phenomena observed in the experiments previously described the melt was continuously mixed with an air-driven impeller. LiMCA samples were taken under the following conditions:

Metal Temperature	-	690-720°C
Orifice Diameter	-	0.30 mm
Current	-	60 Amperes
Differential Pressure	-	5" Hg (16.8 kPa)
Region of Interest	-	50-510 (d > 19 μm)
Pre-Amplifier Gain		1000
Sampling Time (Volume)		60 sec. (16 mL)

Figure 2 shows the results obtained using LiMCA and PoDFA as a function of the titanium concentration as determined by emission spectrometry. It can be seen that while the LiMCA responds linearly with the quantity of grain refiner addition PoDFA results show no relation to either LiMCA or the level of titanium. The final PoDFA value (3.1 mm^2/kg) was extremely elevated and presumably was the result of the grain refiner nuclei bridging the gaps in the filter and thus acting as "filter aids" causing a large quantity of small (<3 μm) TiB_2 particles to be captured.

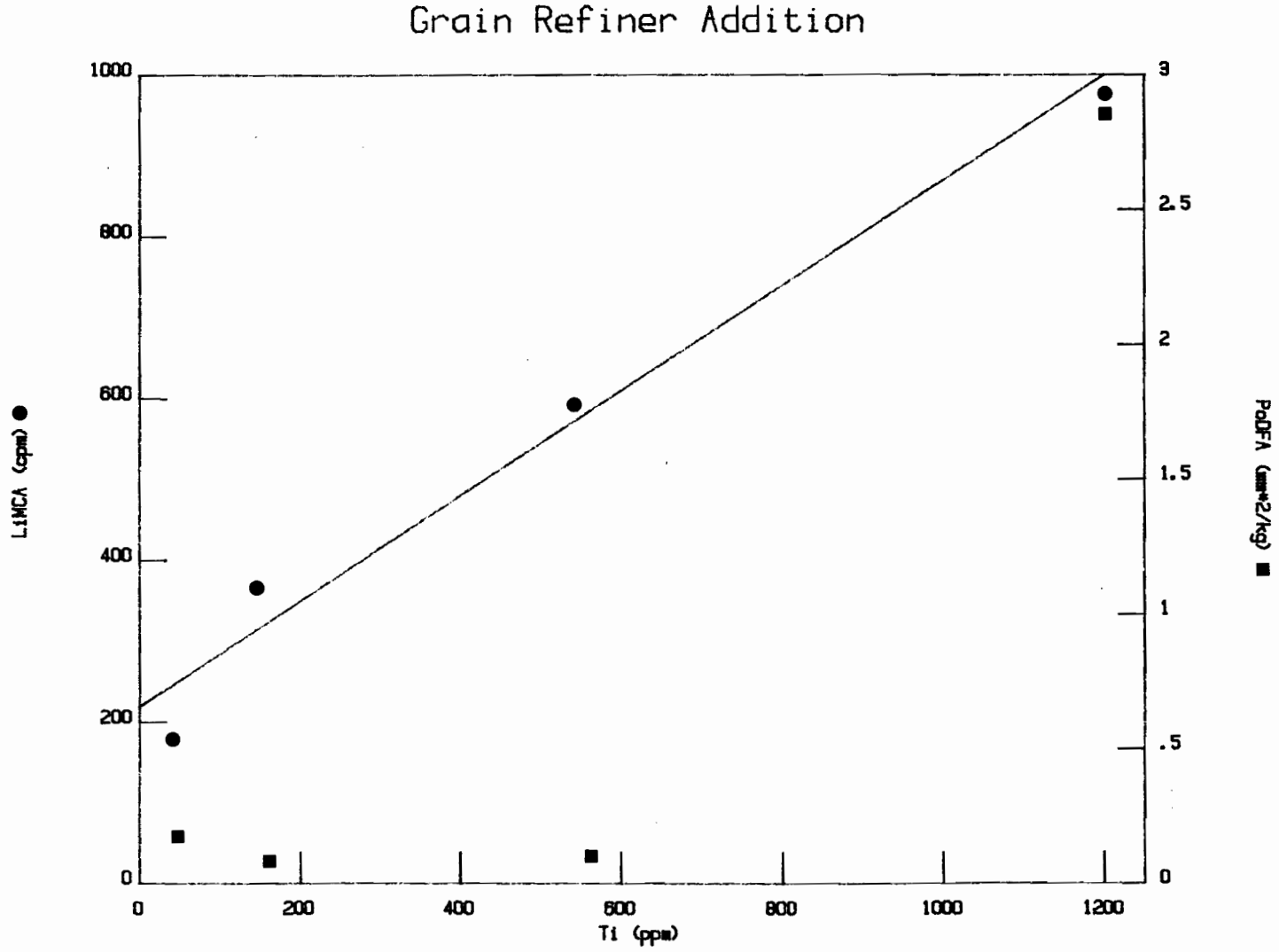

Figure 2: LiMCA and PoDFA readings as a function of the quantity of grain refiner rod (5% Ti 1% B) added to an aluminium melt.

2.4 Discussion of Laboratory Results

The laboratory results while promising, did not permit an unequivocal evaluation of the performance of the LiMCA. In the relatively small furnaces used the exposed surface area to metal volume was high leading to the generation of substantial quantities of large oxide films which are rarely observed in metal produced on a commercial scale. The lack of success attained in adding particles of known size and composition to the melt and the difficulties encountered in keeping existing inclusions in suspension made quantitative measurements of metal cleanliness difficult. With regard to the observations of particle settling it must be emphasized that the sampling probe was immersed to a depth of only 50 to 80 mm with respect to the melt surface, thus the rapid decline in count rates observed in these experiments would take significantly longer in industrial scale furnaces where the total metal depth is typically an order of magnitude larger.

3. PLANT TESTS

The laboratory experiments described in the previous section clearly demonstrated the potential of the apparatus and highlighted some of the difficulties experienced in manipulating molten aluminium on a small scale, in particular the production and maintenance of inclusion laden metal without the simultaneous generation of excessive quantities of oxide films. Thus it was felt that the relevance of the present work could be considerably enhanced by conducting a series of experiments in a production environment.

The advantages of working under production conditions also included a stable metal temperature, the option of taking large numbers of PoDFA samples in rapid succession and the fact that a variety of commercial wrought alloys could be used in the evaluation. This approach was not without its drawbacks which included no control over the alloy composition or batching process at any given time and the timing of the experiments.

3.1 Apparatus and Procedure

In order to facilitate transport and to protect the equipment the LiMCA device was modified as shown in Figures 3 and 4. The battery, ballast resistors, shunt, panel meters, vacuum pump reservoir and valve manifold were attached to a modified dolly. A large mechanics tool chest was modified to hold the electronic test equipment, the isolation transformer, spare batteries, tools, the gas cylinder and other miscellaneous equipment. A support jig, clamped onto the metal transform launders and held the electrodes and the sampling cell holder assembly (Figure 5). Figure 6 shows a close-up of the sampling cell holder assembly and Figure 7 shows the sampling head in use sampling metal directly from a transfer launder.

The battery, as before was a 6 V heavy duty automotive lead-acid battery and the ballast resistor consisted of six parallel 0.5 Ω 100W wire wound power resistors. This assembly gave a stabilized current of 55 to 60 amperes depending upon the state of the battery. The difference between the theoretical current, 72A of such an arrangement of circuit elements and

Figures 3 and 4: General view of the LiMCA apparatus as modified for carrying out in-plant trials.

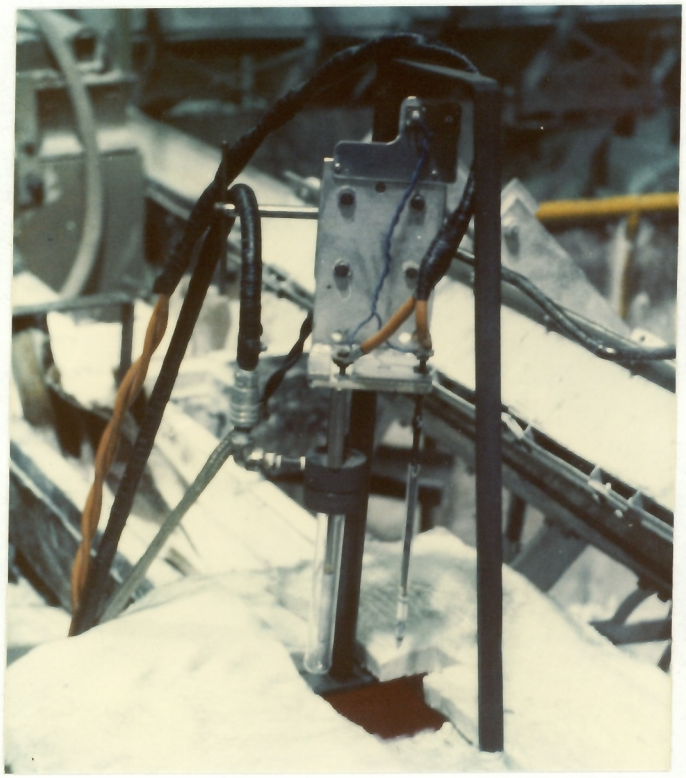

Figure 5: The metal sampling cell, cell holder assembly and support jig used to sample aluminium directly from metal transfer launders.

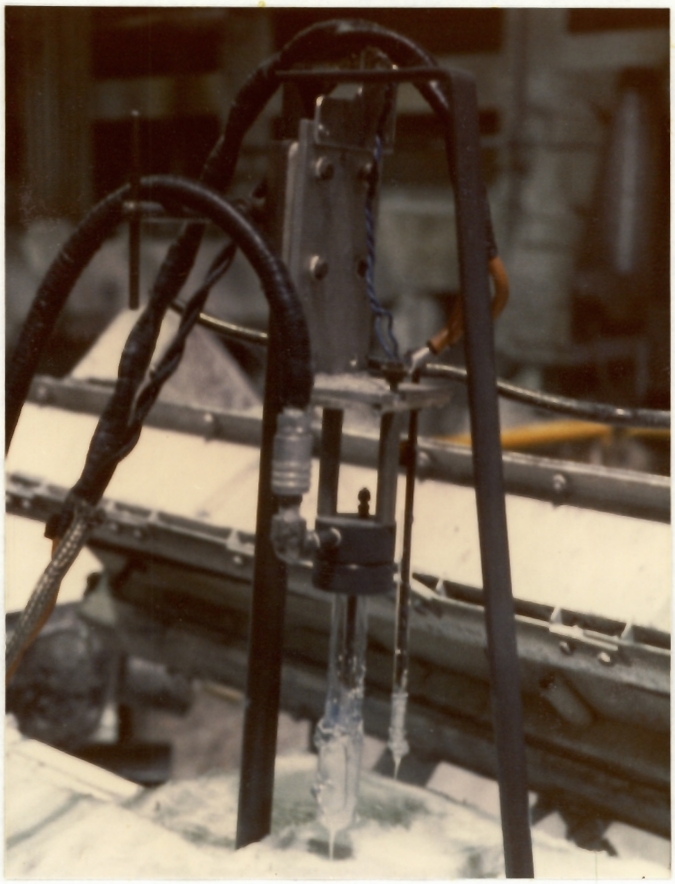

Figure 6: Closeup of the metal sampling cell and cell holder assembly after use.

Figure 7: The LiMCA apparatus in use sampling directly from a transfer launder.

the observed current 60A (new battery, full charge) was due to the resistance of the cables, contacts and the steel rods used as electrodes and to hold the resistor bank.

Generally 2 hours of testing, approximately thirty 60-second samples, could be performed before the battery had to be charged. Battery replacement took approximately five minutes and was done when the current fell below 55A or when the short-circuiting current (see Part I sec. 6.4) was insufficient to stabilize the base line at a suitable noise level, typically ± 5 μV P-P.

Installation consisted of rolling the two pieces of equipment into position, connecting the necessary power leads and argon/vacuum hoses, clamping the jig onto the transfer trough and installing the glass-sheathed electrodes and sampling cell. The cell was lowered to about one inch above the surface of the metal and preheated for 2 to 3 minutes. The argon was then switched on, ∿ 2 psi (13.7 kPa), and the cell and counter electrode immersed in the molten metal. The vacuum reservoir was then adjusted to the desired pressure (generally 5" Hg, 16.8kPa) and the system was depressurized. Once the metal had climbed to the level of the inner electrode there was an abrupt change in the noise level on the oscilloscope display due to the establishment of contact between the leads to the two inputs of the differential amplifier, at that point the current was switched on and the baseline observed. If the baseline was stable sampling was commenced by depressing the start button on the multichannel analyser and counting for a

fixed period of time (generally 60 or 30 seconds), if the baseline was not stable When the current was applied then the resistor bypass switch was used to apply a large (200-300 A depending upon the condition of the battery) current to the circuit for 2 to 3 seconds. This generally solved any 'noise' problem, if it did not the 'treatment' was repeated and if the second 'treatment' did not work then all electrical contacts were examined and secured as necessary. In the very rare event that this did not solve the problem the sampling cell was replaced and the electrodes inspected and replaced if necessary and the start-up procedure repeated.

After each sample had been acquired the current was switched off, the system was pressurized with argon and the results were transcribed or recorded on magnetic tape. Since a 511 channel histogram was considered too unwieldy the counts were integrated using the region of interest option on the multichannel analyser. The areas integrated and the corresponding equivalent spherical diameters of the limits of integration under the conditions normally used (pre-amplifier gain of 1000, current of 60 amperes and 0.30 mm diameter orifice) are shown below.

Region	d: Particle Equivalent Spherical Diameter (μm)
2-60	16 to 20
61-122	20 to 25
123-172	25 to 30
173-215	30 to 35
216-252	35 to 40
253-285	40 to 45
286-314	35 to 50
> 314	> 50

Once the data had been acquired the sampling cell was normally emptied and ready for reuse.

4. Plant Trials: Results

The LiMCA apparatus was used at five of Alcan's casting centres, the Saguenay Works, the Lapointe Works, the Oswego Works and at casting centres numbers 45 and 32 of the Sécal (Société d'électrolyse et de chimie Alcan Limitée) Works. Unless otherwise noted the instrumental settings and conditions were as follows:

orifice diameter	:	0.30 mm
current	:	60 amperes
differential pressure	:	5" Hg (16.8 kPa)
pre-amplifier gain	:	1000
sampling time (volume)	:	60 seconds (16 mL)
detection limit	:	d>20 μm

PoDFA samples, when taken, were analysed by the Metallography Department of the Alcan (Arvida) Research Centre.

4.1 Saguenay Works

The Saguenay Works produces aluminium sheet by a twin belt casting process. There are four tilting reverberatory furnaces which are charged with virgin molten metal from Sécal's electrolysis plant and recycled internal scrap. Grain refiner additions are made at the furnace outlets and the metal is conveyed via a launder to one of the three belt casters. The plant layout is shown schematically in Figure 8. Due to the long distances between the furnaces and the casters only the initial

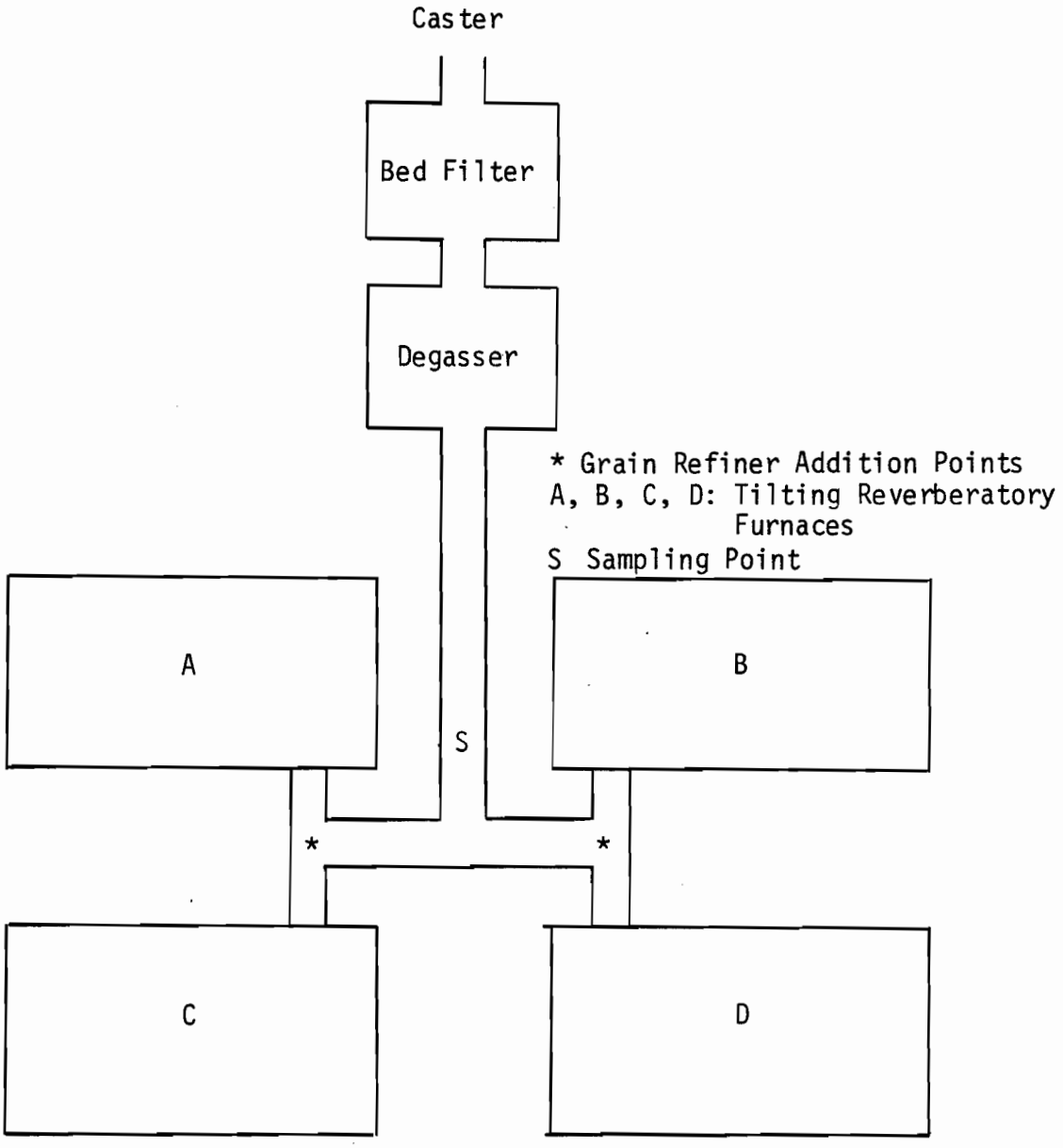

Figure 8: Plant layout Saguenay Works (schematic).

portion of the transfer launder is open, the rest being a heated, closed pipeline. Thus it was not possible to sample the metal downstream of either of the treatment units indicated in Figure 8.

Casting is carried out continuously for periods of up to six hours with provisions to automatically change over from furnace to furnace as they are emptied.

LiMCA and PoDFA samples were taken at the entry to the closed section of the launder downstream of both a glass cloth filter and the point of addition of the grain refiner rod. The results obtained by these two techniques are shown as a function of time in Figures 9 and 10. In both cases the LiMCA results represent the summation of all peaks appearing above channel 61 of the multichannel analyser (i.e. > 20 μm equivalent spherical diameter). Figure 11 is identical to Fig. 10 except that in this case the summation of all counts appearing above the threshold (ca 16 μm ESD) are plotted. Figure 12 shows the particle size distribution as measured by the LiMCA for the three points indicated on Figure 9.

Inspection of Figures 9, 10 and 11 clearly shows that the LiMCA and PoDFA results are in excellent qualitative agreement. After each furnace charge there occurred a large increase in the level of suspended inclusions which decayed throughout the cast and again rose sharply upon subsequent changeover. The PoDFA results indicated that the inclusions were predominantly composed of titanium diboride, of which there were two sources;

the grain refining addition that was made continuously upstream of the sampling point and recycled grain refined scrap (edge trim, damaged coils). Since the grain refiner was added continuously it should, in principle, have contributed a constant level of suspended particulates to the metal. The scrap on the other hand, was charged to the furnaces where the boride particles have the opportunity to agglomerate and settle and this is believed to be the cause of the cyclical variation observed in the inclusion content of these melts. The possibility that the "bursts" are the result of entrained refractory particles washed off the fresh sections of launder exposed after furnace changeover appears unlikely due to the qualitative PoDFA results and the fact that stirring the metal in the transfer trough upstream of the sampling point has no measurable effect on the LiMCA results.

Figure 11 is included also to demonstrate one way of increasing the sensitivity of the LiMCA. As was pointed out in Part One the initial goal was to detect and count particles larger than d = 20 μm, however, by lowering the detection limit the number of counts observed rises dramatically. This is further substantiated by Figure 12 which demonstrates the predominance of the smaller particles. Figure 12 also shows that the larger particles sediment faster than the smaller ones (not an unexpected result) and is included to demonstrate the ability of the LiMCA to provide particle size distributions. The quantitative relation between the LiMCA and PoDFA results will be discussed in a later section.

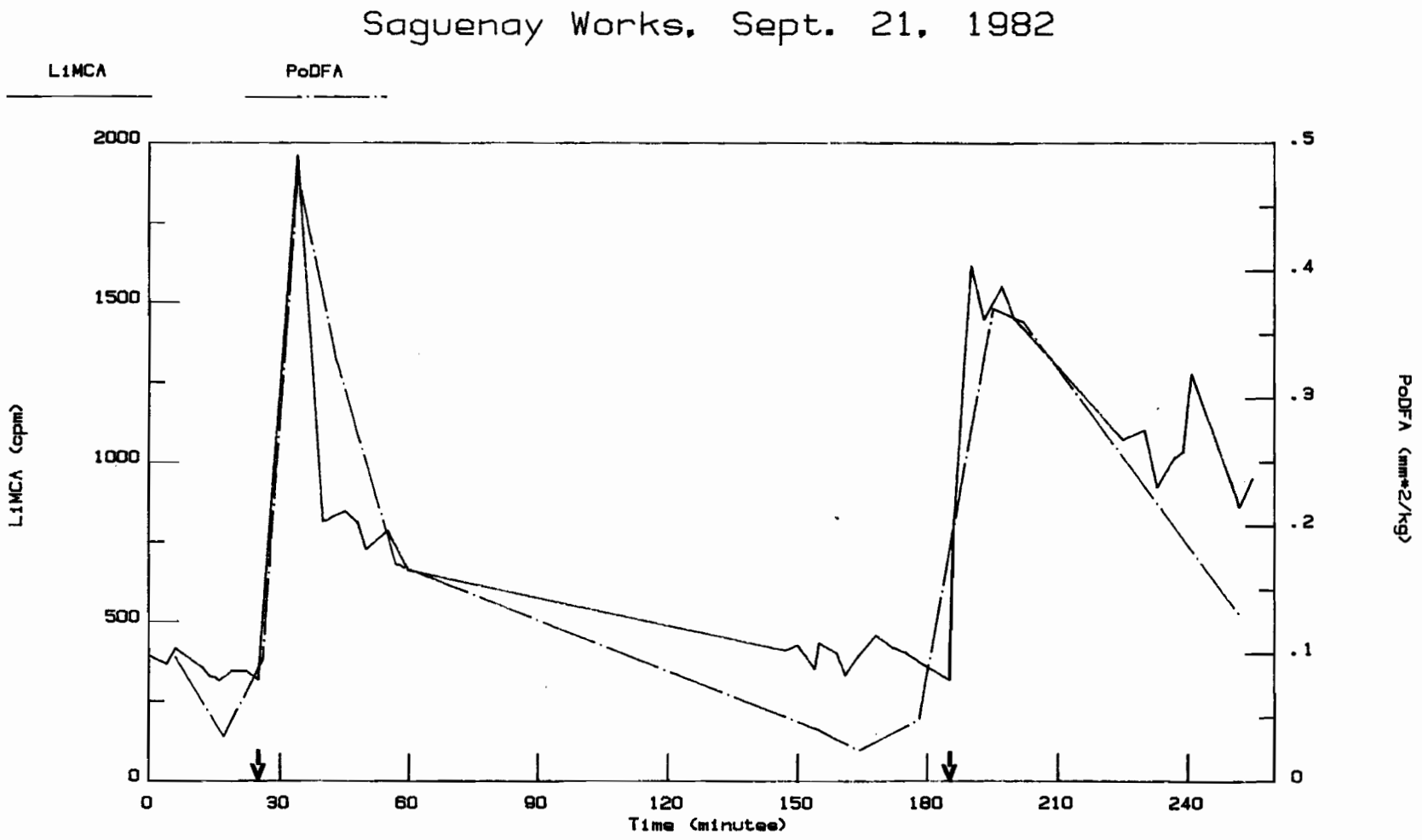

Figure 9: LiMCA and PoDFA results as a function of time into cast, Saguenay Works, September 21, 1982. Arrows indicate time at which furnace change took place.

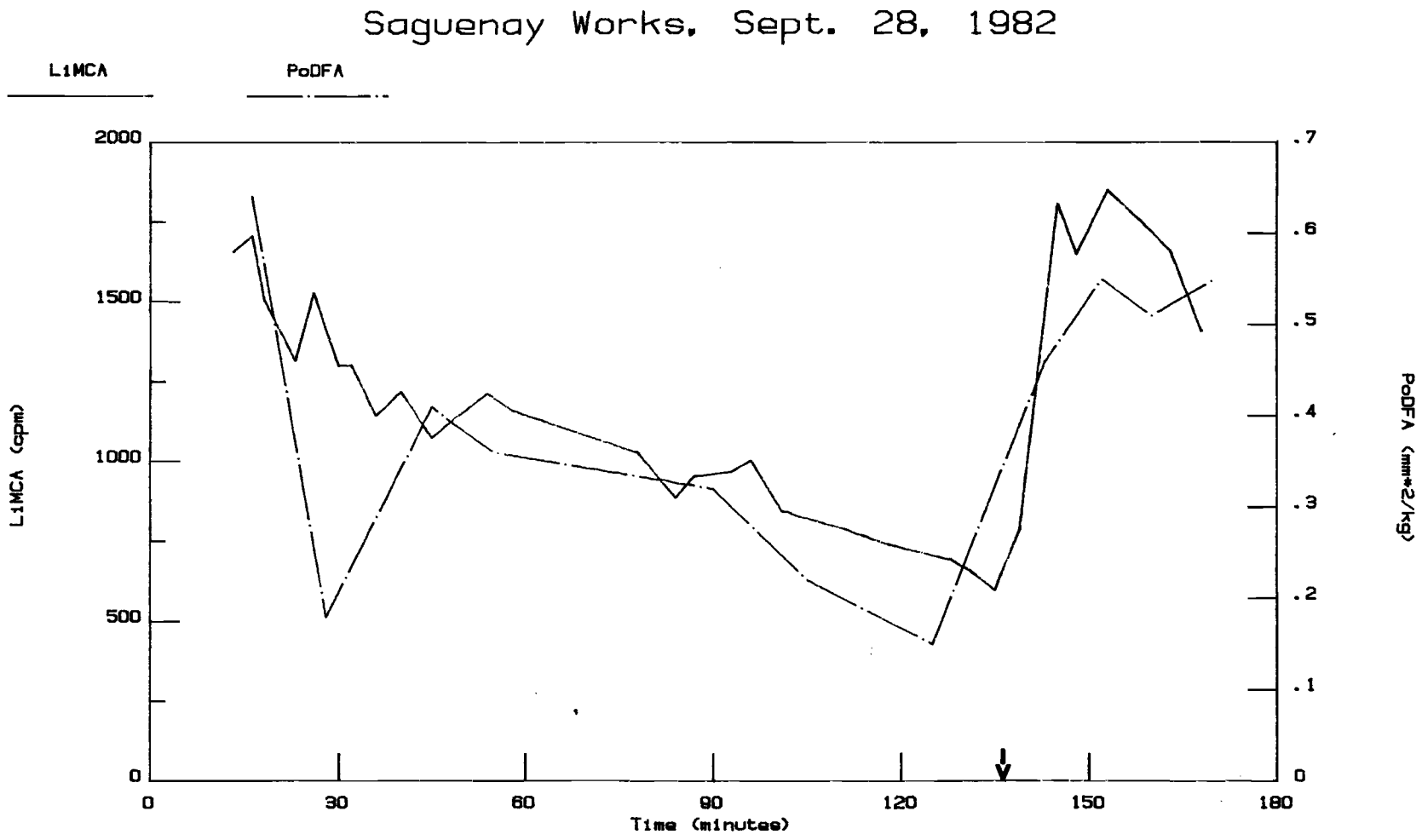

Figure 10: LiMCA and PoDFA results as a function of time into cast, Saguenay Works, September 28, 1982. Arrow indicates time at which furnace change took place.

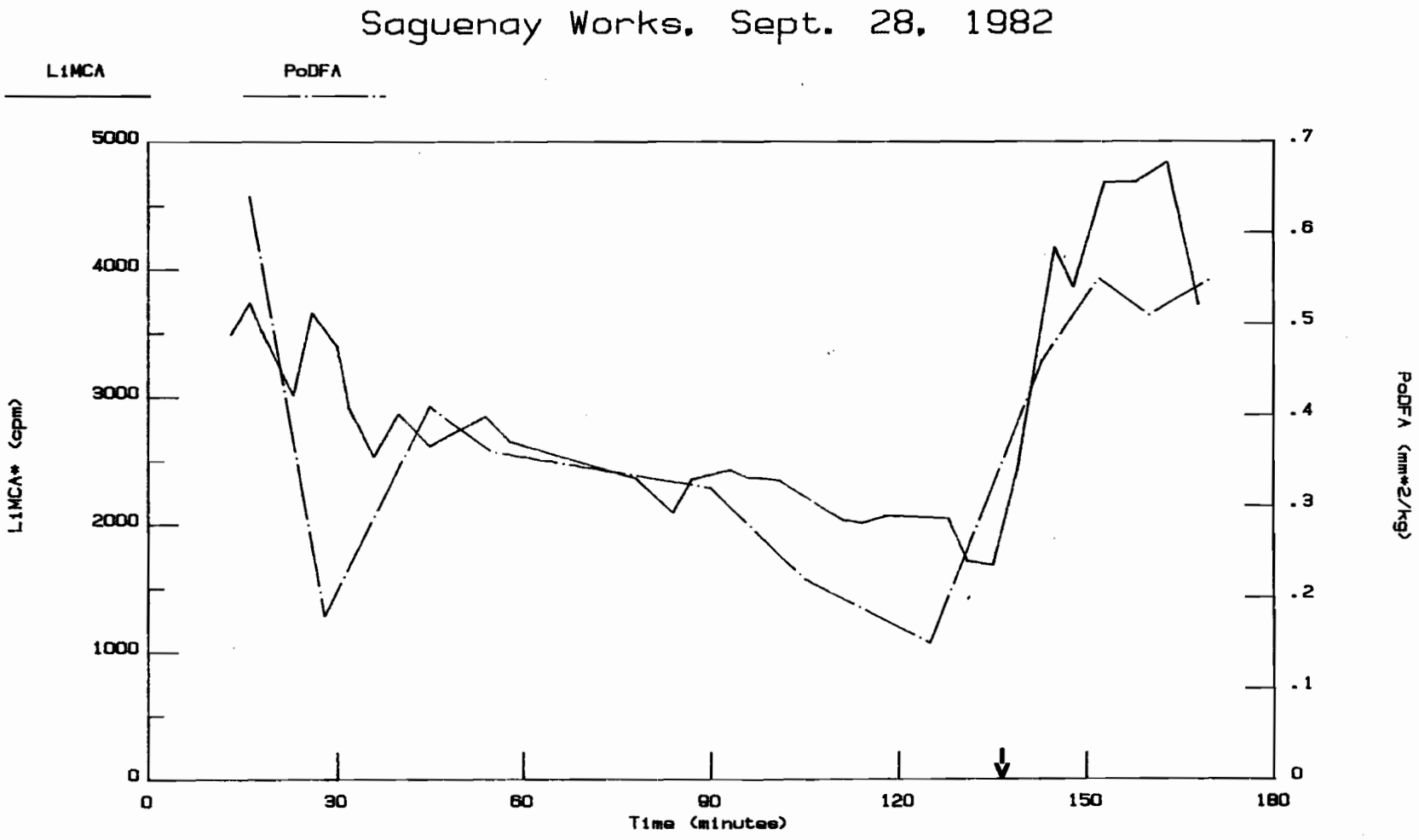

Figure 11: LiMCA and PoDFA results as a function of time into cast, Saguenay Works, September 28, 1982. In this case all counts corresponding to particles larger than d =16 μm have been included in the LiMCA results. Arrow indicates time at which furnace change took place.

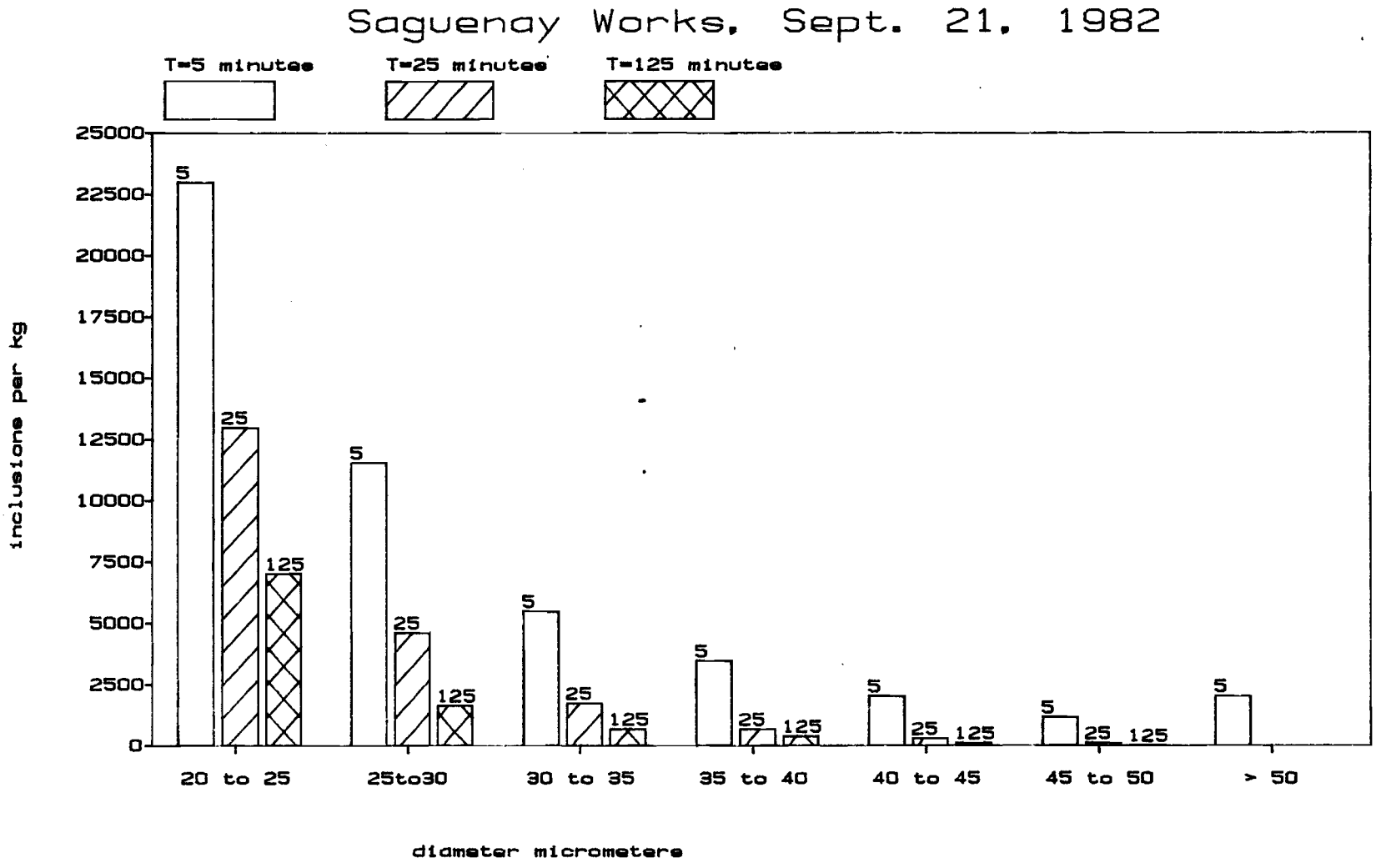

Figure 12: The particle size distributions obtained using the LiMCA for times t = 40, 60 and 160 minutes in Figure 9 (5, 25 and 125 minutes after the first furnace changeover). The results are expressed in terms of particle number per kg based on a sample volume of 16 ml.

4.2 Lapointe Works

The Lapointe Works produces aluminium wire by the Properzi process. The plant layout is shown schematically in Figure 13. There are four reverberatory furnaces, two of them stationary which are used for remelting scrap and accepting hot metal from a nearby electrolysis plant and two tilting furnaces used for casting. LiMCA and PoDFA samples were taken at the point indicated, which was upstream of the point of addition of the grain refiner rod. In contrast to the Saguenay Works, the Lapointe Works does not change furnaces continuously and thus the sampling period was limited to the time required to cast one furnace (typically two to three hours). During the time in which the tests were carried out electrical conductor (E.C.) grade aluminium wire was being produced. In order to meet the conductivity specification for E.C. grade wire the metal is treated with boron in order to precipitate vanadium in the form of titanium-vanadium boride particles (Ti-V)B which are removed by decantation before the start of casting. Figures 14 and 15 show typical LiMCA and PoDFA values observed as a function of casting time. It can be seen that the PoDFA values and the LiMCA count rates are both considerably lower than those observed at the Saguenay Works. This is due to the fact that considerably less process scrap is generated by the Properzi process leading to a lower recirculating scrap load. In addition, the concentration of grain refiner added was much lower than at the Saguenay Works. The overall effect being that at the Lapointe Works, the furnace charges typically contain less particle laden scrap, and the scrap they do contain is 'cleaner' than at the Saguenay Works. Figure 16 was obtained on a cast in which,

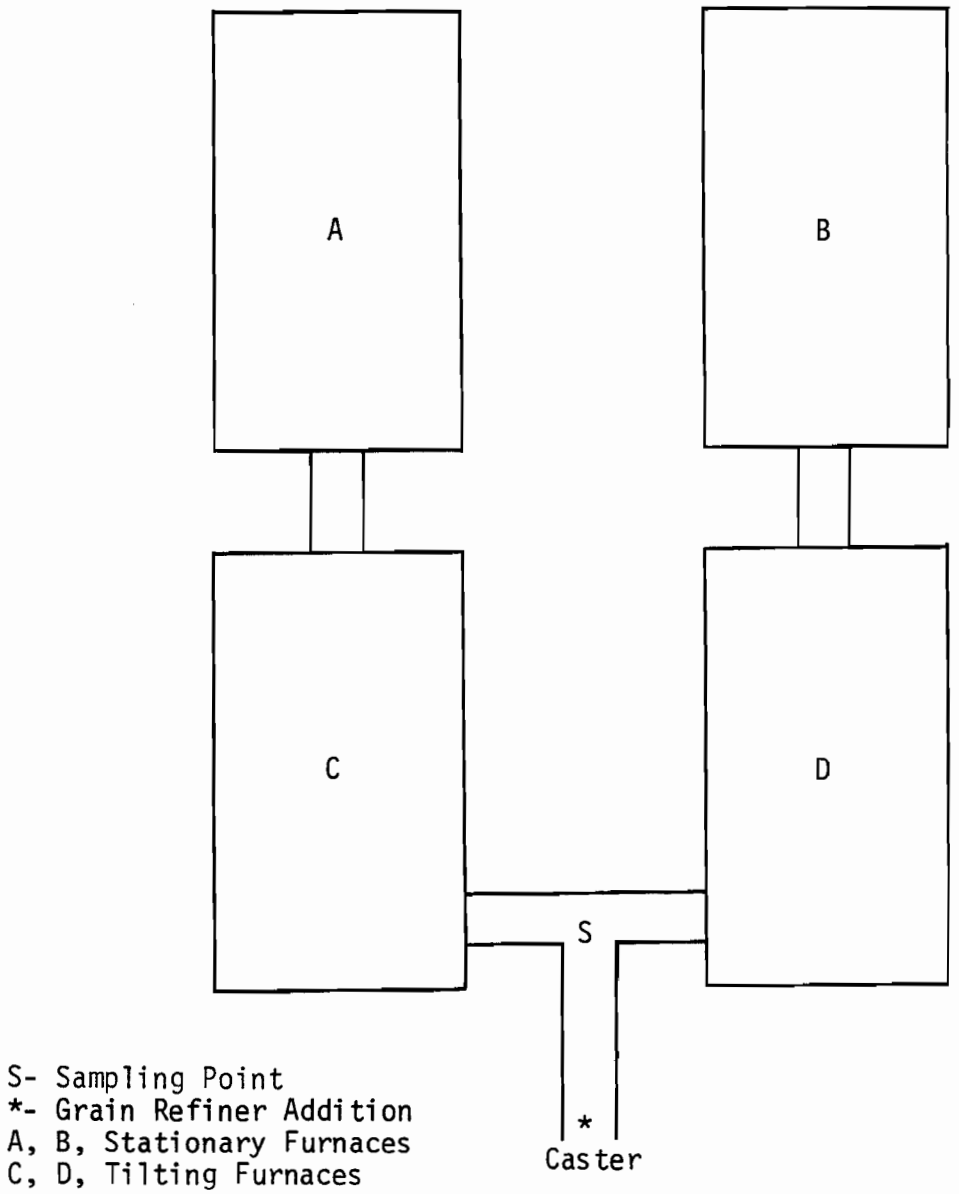

Figure 13: Plant layout, Lapointe Works (schematic).

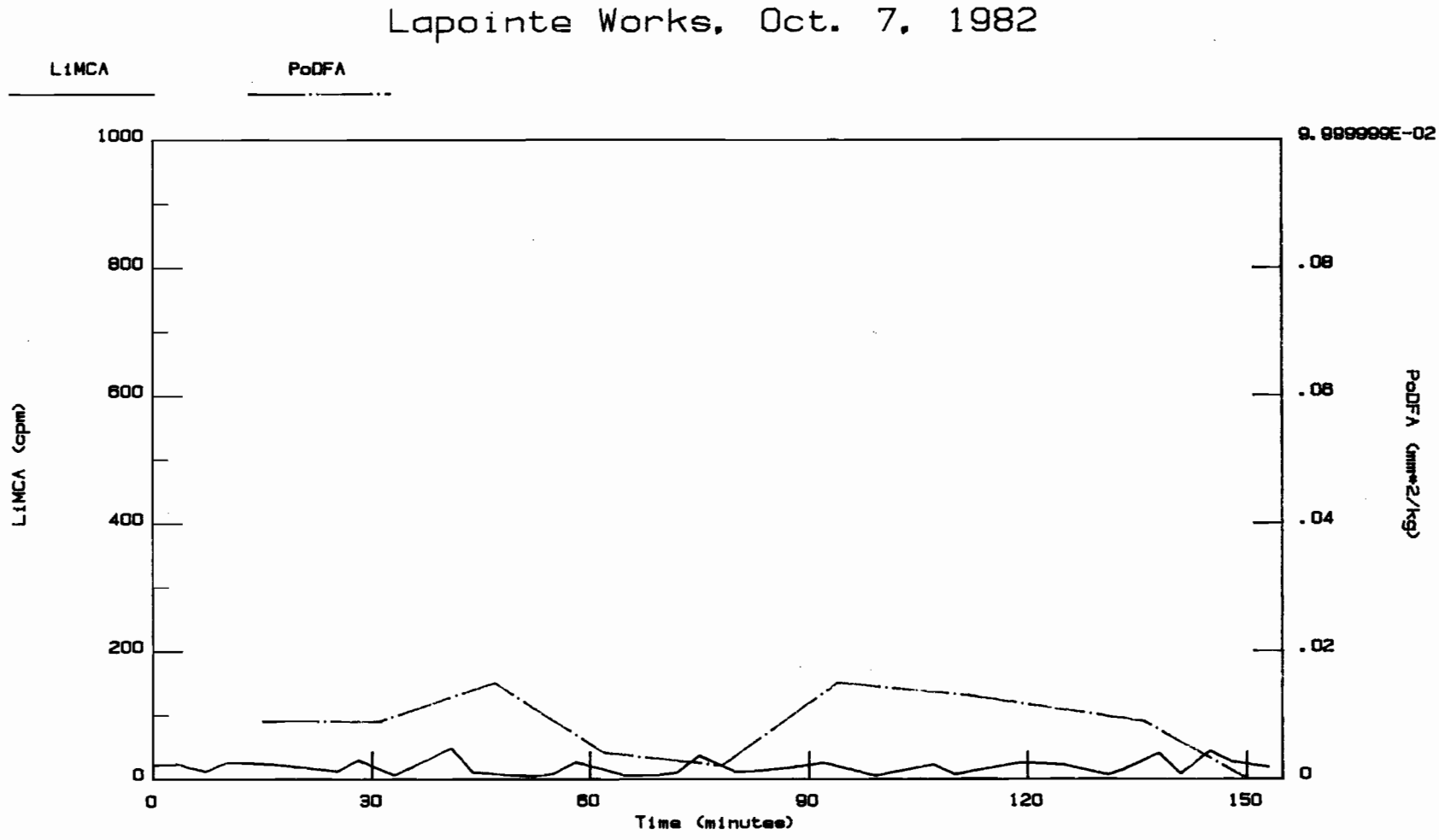

Figure 14: LiMCA and PoDFA results as a function of time into cast, Lapointe Works October 7, 1982.

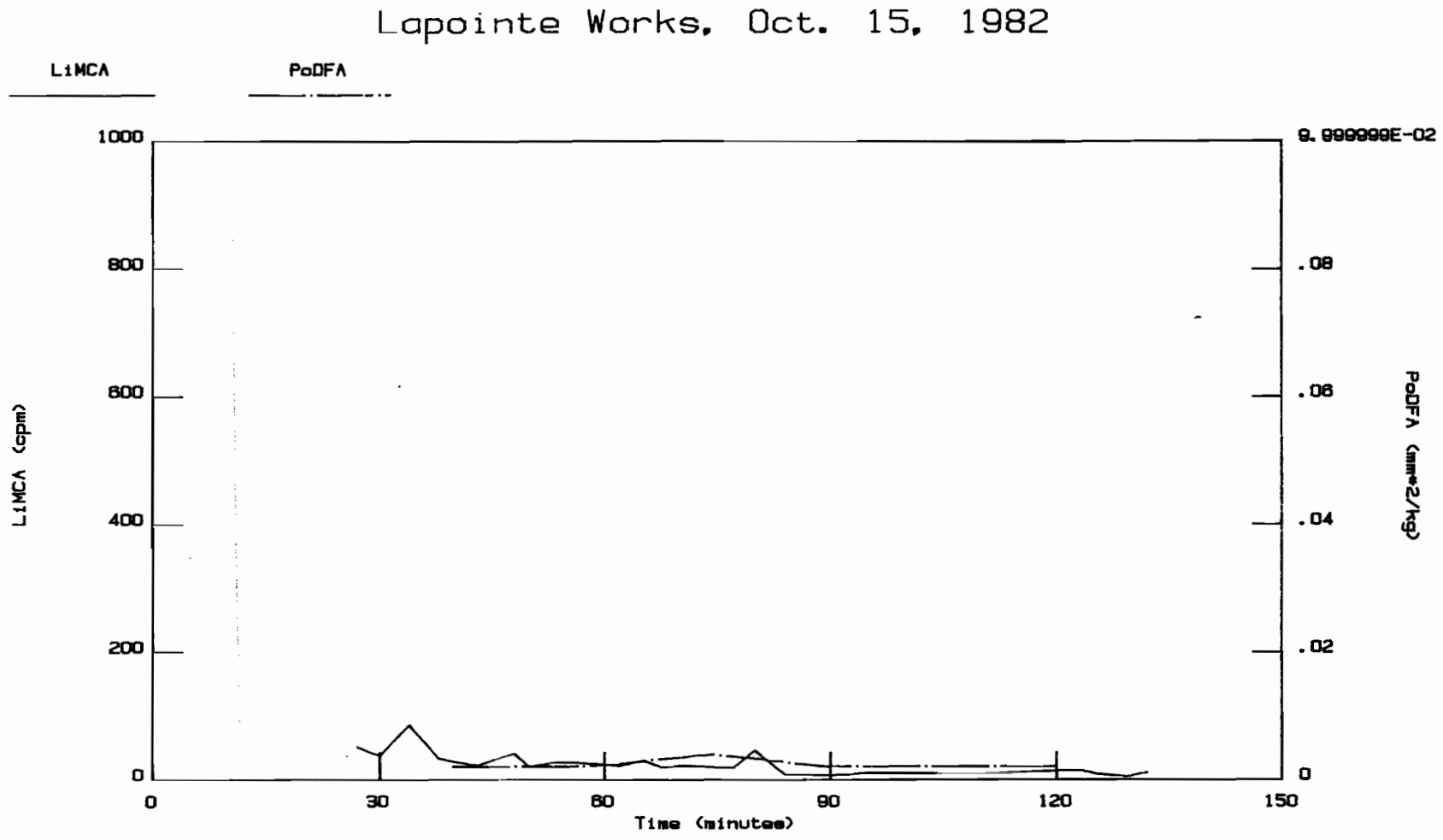

Figure 15: LiMCA and PoDFA results as a function of time into cast, Lapointe Works, October 15, 1982.

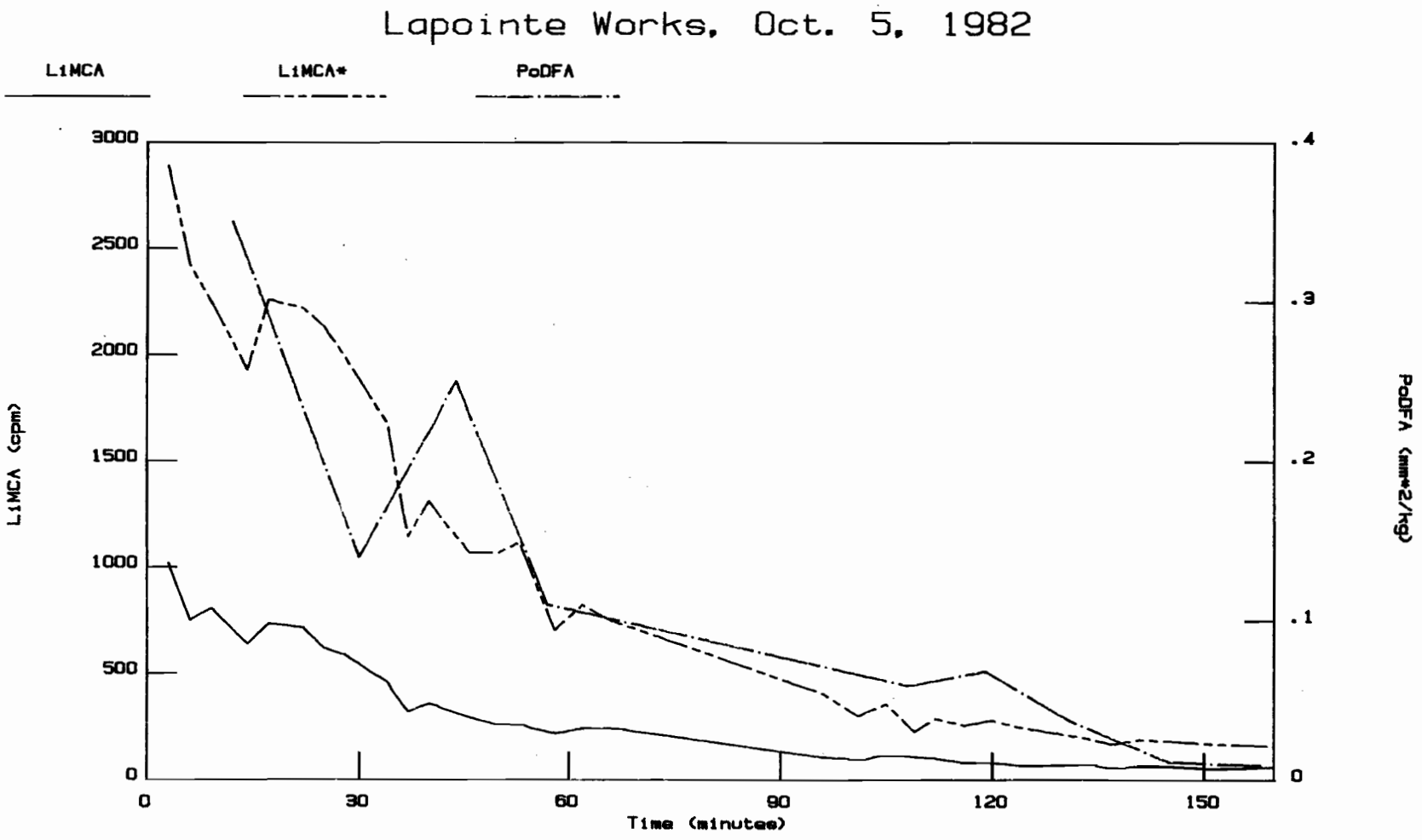

Figure 16: LiMCA and PoDFA results as a function of time into cast, Lapointe Works, October 5, 1982. In this case the metal in the furnace was well mixed at the outset due to production difficulties. The upper solid line represents all counts corresponding to particles larger than 16μm in diameter.

due to production difficulties, the metal was cast immediately after it has been transferred from one tilting furnace to the other. In this case both LiMCA and PoDFA indicated that particle settling during the cast was occurring. The rapid transfer of metal resuspended the sediment in the receiving furnace leading to a much larger than normal inclusion concentration which, after thirty minutes of casting, had fallen to one half of the initial value and was approaching 'typical' levels after two hours.

Table 3 shows the particle size distribution three minutes, one hour and two hours after the end of the metal transfer operation. It is evident that the rate of disappearance (settling) increases with particle size.

Figure 17 shows a cast in which the LiMCA results indicated that the metal was quite clean whereas the PoDFA results suggested the opposite. This discrepancy was caused by the presence of small particles, tentatively identified as borocarbides. Examination of the PoDFA concentrate using scanning electron microscopy revealed the presence of a network of very fine, acicular particles (0.25x2 micrometers) covering the surface of the PoDFA disc. This mat of particles likely acted as a filter aid increasing the capture efficiency of the PoDFA disc for small ($d < 20$ μm) particles leading to the anomalously high PoDFA values.

TABLE 3

PARTICLE SIZE DISTRIBUTIONS OBTAINED FROM THE LIMCA DATA FOR TIMES t =3, 60 and 120 MINUTES IN METAL FROM AN INITIALY WELL-MIXED FURNACE (SEE FIG. 16)

	Diameter Interval μm (CPM)							
Time (min.)	16 to 20	20 to 25	25 to 30	30 to 35	35 to 40	40 to 45	45 to 50	>50
0	1871	690	177	72	37	17	7	18
60	582	151	31	12	9	9	1	3
120	181	36	10	4	5	1	1	7

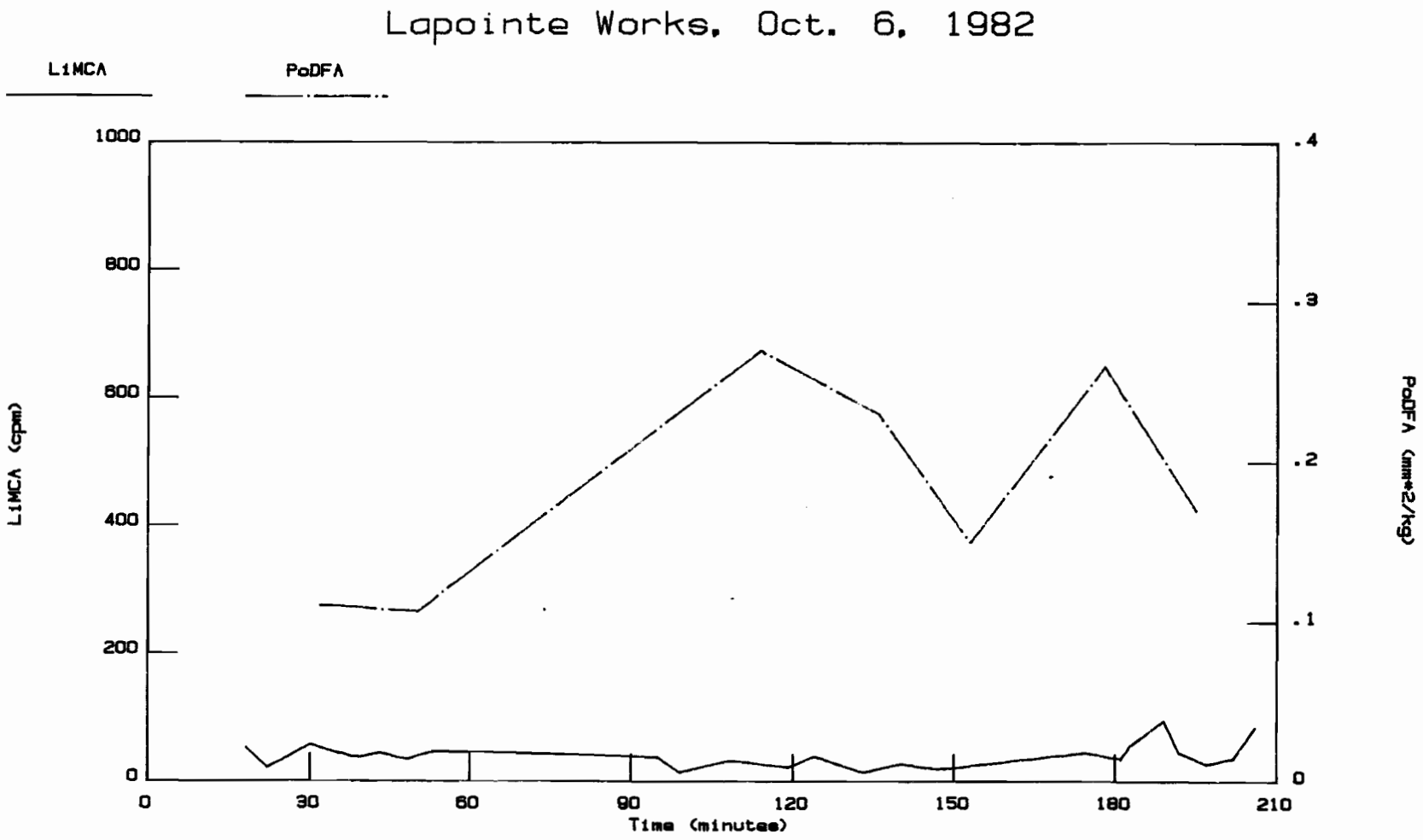

Figure 17: LiMCA and PoDFA results as a function of time into cast, Lapointe Works, 1982. (In this case the metal contained small "borocarbide" particles which led to the anomolously high PoDFA results).

4.3 DC 32 Sécal Works

The relevant layout of this casting center is shown schematically in Figure 18. There is a tilting reverberatory furnace in which all the batching operations are carried out. During the period of these tests the center was producing rolling ingots for the production of can bodies (alloy AA-3004B). Since this is an inclusion sensitive product a Banbury Bed Filter (BBF) was in use. (A Banbury Bed Filter is essentially a large heated box filled with small pieces of tabular alumina through which the metal to be filtered passes with a low superficial velocity.) Grain refiner addition (5% Ti, 1% B) was made at the furnace outlet upstream of the BBF. Due to the limited space available at this location it was not possible to install the LiMCA, on-line upstream of the BBF. As there is not enough casting capacity at this center to cast the entire contents of the furnace in one go, two 'drops' are made from each furnaceful of metal. As there is a delay of approximately one hour between drops while the ingots are removed and the molds prepared, metal for the second drop effectively received an additional period of settling prior to the start of casting.

Figure 19 shows LiMCA and PoDFA results as a function of time into cast for two successive drops from one batch of metal. It can be seen that, during the first drop the inclusion concentration falls rapidly over the first thirty minutes and levels off thereafter. The second drop, in this case, was at any time approximately twice as clean as the first reflecting the beneficial effect of the increased settling period arising from the time interval between drops. Unfortunately it was not always

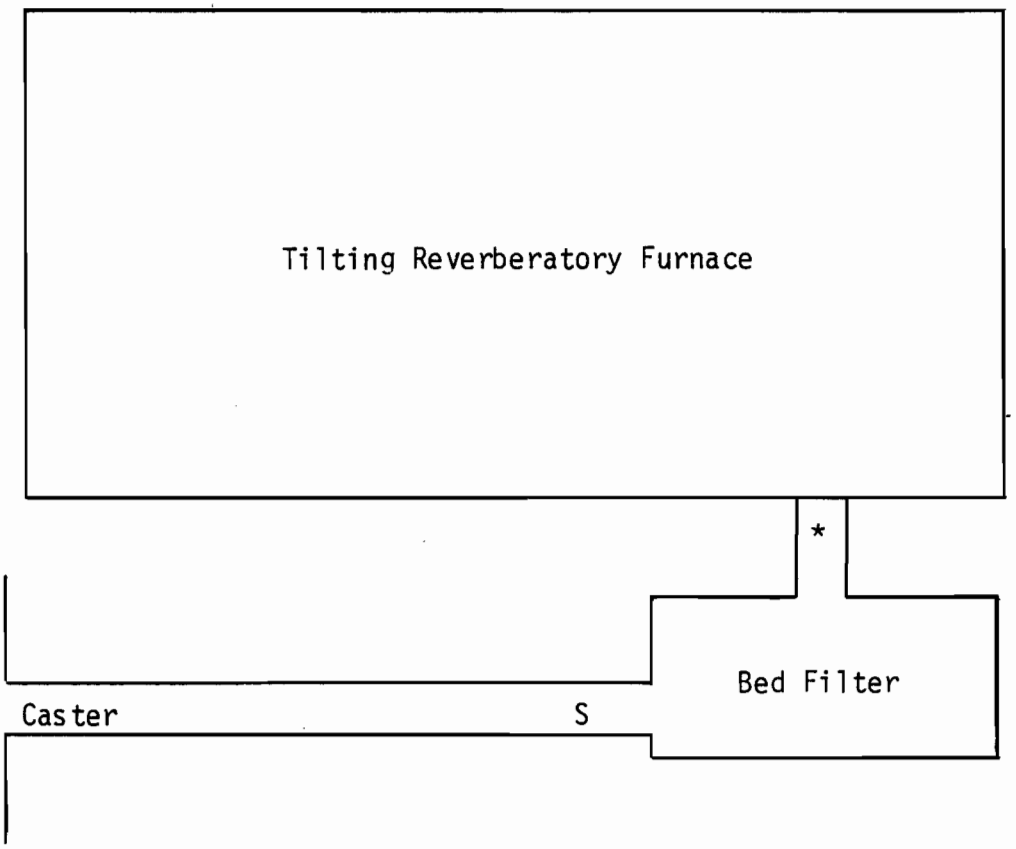

S- Sampling Point
*- Grain Refiner Addition

Figure 18: Plant layout, Sécal DC 32 (schematic).

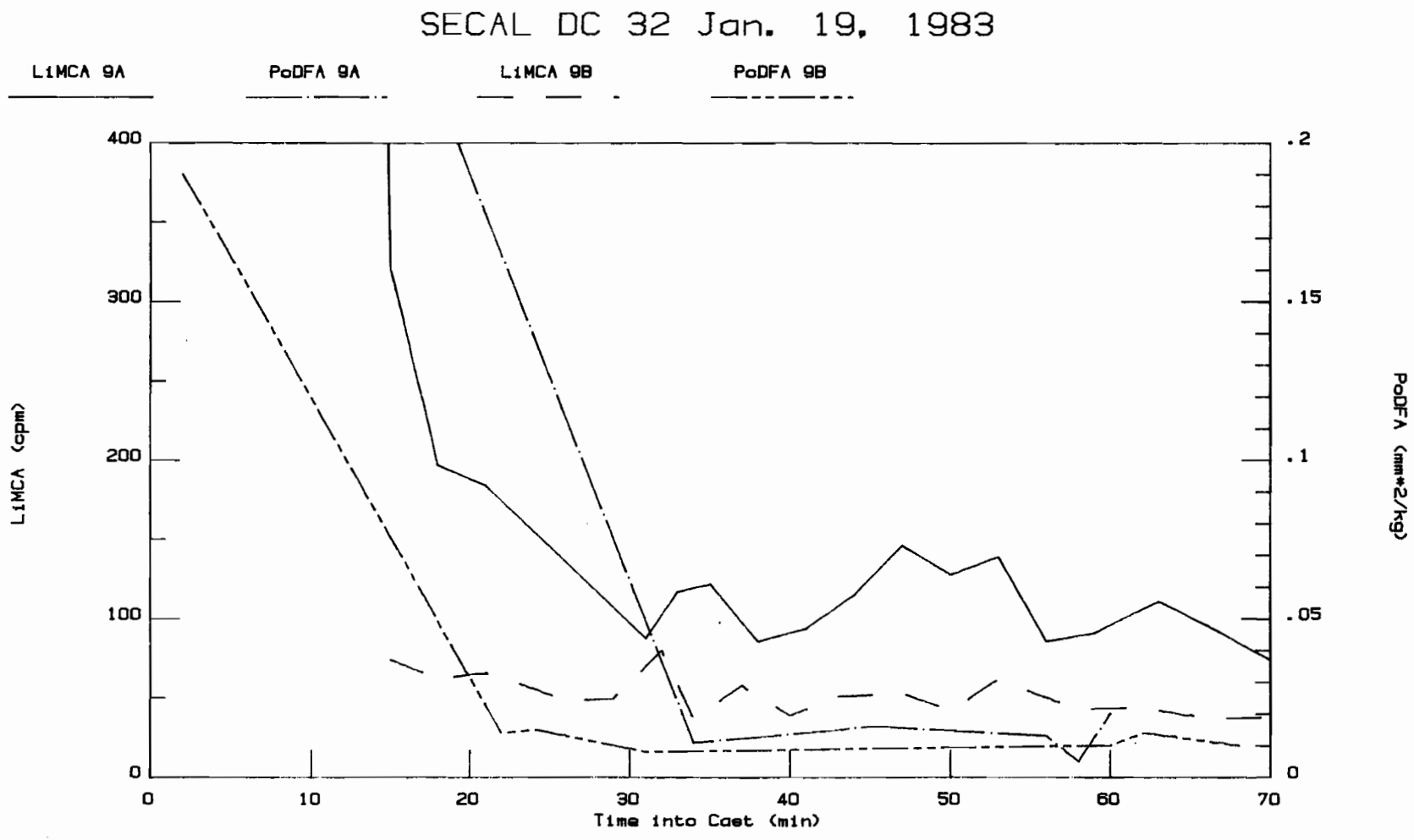

Figure 19: LiMCA and PoDFA results as a function of time into cast for two successive drops from the same original batch.

possible to obtain samples during the first 15 minutes of casting due to the necessity of not impeding the casting crew's full access to the bed filter.

Figure 20 shows the results obtained on a second drop in which samples during the initial period of casting were obtained. In this case both techniques showed that an initial 'surge' of inclusion laden metal occurred which decayed very rapidly. It is believed that this phenomenon was caused by the initial rush of metal through the bed filter washing out particles previously captured and not as a result of particle settling within the furnace.

Figure 21 shows the results obtained on two successive drops in which the metal, due to production delays, had been held in the furnace for three hours rather than the one hour settling period normally allowed prior to the first drop. This demonstrates that the additional settling time virtually eliminated the settling during the first drop observed in Figure 19. Hence again according to the LiMCA results the second drop was cleaner than the first as a result of the additional settling time between drops.

Figure 22 shows the response of the LiMCA and PoDFA results to an 'upset' that occurred during a drop. In this case the metal had been settled for approximately 90 minutes prior to the start of casting and was relatively clean at the start of the drop. Both techniques then picked up a large increase in the inclusion concentration starting at approximately

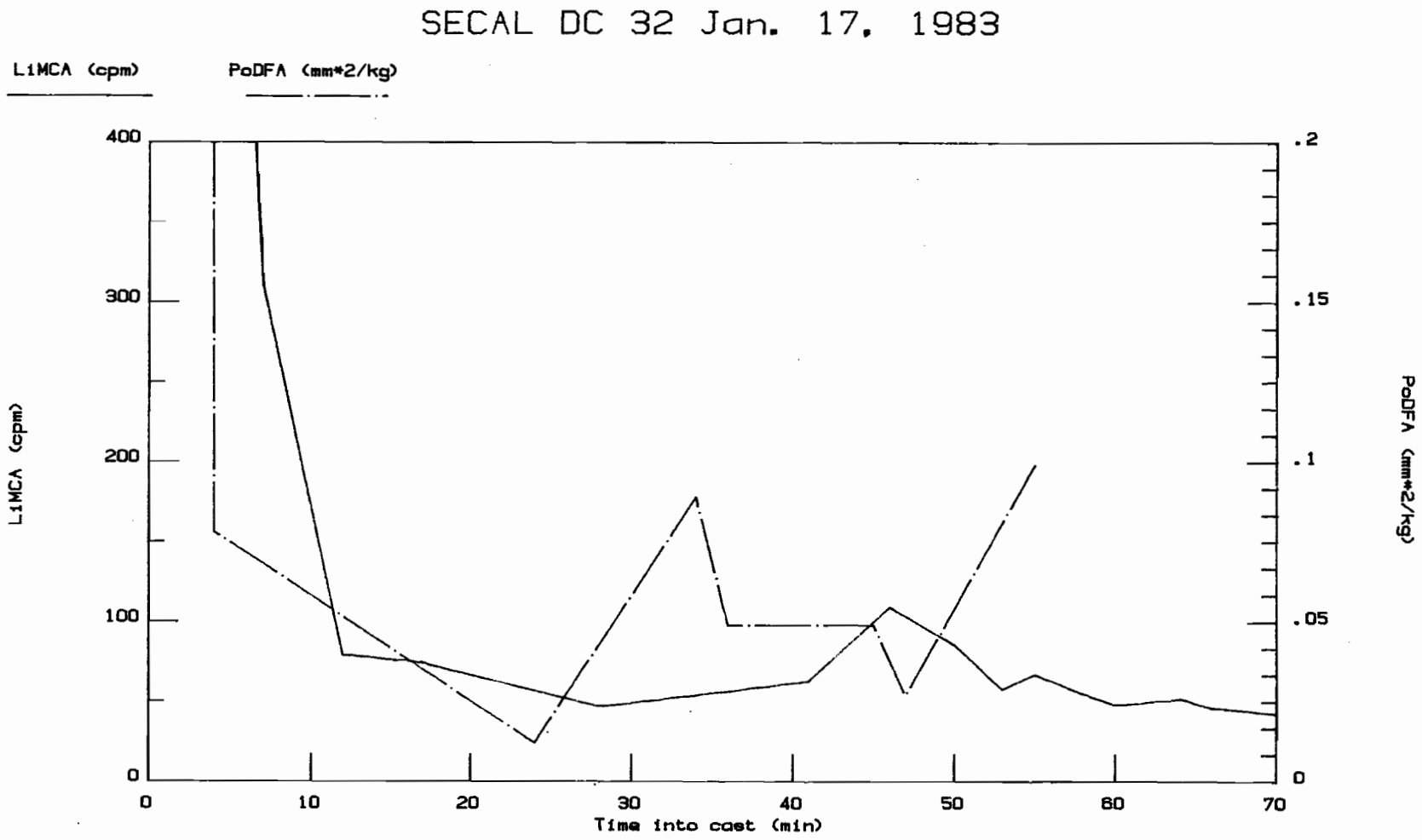

Figure 20: LiMCA and PoDFA results as a function of time into cast, note the initial surge of inclusion-laden metal released from the bed filter.

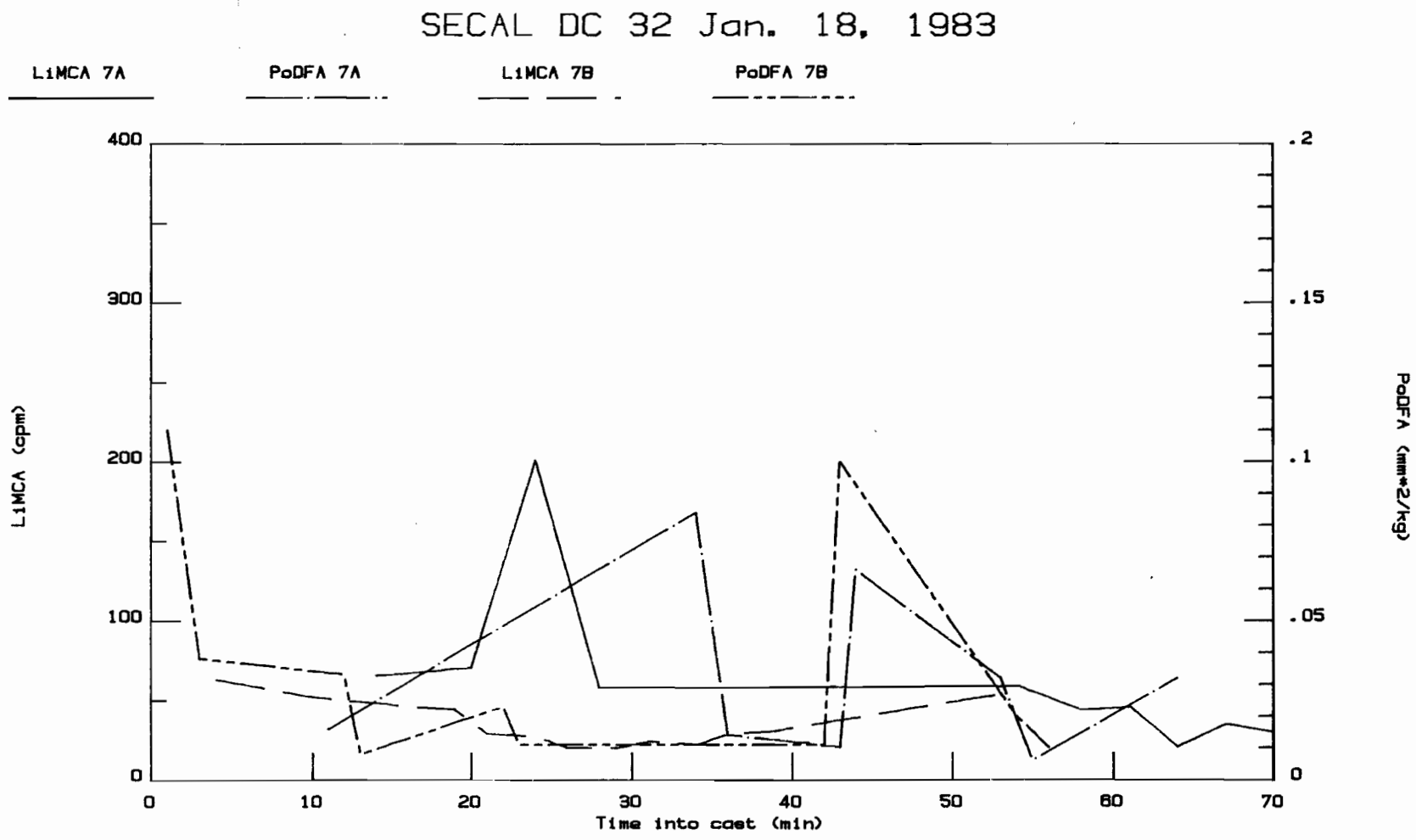

Figure 21: LiMCA and PoDFA results as a function of time into cast. The first drop (7A) had received an additional two hours of settling compared to the example in Figure 19.

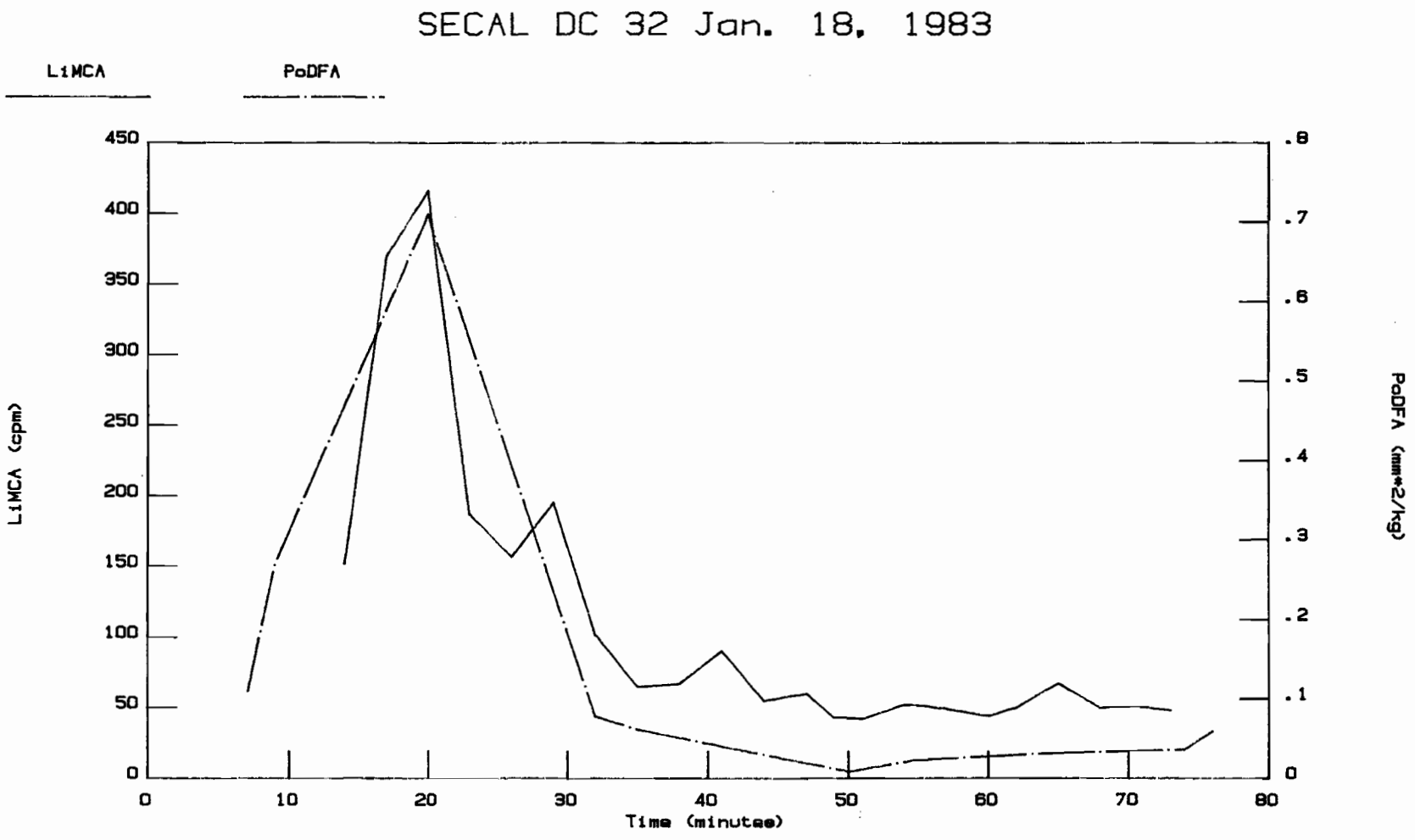

Figure 22: LiMCA and PoDFA results as a function of time into cast, in this example an 'upset' occurred approximately 15 to 20 minutes into the cast.

15 minutes into the drop. Although the cause of the upset was not known it seems possible that it was caused by a transient surge of metal through the filter which liberated some of the inclusions previously captured.

Figure 23 illustrates an off-line use of the apparatus to measure the performance of the bed filter at DC32. Metal samples weighing approximately 2 kg were taken from the transfer launder before and after the bed filter and held in pre-heated crucibles in an insulated bucket. The LiMCA probe was then lowered into the crucible and two one minute readings were taken for each sample. The results of three 'before' and two 'after' samples (six and four readings respectively) were averaged for each particle size range to produce the histogram shown in Figure 23. The removal efficiency of the bed filter was approximately 70% and independent of particle diameter over the range 16 to 40 μm. The apparent drop in removal efficiency for the three largest size ranges is likely the result of the large relative counting error inherent in the technique at low count rates and not a decrease in filter performance (sources of error and counting statistics will be discussed in a later section).

These results once again show that these two techniques of metal cleanliness assessment (LiMCA and PoDFA) provide much the same picture of the history of melt cleanliness. Whereas both techniques provide an overall measure of melt cleanliness, the LiMCA also provides immediate results and the particle size distribution while the PoDFA additionally provides information about the type(s) of inclusions present.

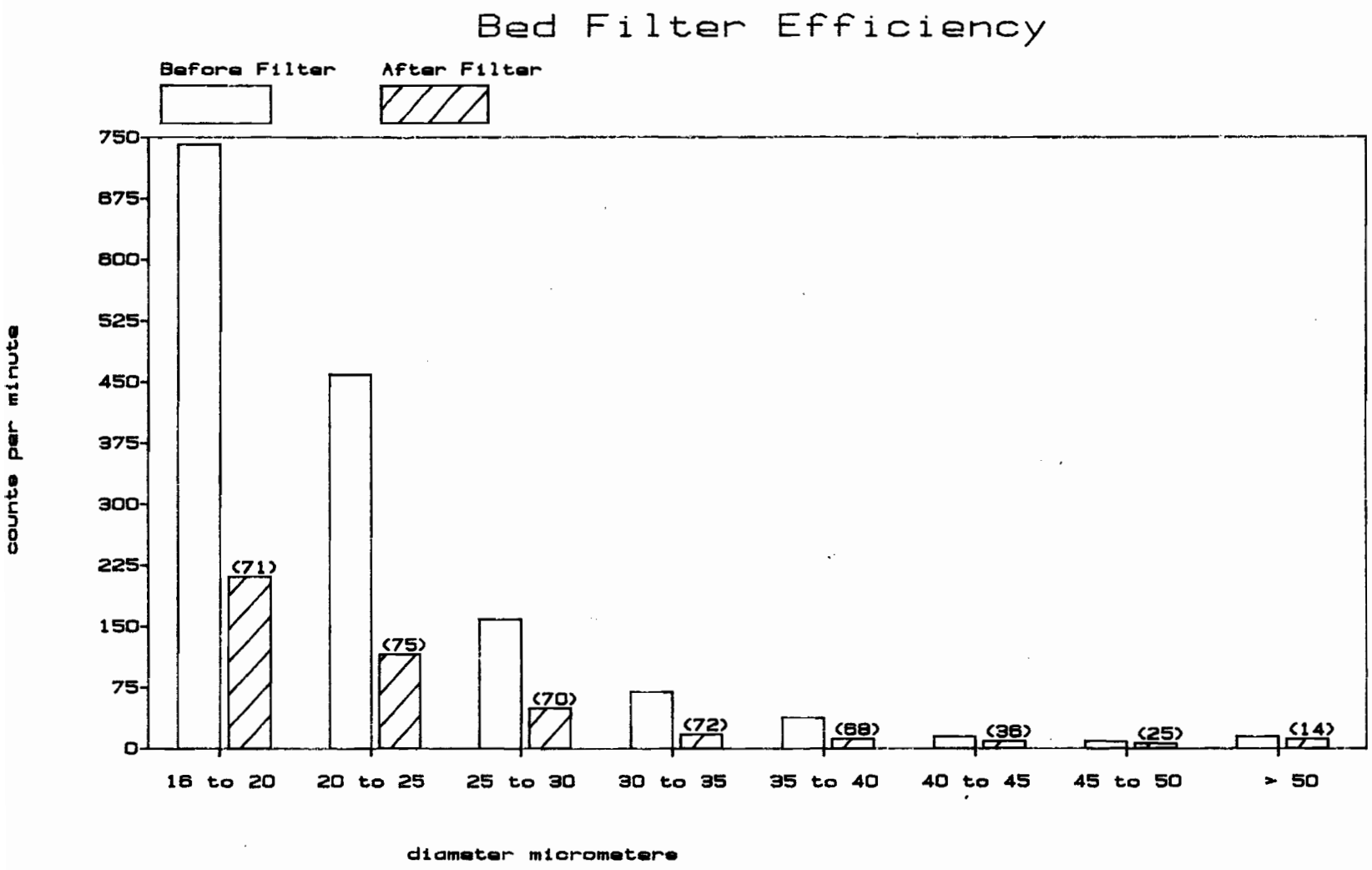

Figure 23: Bed Filter Efficiency: Count rates recorded in metal samples taken before and after a bed filter as a function of particle size. The figures in parentheses give the percentage removal.

4.4 DC45 Sécal Works

The DC45 casting center produces extrusion ingot and rolling stock by the direct chill process. There are three tilting furnaces which may be charged with scrap, hot metal or a combination of both. The plant layout is shown schematically in Figure 24. Grain refiner additions are made at the furnace outlet upstream of the sampling point used. Although there is an Alcoa 622 melt treatment unit, it was not in use during the period of this study. Casting rates at this center are considerably higher than at either the Saguenay or Lapointe Works with a typical drop lasting 50 to 60 minutes. PoDFA and LiMCA samples were taken at the point indicated in Figure 24. The results obtained on two casts are shown in Figures 25 and 26.

The effect of the rate of sampling was investigated during a third cast by taking readings while sampling at twice and three times the standard differential pressure (10 and 15 in. Hg, 24 and 51 kPa). These results are shown in Table 4.

These results again demonstrate the beneficial effect of allowing the metal to settle for extended periods of time prior to casting. For the cast shown in Figure 25 there was a substantial delay prior to casting due to mechanical problems with the casting table, whereas in the second example (Figure 26) the metal received only thirty minutes of settling and the LiMCA results were approximately four times higher than those shown in Figure 25.

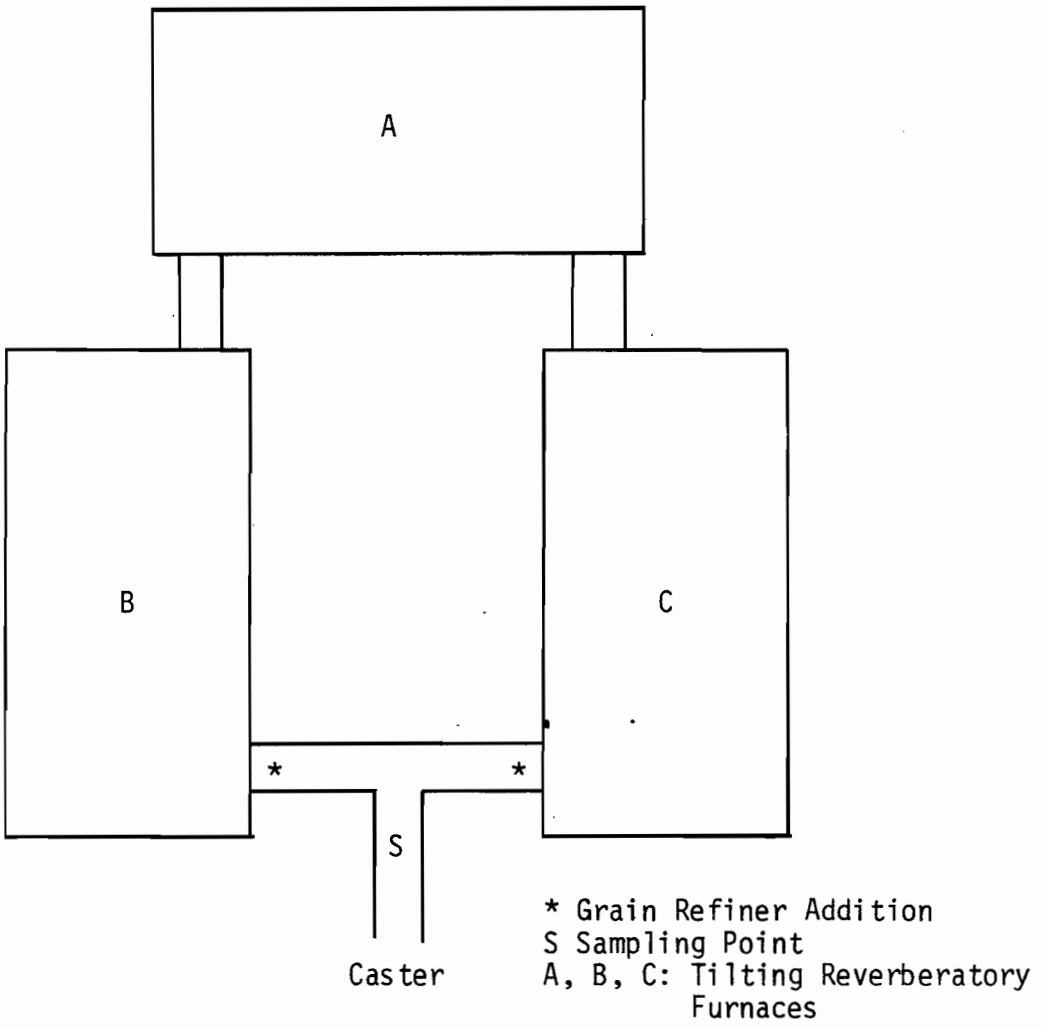

Figure 24: Plant layout: Sécal DC 45 (schematic).

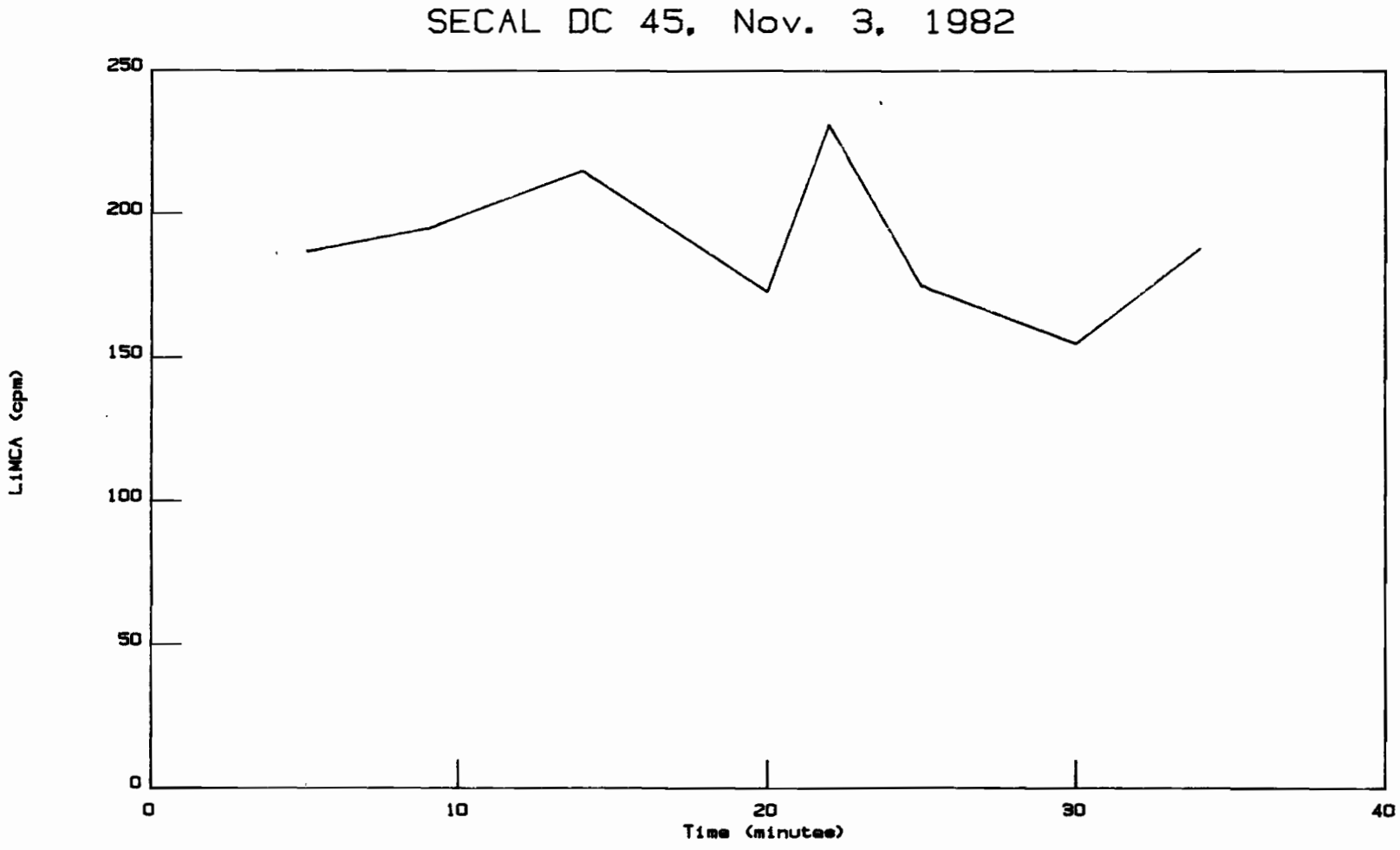

Figure 25: LiMCA results as a function of time into cast, DC 45, November 3, 1982. In this case there was a substantial delay prior to the start of casting.

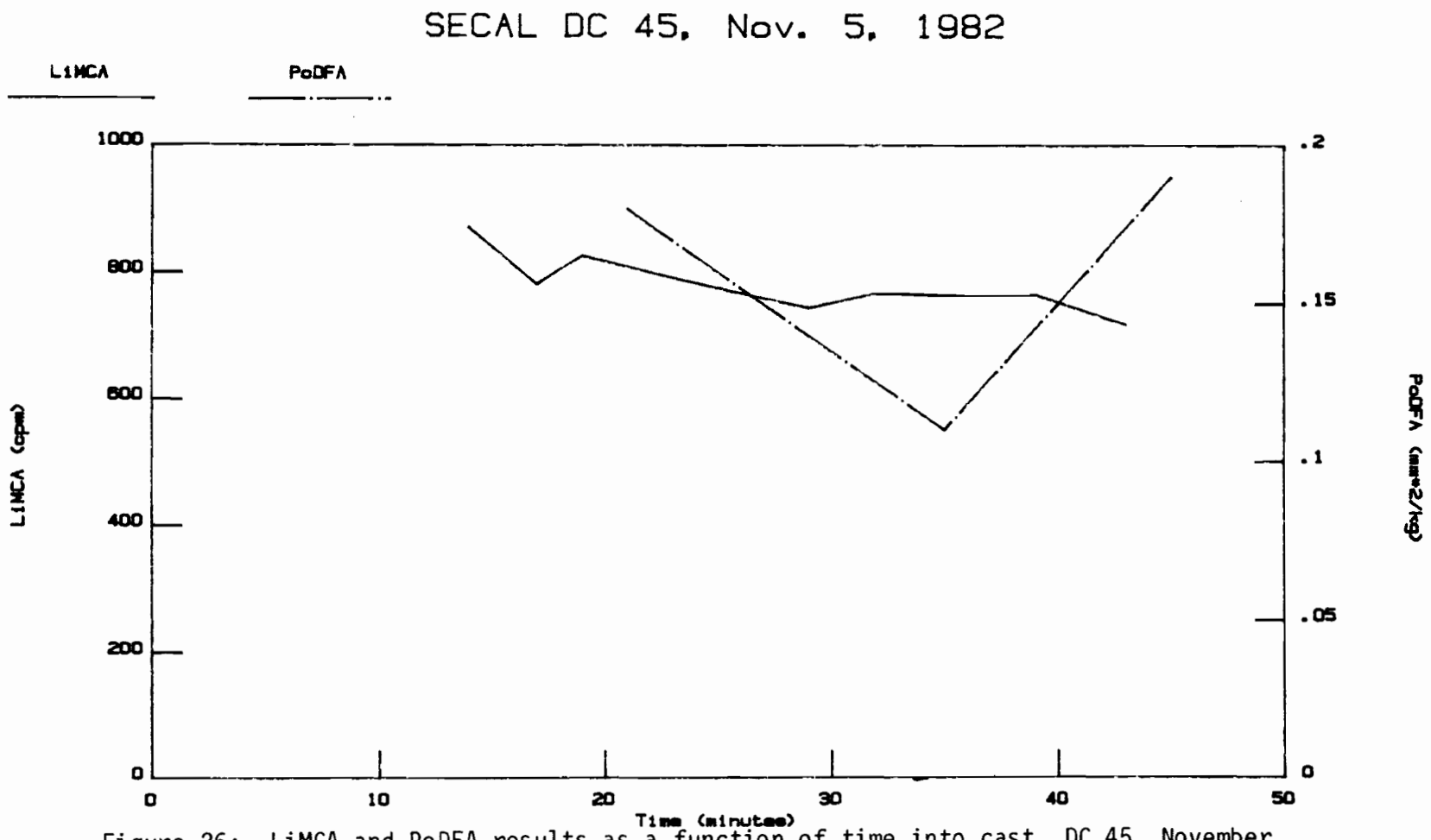

Figure 26: LiMCA and PoDFA results as a function of time into cast, DC 45, November 5, 1982. The metal was settled for approximately 30 minutes prior to casting.

In order to investigate the homogeneity of the metal stream two of the samples in Figure 26 (t = 29 and t = 32 minutes) were taken while using a large 'spoon' to isolate the metal being sampled from the flowing stream. This had no apparent effect on the LiMCA readings and, although admitedly inconclusive, suggests that the metal in the transfer troughs is fairly homogenous with regard to inclusions and that the relatively large scatter observed in duplicate PoDFA results arises from other factors such as the rate of metal flow through the disc and the exact nature of the discs themselves (porosity, capture efficiency, etc.).

In order to assess the effect of the rate of aspiration on the LiMCA results two samples were taken at differential pressures other than the 5 inches of mercury normally used. One sample was taken at a differential pressure twice normal (i.e. 10" Hg, 34 kPa) and another at three times normal (15" Hg, 51 kPa). In the latter case the sampling period was reduced to 30 seconds to avoid overflowing the sampling tube. Apart from the fact that the observed peaks were of shorter than normal duration (due to the decreased residence time of the particles within the orifice) no other effects were apparent. Table 4 gives the count rates observed and the differential sampling pressure for these two samples as well as those taken immediately before and after using standard conditions.

TABLE 4

EFFECT OF DIFFERENTIAL SAMPLING PRESSURE (FLOW RATE) ON THE LiMCA RESULTS

ΔP	Count Rate (CPM)	Corrected Count Rate
5 in. Hg	717	717
10 "	1056	746
5 "	766	766
15 "	625 x 2	722
5 "	722	722

When the observed count rates are normalized to the volume of metal sampled under standard conditions using the following equation

$$N = Nobs\sqrt{\frac{\Delta P_{st}}{\Delta P_{test}}}$$

the results are indistinguishable. Thus if desired the sampling rate could have been increased at least 73%, by increasing the differential sampling pressure by a factor of three, with no apparent effect on the performance of the device.

4.5 Oswego Works

Alcan operates a large remelt and rolling facility at Oswego, New York. LiMCA tests were carried out at two of the Oswego casting centers producing can body alloy rolling ingots. For this product the metal is fluxed with a nitrogen/chlorine mixture in a holding furnace, allowed to settle for a specified minimum period of time then passed through a Banbury Bed Filter (BBF) immediately prior to casting (Figure 27).

LiMCA sampling was carried out "on-line" upstream of the BBF at the holding furnace outlet and "downstream" just prior to the casting pit. The results obtained are shown in Figures 28 to 30 and in Table 5.

The results shown in Fig. 28 are typical of what was observed at this location. The upper line represents the count rate of particles larger than d = 20 μm at the furnace outlet as a function of time into cast. It can be seen that the count rate decays steadily with time, due presumably to the settling (or floating) of suspended inclusions. The lower curve, representing metal sampled after filtration, also shows a decrease in the count rate with time and all the values are markedly lower than those of the unfiltered metal indicating that the BBF was removing approximately 95% of the incoming inclusions.

Since the apparatus had only one sampling head it was not possible to take "before and after filter" samples simultaneously and the results shown in Figure 28 were obtained on two separate casts. Figure 29 shows the results obtained by alternately sampling metal before and after filtration during a single cast. Again it is evident that settling was occurring

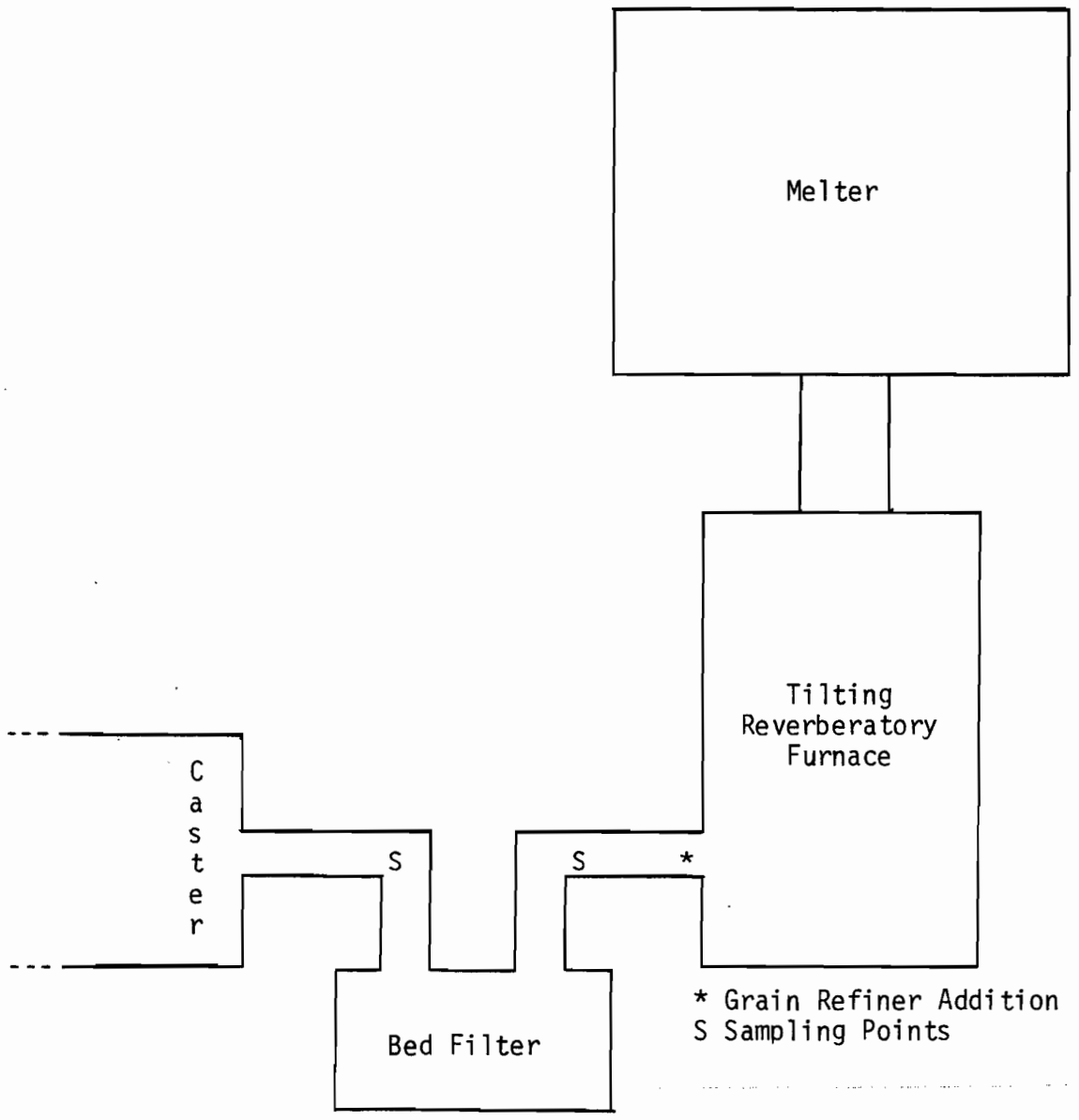

Figure 27: Plant layout, Oswego DC 4 and DC 5 (schematic).

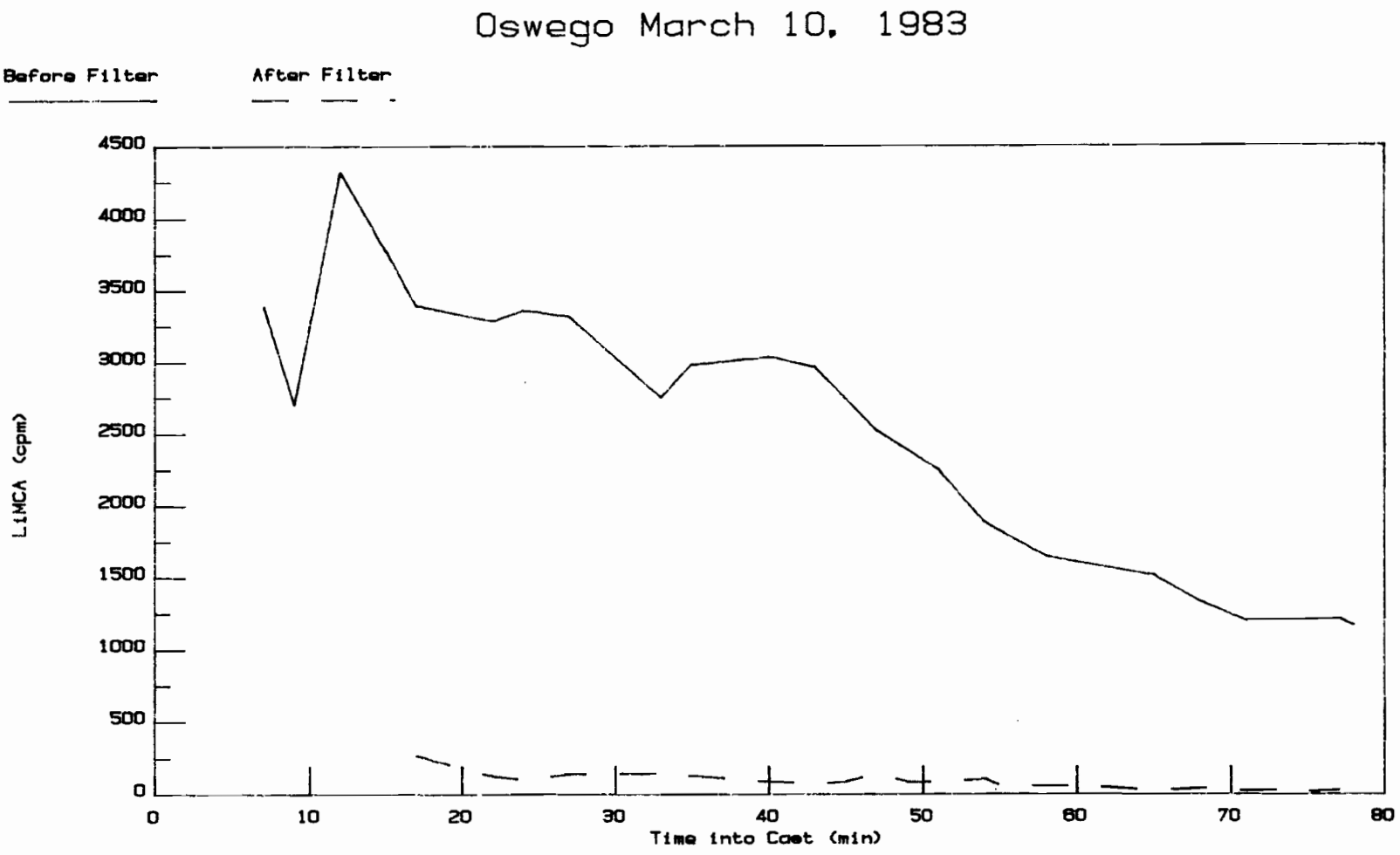

Figure 28: LiMCA results as a function of time into cast and position with respect to the bed filter, Oswego, March 10, 1983.

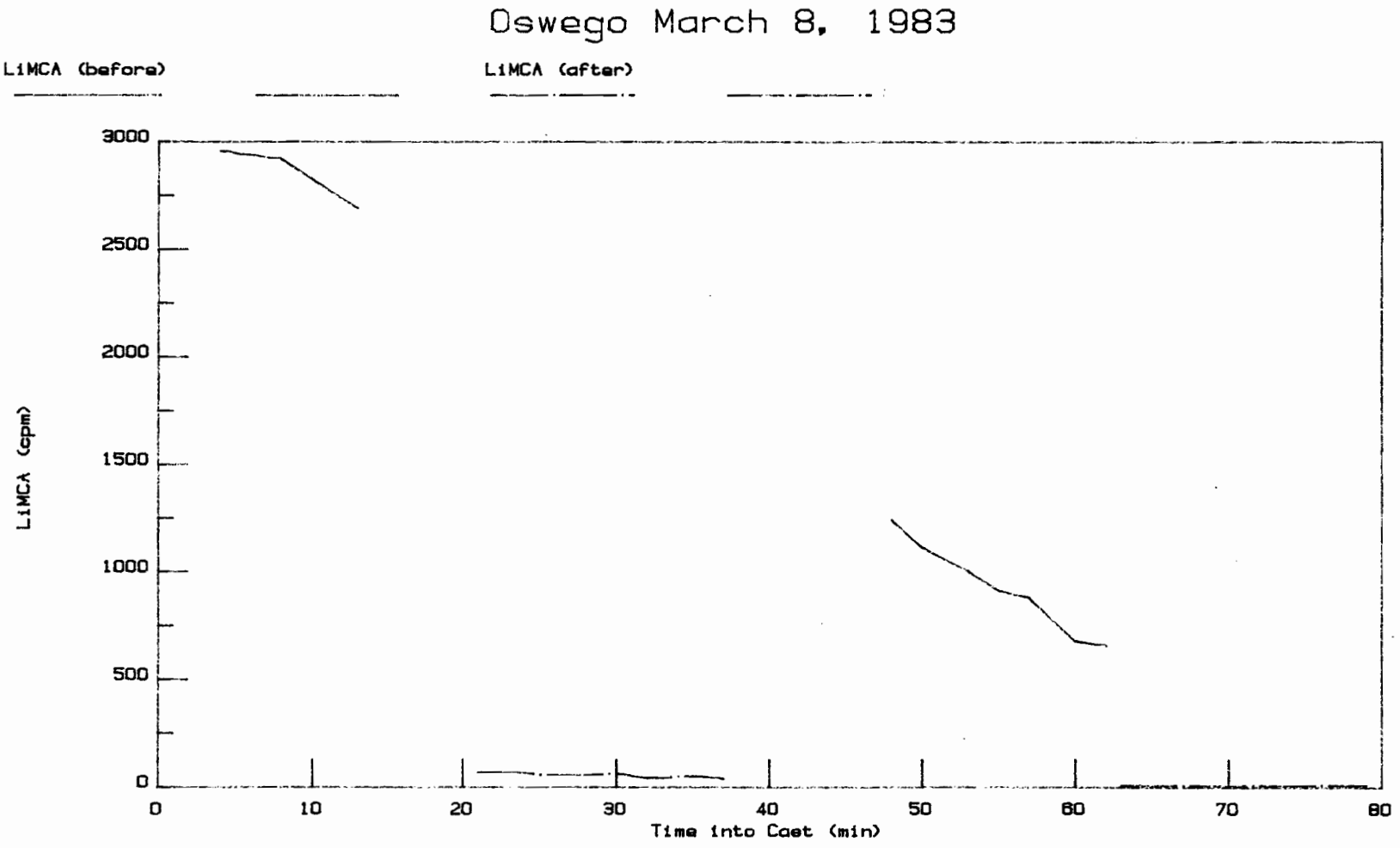

Figure 29: LiMCA results as a function of time into cast and position with respect to the bed filter, Oswego, March 8, 1983.

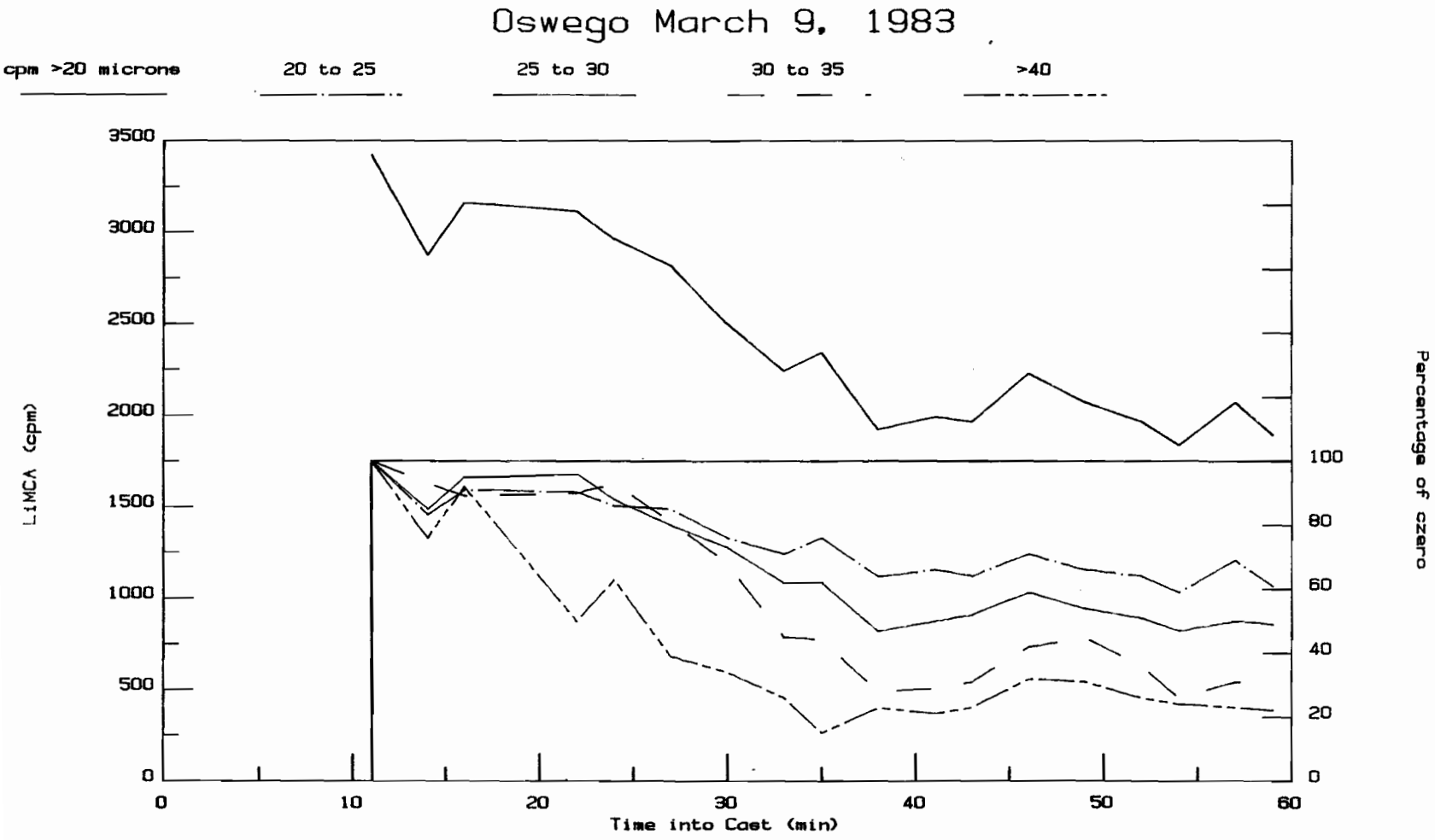

Figure 30: LiMCA results as a function of time into cast, Oswego, March 9, 1983. The lower curves give the relative count rates for the indicated particle size ranges as a percentage of the initial readings at t = 11 minutes.

and that the BBF was removing the majority of the incoming inclusions.

As mentioned previously the LiMCA also provides particle size distribution data. Figure 30, in addition to giving the total count rate also shows the count rates according to particle size as a percentage of their initial values recorded at the t = 11 minutes. This indicates that the particles responsible for the observed counts are behaving as one would expect with the larger particles disappearing faster than the smaller ones. Table 5 lists the actual readings taken during this cast which were used to generate Figure 30.

	LiMCA (counts per minute)							
Time	Total	20 μm to 25	25 μm to 30	30 μm to 35	35 μm to 40	40 μm to 45	45 μm to 50	>50 μm
11	3423	2341	693	246	81	41	10	11
14	2877	1949	590	228	62	31	6	11
16	3160	2127	658	220	98	31	16	10
22	3113	2113	666	221	82	18	8	5
24	2964	2014	607	228	76	28	8	3
27	2819	1989	556	200	50	16	4	4
30	2500	1769	504	167	39	12	4	5
33	2245	1657	428	111	33	12	1	3
35	2342	1776	429	109	19	6	3	0
38	1925	1494	325	69	23	5	5	4
41	1991	1548	348	71	11	6	5	2
43	1965	1494	362	75	20	9	2	3
46	2228	1668	411	102	29	6	6	8
49	2073	1543	376	111	24	10	6	3
52	1966	1494	353	89	14	7	4	5
54	1837	1385	324	64	31	14	7	12
57	2069	1607	346	76	25	5	8	2
59	1895	1436	340	79	26	6	2	6
62	1550	1186	262	64	22	5	0	11
71	1272	982	200	49	22	7	6	6
73	1216	941	164	54	20	6	1	10
77	1347	1022	228	69	12	9	4	3
79	1390	1058	231	72	15	9	3	2

Table 5: Count rates for the indicated particle size ranges for each data point shown in Figure 30.

5. DISCUSSION

5.1 General Observations

Perhaps the most striking observation. is the fact that molten aluminium contains a considerable number of suspended inclusions even after melt cleaning treatments such as settling, fluxing and filtration. Taking as an example the DC32 results where, by the time it had reached the sampling point, the metal had received all three of the above treatments, the LiMCA still registered 50 to 100 counts per minute. Based on a sample volume of 16 mL this corresponds to 3 to 6 particles per mL. On a volume basis however, this concentration of inclusions is very low, 25 to 50 ppb (parts per billion) based on an average particle diameter of 25 μm. In this respect the LiMCA is a very sensitive device. In the laboratory, even using pure metal and prolonged (days) settling periods; "zero" count rates were seldom observed. This is not particularly surprising considering that the detection limit of the device, based on detecting one 16 μm particle in 16 mL of aluminium (the volume of metal sampled in one minute under "standard" conditions) corresponds to 100 parts per trillion (10^{12}) on a volume basis.

5.2 Sources of Error

Before further discussion of the results it would be useful to consider the major sources of error and the expected variability of the LiMCA results. Contributing sources of error were variations in the current supplied by the battery, the actual dimensions of the orifice, the vacuum reservoir pressure and the counting error inherent in instruments of this type.

5.2.1 Counting Statistics

Since the LiMCA apparatus effectively examines many samples of the melt each equal in volume to the volume of the aperture, the Poisson distribution applies[6]. Accordingly the standard deviation of the observed number of counts (N_o) is equal to the square root of the count number, that is:

$$S_1 = (N_o)^{\frac{1}{2}} \qquad (1)$$

A second source of error arises from variations in the exact amount of metal sampled. Since, for the purposes of these experiments, the measurements were taken over a fixed period of time (one minute) these variations arise from the precision with which the pressure in the vacuum reservoir could be set and from tube to tube variations in both the overall form (and thus discharge coefficient) of the orifices and their exact minimum diameters. A rigorous treatment of this second source of error would be impractical particularly in view of the unknowns regarding the form of the orifices. However, the results presented in Table 5 of Part One provide a means of estimating the standard deviation arising from these sources, since the measured volumes were effectively subject to variability arising from the above mentioned sources. From these results we have two estimates of the relative standard deviation arising from these sources, one representing variation in the volume sampled with repeated sampling using the same tube $\left(\frac{S_2}{V}\right)$ and the other also including variations caused by tube to tube variations in the form and the diameter of the orifice $\left(\frac{S_3}{V}\right)$.

For repeated measurements with different sampling tubes the 95% confidence limits in the number of counts (per minute) considering only the variations in the sample volume are:

$$N = No \pm 2\left(\frac{S_3}{V}\right) No \qquad (2)$$

where: No = the observed number of counts

$\left(\frac{S_3}{V}\right)$ = the relative standard deviation of the sample volume.

The confidence interval due to the "Poisson" error is likewise:

$$N = No \pm 2\sqrt{No} \qquad (3)$$

The 95% confidence interval considering both sources of error is thus:

$$N = No \pm 2\left(\left(\left(\frac{S_3}{V}\right) No\right)^2 + \left(\sqrt{No}\right)^2\right)^{\frac{1}{2}} \qquad (4)$$

Table 6 shows the magnitude of the total error $\left[\left(\left(\frac{S_3}{V}\right) No\right)^2 + No\right]^{\frac{1}{2}}$ and the independent contributions of each of the contributing errors $\left(\left(\frac{S_3}{V}\right)No \text{ and } \sqrt{No}\right)$ as well as the relative magnitudes of the two error sources $\left(\frac{\sqrt{No}}{\left(\frac{S_3}{V}\right)No}\right)^2$.

It can be seen that, at low count rates ($\sim$ <200) the Poisson contribution dominates and that the two sources of error contribute equally to

the total error at $N = \left(\frac{S_3}{V}\right)^{-2} = 590$ cpm, above which error arising from variations in the sample volume becomes increasingly dominant.

Similarly the confidence intervals from the situation of repeated sampling with the same tube can be calculated by substituting $\left(\frac{S_2}{V_2}\right)$ in the place of $\left(\frac{S_3}{V_3}\right)$ in equation 4. In this case the Poisson error again dominates at low count rates and the two contributions are equal to No ≃ 1765.

This analysis indicates that, at low count rates (clean metal) the precision of the technique can be increased by simply taking larger samples. When the Poisson error dominates taking N small samples and summing the results is equivalent to taking one sample N times larger. Thus two avenues are available if it were deemed desirable to decrease the error when measuring clean metal.

5.2.2 Coincidence Effects

A further potential source of error is coincidence, that is the presence of two or more particles in the sensing zone at the same time.

Bader and Gordon[6] distinguished two different coincidence effects occurring in resistive pulse and optical particle counters:

Primary coincidence - which lowers the number of counts observed and occurs when two particles, which should have been counted individually, appear simultaneously in the sending volume and are recorded as a single larger particle and Secondary Coincidence - which raises the count rate

TABLE 6

EXPECTED TOTAL ERROR (STANDARD DEVIATION) FOR THE INDICATED NUMBER OF COUNTS ARISING FROM THE COUNTING (POISSON) ERROR AND THE VARIATION IN SAMPLE VOLUME, AS WELL AS THEIR RELATIVE CONTRIBUTION

	ERROR (STANDARD DEVIATION)			
Count Number	Total $\left[\left(\frac{S_3}{V} No\right)^2 + (No^{\frac{1}{2}})^2\right]^{\frac{1}{2}}$	Poisson* (P) $(No)^{\frac{1}{2}}$	Volume (V) $\left(\frac{S_3}{V} No\right)$	Relative $(P/V)^2$ $\left[\frac{(No)^{\frac{1}{2}}}{\left(\frac{S_3}{V} No\right)}\right]^2$
5	2.2	2.2	0.2	118
10	3.2	3.2	0.4	59
20	4.6	4.5	0.8	30
40	6.5	6.3	1.6	15
75	9.2	8.7	3.1	7.9
100	11	10	4.1	5.9
200	16	14	8.2	3.0
400	26	20	17	1.5
500	30	33	21	1.2
590	34	24	24	1.0
750	41	27	31	0.8
1,000	52	32	41	0.6
2,000	94	45	82	0.3
4,000	176	63	165	0.15
10,000	423	100	411	0.06

* For small values of No the Poisson distribution is skewed and the confidence limits should be calculated or obtained from tables. However, for No greater than 10, this approximation is satisfactory.

and occurs when two small (non-detectable) particles are present in the sensing zone simultaneously and together produce a detectable signal.

5.2.2.1 Primary Coincidence

The Poisson distribution gives the probability of finding "r" particles in a volume (v) when the average concentration of particles per unit volume is (n/V) as

$$P(r) = \frac{\varepsilon^r e^{-\varepsilon}}{r!} \qquad (5)$$

where $\varepsilon = \left(\frac{n}{V}\right)v$ (i.e. the average number of particles in the sensing volume). The probability of finding no particles is thus:

$$P(0) = \frac{\varepsilon^0 e^{-\varepsilon}}{0!} = e^{-\varepsilon} \qquad (6)$$

The probability of finding one or more particles is then

$$P(r \geq 1) = 1 - P(0) = 1 - e^{-\varepsilon} \qquad (7)$$

Therefore the frequency with which one and only one particle is detected is:

$$\frac{P(1)}{P(r \geq 1)} = \frac{\varepsilon e^{-\varepsilon}}{1-e^{-\varepsilon}} \qquad (8)$$

During this investigation the highest particle concentration measured was 4500 cpm or $2.8 \times 10^8/m^3$ (based on a 16 ml sample volume) and the volume of the sampling zone (v) was approximately 1×10^{-10} m^3. For this case equation 8 gives

$$\frac{P(1)}{P(r \geq 1)} = 0.99$$

(For smaller values of ε equation 8 can be simplified by expanding the denominator in a Taylor series, neglecting terms higher than order 1 to give:

$$\frac{P(1)}{P(R\geq 1)} = e^{-\varepsilon} \quad .)$$

That is, 99% of the particles arrive in the sampling zone individually.

The primary coincidence loss is given by one minus the probability of finding one or more particles in the sensing volume divided by the average number (ε).

$$1 - \frac{P\geq 1}{\varepsilon} = 1 - \frac{1-e^{-\varepsilon}}{\varepsilon} = 0.014 \qquad (9)$$

Since the primary coincidence loss was less than 2% in this extreme case errors arising from this source were considered negligible.

5.2.2.2 Secondary Coincidence

In order to estimate the importance of secondary coincidence (two small, individually non-detectable particles appearing together as a detectable pulse) it is necessary to extrapolate the size distribution beyond the lower limit. In this work the threshold (detection limit) was arbitrarily set at channel number 61 of the multi-channel analyser ($d = 20$ μm) actually data were recorded down to $d \simeq 16$ μm a fact which allows the effect of secondary coincidence to be calculated since two particles larger than 16 micrometers in diameter arriving together would appear as a single particle larger than 20 μm.

In general the region corresponding to particles of diameters ranging from 16 to 20 μm contained about twice the number of counts recorded for d > 20 μm. Again taking the highest observed count rate as 4500 cpm this corresponds to $2 \times 4500 = 9000$ cpm or 5.6×10^8 particles/M^3. Substituting this value into equation 5 and dividing by the probability of finding one or more particles in the size range of interest (Equation 7) gives:

$$\frac{P_2 \text{ (Equation 5, } n = 5.6 \times 10^8/cm^3)}{P>1 \text{ (Equation 7, } n = 2.8 \times 10^8/cm^3)} = 0.054$$

the fractional increase in count rate occurring in this situation due to secondary coincidence. Thus in this (the worst) case secondary coincidence would have increased the count rate by approximately 5%. At lower count rates the effect becomes increasingly insignificant.

5.2.3. Variations in Orifice Diameter

The diameters of the orifices used during these experiments was 300 ± 10 μm. Variations in orifice diameter affect the count rate in two ways:

1. by changing the actual volume of metal samples during the fixed (1 minute) sampling period,

and

2. by altering the particle size detection limit which was arbitrarily chosen as channel number 61 of the multichannel analyser (d = 20 μm for D = 300 μm and I = 60 A).

Fortunately these two effects act in opposition, for instance, when using a 310 μm orifice the sample volume was increased, on average, by a factor of $\left(\frac{310}{300}\right)^2 = 1.07$ (due to the fact that the volumetric flow rate is proportional to the orifice area). At the same time channel number 61 then corresponds to a particle of 21 μm E.S.D. (and particles of 20 μm E.S.D. appear in channel 47). Particles ranging from 20 to 25 μm in diameter normally accounted for one-half the two-thirds of the total count rate (d > 20 μm) thus the observed count rate for d > 21 μm would be roughly: $\frac{1}{5} \times \frac{1}{2}$ to $\frac{2}{3}$ = 10 to 14% lower due to the "missing" particles. This roughly compensated for the increased sample volume. Experimentally sequential results obtained with different tubes did not lead to any abrupt changes in the observed count rates, although it is possible to imagine particle size distributions in which this coincidental annulment of errors would not occur.

5.2.4 Variations in Current

Variations in the current can affect the results by altering the magnitude of the observed peaks thus changing both the apparent size and the concentration of particles counted. Typical current variations within a 90 minute sampling period were approximately two amperes between the first and last samples.

At a current of 60 amperes a count due to a particle 20 μm in diameter appeared in channel number 61, at 58 amperes it would have appeared in channel number 59. The effect of neglecting one channel at the lower limit

of integration was estimated to be no larger than 1 to 2%, thus small long-term variations in current were considered to have had a negligible effect on the results.

5.2.5 Random Noise

On occasion very high count rates (> 10000 cpm) were recorded for an individual measurement. These anomalous readings arose from a number of sources including loose electrical contacts, heavily oxidized electrodes, orifice blockage and mechanical vibrations. Spuriously high counts were compared with those taken immediately prior and following and rejected.

5.3 Comparison Between the Metallographic (PoDFA) and Resistive Pulse LiMCA Results

The PoDFA and LiMCA techniques were both developed to provide information about the concentration of suspended particles in aluminium and as such, a relation should, in principle exist between the results obtained using each technique. Table 7 shows the slope, intercept and correlation coefficients between the results of the two techniques obtained at the Saguenay Works (Figures 9 and 10) and at the Lapointe Works (Figures 14, 15 and 16). The data from several casts at each location were combined in order to provide sufficient data points and a reasonable range over which to perform the linear regressions. Previous experience with the PoDFA technique suggested that the expected reproducibility of the results is of the order of ± 40%. In the case of the LiMCA results Table 6 was used to

obtain an estimate of their variability. Thus for the regression analysis of the Saguenay Works data where the average LiMCA result was 1044 (i.e. 2s= ± 2 x 54 or 10%) the regression was performed minimizing the ordinate (PoDFA) deviation from the least-square regression line.

For the Lapointe Works data the average LiMCA value was 400 (i.e. ± 15%) and again the regression was performed minimizing the PoDFA deviations (the results of Figure 17 were omitted due to the systematic error in the PoDFA results mentioned earlier).

The data points and the regression lines are plotted in Figures 31 and 32. Further data analysis showed that the two regression lines did not significantly differ with respect to slope or intercept.

TABLE 7

SLOPES, INTERCEPTS AND CORRELATION COEFFICIENTS OBTAINED BY LINEAR REGRESSION ANALYSIS OF THE LiMCA AND PoDFA DATA FROM THE SAGUENAY AND THE LAPOINTE WORKS

Location	Slope	Intercept	Correlation Coefficient
Saguenay	3155	150	0.89
Lapointe	2860	-31	0.93

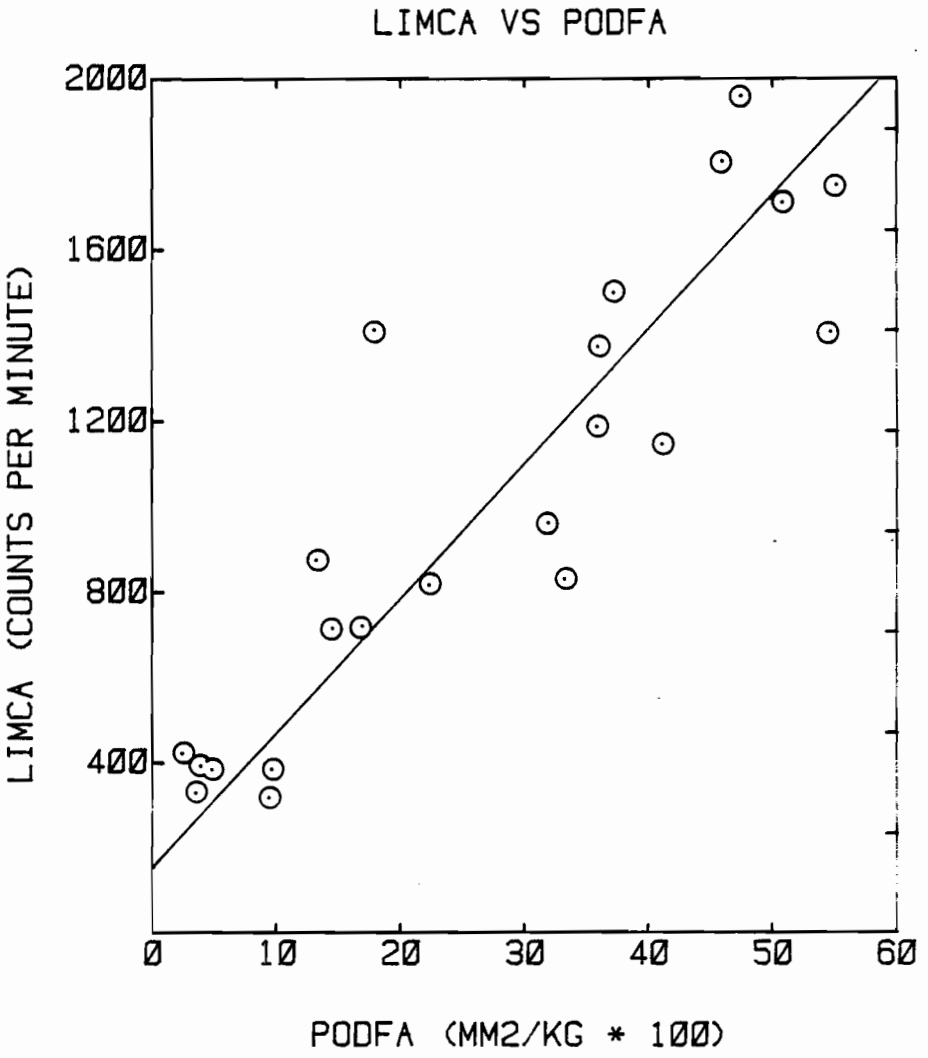

Figure 31: LiMCA results as a function of PoDFA results for the combined Saguenay Works data (Figures 9 and 10). The line was calculated by a linear least-squares regression.

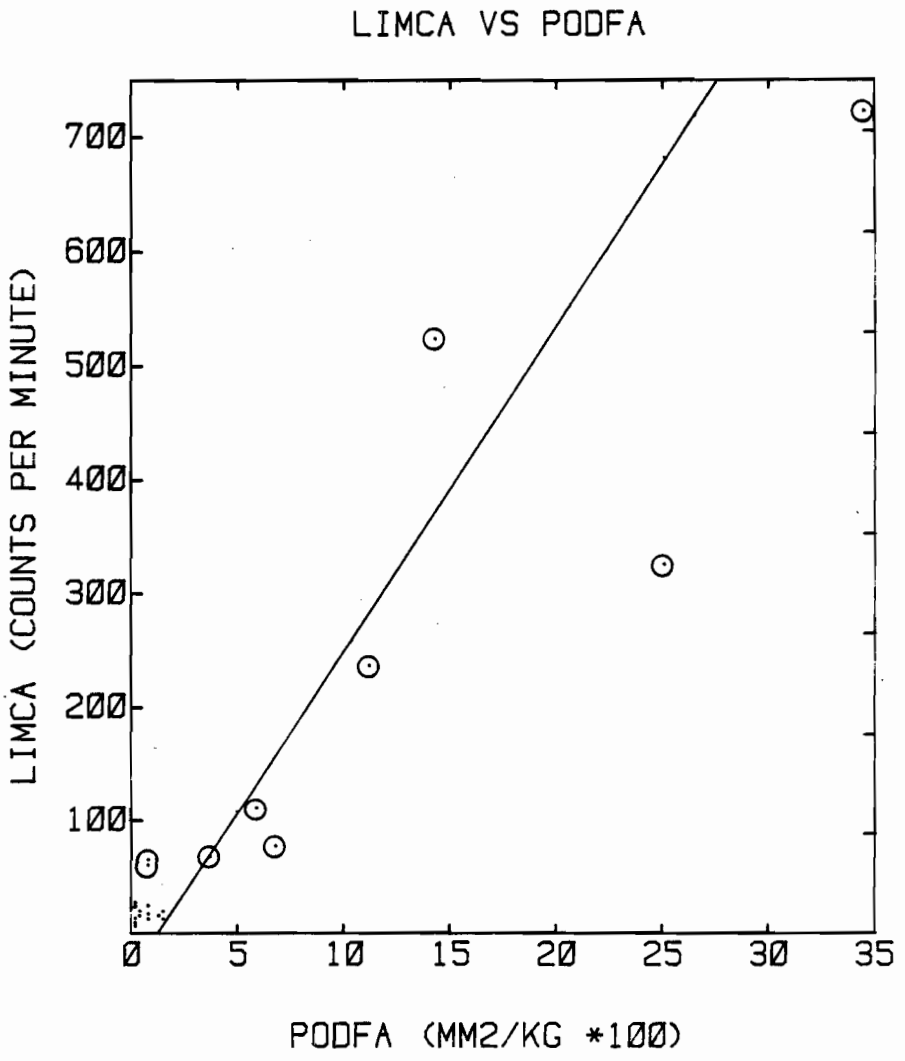

Figure 32: LiMCA results as a function of PoDFA results for the combined Lapointe Works data (Figures 14, 15 and 16). The line was calculated by a linear least-squares regression.

In the PoDFA test a known mass (typically 1.5 kg) is filtered through a disc 12.7 mm in diameter. The volume of the concentrate is thus:

$$\frac{\pi D^2 h}{4}$$

where: D = the filter diameter

h = the thickness of the filter cake.

The disc is then sectioned at a right angle to its surface in the plane passing through its center and this surface is examined. The volume examined is thus:

$$Dh\,\delta$$

where: δ is the depth of field.

The fraction of the concentrate examined (f) is thus

$$f = \frac{Dh\,\delta}{\frac{\pi D^2}{4} h} = \frac{4\delta}{\pi D}$$

Assuming that the depth of field "δ" is 25 μm f becomes:

$$f = \frac{4\ 25\times10^{-6}}{\pi\ 12.7\times10^{-3}} = 2.5\times10^{-3}$$

Thus the volume of metal actually examined per kg of metal filtered is

$$f = \frac{1000\ g}{2300\ g/mL} = 1.1\ mL$$

Taking the slope of the regression line as 3000 cpm/(1.0 mm^2/kg) the expected number of particles of $d \geq 20$ μm per mL is 3000/16 = 187.

Assuming that they present an average cross-sectional diameter of 25 μm in the PoDFA section the total area presented by 1.1 mL of metal would be:

$$\frac{\pi D^2}{4} \times 187 \times 1.1 = 0.10 \text{ mm}^2$$

a factor of ten below the value expected from the LiMCA vs PoDFA regression.

This discrepancy* is believed to be due to the capture of particles smaller than d = 20 μm by the PoDFA disc. Although the discs are selective for particles larger than 20 μm the capture efficiency for 15 μm particles is estimated to be 70% and is still 40% for 10 μm particles. The particle size distribution data shown in Table 3 suggests that these smaller particles are present in relatively large concentrations thus despite the lower capture efficiency and their smaller cross-sectional area they probably contribute significantly to the total inclusion area observed on the PoDFA discs.

5.4 Particle Size Distributions

In addition to providing a gross count (concentration) of particles larger than a predetermined size, the LiMCA also provides a histogram of the particle size distribution. Thus a 511 channel histogram was available for every data point on each graph shown in the Results section. In order to make the results more comprehensible the number of channels per histogram was reduced to eight with six of those corresponding to a 5 μm

---

* The optimistic view is, of course, that there is "order of magnitude" agreement.

diameter increment over the range 20 to 50 μm. Examples of the particle size distributions obtained were given in the Results and Discussion section (Figures 12, 16 and 31, Table 5) and in each case clearly suggested that particle settling (floating) was occurring within the holding furnace with the larger particles, as expected, disappearing faster than the smaller ones.

The general shape of the particle size distributions was always the same as it is evident that the peak (number) concentration of particles lies somewhere below d = 20 μm. The rapid increase in the concentration of particles with decreasing size lends credence to the hypothesis stated in the previous section that attributed the ten-fold discrepancy between the observed and calculated relationship beween the LiMCA and PoDFA results to the presence of large numbers of particles smaller than 20 μm on the PoDFA discs*.

---

* It should be noted that most of the particles were identified as TiB_2 clusters. When these are present as a filter cake it is not possible to distinguish (or measure) individual clusters by metallographic examination.

6. CONCLUSIONS

From these experiments it was found that the apparatus developed could be used to obtain quantitative data about metal cleanliness in both the laboratory and a variety production environments. The results obtained were both reproducible from sample to sample and "reasonable" in that they confirmed conclusions acquired through years of semi-empirical observations about the effects of settling times and bed filters on the cleanliness of aluminium. In addition a highly significant relation was found between the LiMCA results and those provided by an independent technique based upon a completely different measurement principle.

REFERENCES

1- C.J. Siemensen, "A Critical Review of the Literature Concerning the Fluxing of Aluminium Melts with Salts or Gas", Sentralinstitut For Industriell Forskning, Report No. 78-05-11-1, Oslo, Norway, 1978.

2- K. Bauxman, J.D. Bornand and G.B. Leconte, "Impact of Purification Methods on Inclusions and Melt Loss", Light Metals, The Metallurgical Society of AIME, pp. 191-206, 1977.

3- S.A. Levy, J.C. Miller, P. McNanara and D.A. Feitig, "Molten Metal Quality-Particulate Tests", Light Metals, The Metallurgical Society of AIME, pp. 149-170, 1977.

4- T. Tanaka, S. Asami and K. Nishitsuji, "Agglomeration and Settlement of TiB_2 Particles in Molten Aluminium", Aluminium, Vol. 58 (10), pp. 600-604, 1982.

5- C.J. Siemensen and G. Strand, "Analysis of Inclusions in Aluminium by Dissolution of the Samples in Hydrochloric/Nitric Acid", Fresenius Z. Anal. Chem., Vol. 308, pp. 11-16, 1981.

6- H. Bader, J.R. Gordon and O.B. Brown, "Theory of Coincidence Count Correction for Optical and Resistive Pulse Particle Counters", Rev. Sci. Instr., Vol. 43 (10), pp. 1407-1412, 1972.

LIST OF FIGURES

Figure 13: Plant layout, Lapointe Works, (schematic).

Figure 14: LiMCA and PoDFA results as a function of time into cast, Lapointe Works, October 7 , 1982.

Figure 15: LiMCA and PoDFA results as a function of time into cast, Lapointe Works, October 15 , 1982.

Figure 16: LiMCA and PoDFA results as a function of time into cast, Lapointe Works, October 5 , 1982. (In this case the metal in the furnace was well mixed at the outset due to production difficulties). The upper solid line represents all counts corresponding to particles larger than 16 μm in diameter.

Figure 17: LiMCA and PoDFA results as a function of time into cast, Lapointe Works 1982. (In this case the metal contained small "borocarbide" particles which led to the anomalously high PoDFA results).

Figure 18: Plant layout, Sécal DC32 (schematic).

Figure 19: LiMCA and PoDFA results as a function of time into cast for two successive drops from the same original batch.

Figure 20: LiMCA and PoDFA results as a function of time into cast, note the initial surge of inclusion-laden metal released from the bed filter.

Figure 21: LiMCA and PoDFA results as a function of time into cast. The first drop (7A) had received an additional two hours of settling compared to the example in Figure 20.

Figure 22: LiMCA and PoDFA results as a function of time into cast, in this example an "upset" occurred approximately 15 to 20 minutes into the cast.

Figure 23: Bed Filter Efficiency: Count rates recorded in metal samples taken before and after a bed filter as a function of particle size. The figures in parentheses give the percentage removal.

Figure 24: Plant layout, Sécal DC45 (schematic).

Figure 25: LiMCA results as a function of time into cast, DC45, November 3, 1982. In this case there was a substantial delay prior to the start of casting.

Figure 26: LiMCA and PoDFA results as a function of time into cast, DC45, November 5, 1982. The metal was settled approximately 30 minutes prior to casting.

Figure 27: Plant layout, Oswego DC4 and DC5 (schematic).

Figure 28: LiMCA results as a function of time into cast and position with respect to the bed filter, Oswego, March 10, 1983.

Figure 29: LiMCA results as a function of time into cast, and position with respect to the bed filter, Oswego, March 8, 1983.

Figure 30: LiMCA results as a function of time into cast, Oswego, March 9, 1983. The lower curves give the relative count rates for the indicated particle size ranges as a percentage of the initial readings at t = 11 minutes.

Figure 31: LiMCA results as a function of PoDFA results for the combined Saguenay Works data (Figures 9 and 10). The line was calculated by a linear least-squares regression.

Figure 32: LiMCA results as a function of PoDFA results for the combined Lapointe Works data (Figure 14, 15 and 16). The line was calculated by a linear least-squares regression.

LIST OF TABLES

CONCLUSIONS TO THE THESIS

CONCLUSIONS TO THE THESIS

The resistive pulse method of particle size analysis has been adapted for use in liquid metals. The apparatus developed is both selective (in terms of particle size) and sensitive (estimated detection limit = less than 1 part per billion V/V). The device can be used to take measurements "on-line" during routine production and provides information about the overall concentration and the particle size distribution of suspended inclusions in one minute. The results were found to be as reproducible as could be expected given the inherent statistical variation characteristics of this type of device. The effects of settling (floating) and filtration were investigated and observed to have a profound influence on the overall level of suspended inclusions. Although most of this work was concerned with molten aluminium the technique was also demonstrated in gallium, zinc and lead and should be generally applicable to all molten metals. The method and apparatus described are currently "patent pending" in the United States and Alcan Limited has undertaken a development program to implement the technique for on-line process control at casting centres producing inclusion sensitive alloys.

CLAIMS TO ORIGINALITY

Aspects of this work constitute in the author's opinion new and distinct contributions to knowledge, these include:

1. While the resistive-pulse technique has been widely used for the measurement of concentrations and size distributions of particles suspended in low temperature aqueous and organic systems, this is the first time it has been successfully applied to the measurement of particles suspended in molten metals.

2. Furthermore, this is the first time that any method of rapidly measuring the concentration and/or size distribution of inclusions suspended in molten metals has been described.

3. Although it has been previously appreciated that quiescent settling can affect the overall "cleanliness" of liquid metals, this is the first time that the effect of settling on the concentration and size distribution of inclusions suspended in a liquid metal has been documented.

4. Although it has been previously appreciated that filtration can affect the overall cleanliness of liquid aluminium, this is the first time that a quantitative description of the effect of filtration has been given in terms of both concentration and particle size distribution.

There are also several other innovations relating more specifically to the apparatus developed which are not as universal in application:

5. A novel liquid metal sampling vessel was developed which was able to withstand immersion and continued exposure for up to two hours in liquid aluminium.

6. An unexpected method of "conditioning" the orifice of the sampling vessel in order to obtain usable signals was discovered.

ACCOPRESS®

25071 –	BLACK / NOIR	– BG2507
25072 –	BLUE / BLEU	– BU2507
25078 –	RED / ROUGE	– BF2507
25075 –	GREEN / VERT	– BP2507
25074 –	GREY / GRIS	– BD2507
25073 –	R. BLUE / BLEU R.	– BB2507
25079 –	X. RED / ROUGE X.	– BX2507
25070 –	YELLOW / JAUNE	– BY2507
25077 –	TANGERINE	– BA2507

ACCO CANADIAN COMPANY LIMITED
COMPAGNIE CANADIENNE ACCO LIMITÉE
TORONTO CANADA